Copyright Warning & Restrictions

The copyright law of the United States (Title 17, United States Code) governs the making of photocopies or other reproductions of copyrighted material.

Under certain conditions specified in the law, libraries and archives are authorized to furnish a photocopy or other reproduction. One of these specified conditions is that the photocopy or reproduction is not to be "used for any purpose other than private study, scholarship, or research." If a, user makes a request for, or later uses, a photocopy or reproduction for purposes in excess of "fair use" that user may be liable for copyright infringement,

This institution reserves the right to refuse to accept a copying order if, in its judgment, fulfillment of the order would involve violation of copyright law.

Please Note: The author retains the copyright while the New Jersey Institute of Technology reserves the right to distribute this thesis or dissertation

Printing note: If you do not wish to print this page, then select "Pages from: first page # to: last page #" on the print dialog screen

ABSTRACT

SOLIDS SUSPENSION AND POWER DISSIPATION IN STIRRED TANKS AGITATED BY AN IMPELLER NEAR THE TANK BOTTOM

by
Ernesto Uehara Nagamine

In this work, the effect of very small impeller clearances off the tank bottom, C, on complete solid off-bottom suspension, Njs, was investigated. Four types of impellers were used: six-blade flat-disk turbine, six-blade flat-blade turbine, six-blade flat (45°) pitched-blade turbine, and the high efficiency impeller Chemineer HE-3. The effects of the impeller diameter, D, tank diameter, T, and solids loading, X, were quantified. The presence of two impellers was analyzed using impellers of the same type and size.

Typically, Njs and the power consumption were found to decrease with the impeller clearance. However, for lower C/T values, a slight increase was observed for axial impellers, especially for low D/T ratios (less than 0.261). The power consumption was lower for the axial-flow impellers as compared with the radial-flow impellers. For disk and flat-blade turbines, a change in the flow pattern was observed in the range of $0.13 < C/T < 0.19$ and $0.19 < C/T < 0.24$, respectively. No change in flow pattern was observed up to $C/T = 0.25$, for the flat (45°) pitched-blade turbines and the Chemineer impellers. Correlations to predict the value of Njs as a function of impeller clearance were obtained, for each type of impeller.

SOLIDS SUSPENSION AND POWER DISSIPATION IN STIRRED TANKS AGITATED BY AN IMPELLER NEAR THE TANK BOTTOM

by
Ernesto Uehara Nagamine

A Thesis
Submitted to the Faculty of
New Jersey Institute of Technology
in Partial Fulfillment of the Requirements for the Degree of
Master of Science in Chemical Engineering

Department of Chemical Engineering,
Chemistry, and Environmental Science

October 1996

APPROVAL PAGE

SOLIDS SUSPENSION AND POWER DISSIPATION IN STIRRED TANKS AGITATED BY AN IMPELLER NEAR THE TANK BOTTOM

Ernesto Uehara Nagamine

Dr. Piero Armenante, Thesis Adviser — Date
Professor of Chemical Engineering, Chemistry, and Environmental Science,
NJIT

Dr. Gordon Lewandowski, Committee Member — Date
Department Chairman and Professor of Chemical Engineering, Chemistry, and
Environmental Science, NJIT

Dr. Dana Knox, Committee Member — Date
Professor of Chemical Engineering, Chemistry, and Environmental Science,
NJIT

BIOGRAPHICAL SKETCH

Author: Ernesto Uehara Nagamine

Degree: Master of Science

Date: October 1996

Undergraduate and Graduate Education:

- Master of Science in Chemical Engineering,
  New Jersey Institute of Technology, Newark, NJ, 1996

- Bachelor of Science in Chemical Engineering,
  Engineering National University, Lima, Peru, 1984

Major: Chemical Engineering

This thesis is dedicated to my wife

ACKNOWLEDGMENT

I would like to express my sincere gratitude to my thesis advisor, Dr. Piero M. Armenante, for his guidance and support. His efforts were truly appreciated.

I would like to acknowledge to the members of my thesis committee, Dr. Gordon Lewandowski and Dr. Dana Knox, for their constructive criticism.

I appreciate the mixing laboratory members, Dr. Chun-Chiao Chou and Mr. Changgen Luo, for their suggestions and assistance.

TABLE OF CONTENTS

TABLE OF CONTENTS
(Continued)

LIST OF TABLES

LIST OF TABLES
(Continued)

LIST OF TABLES
(Continued)

LIST OF TABLES
(Continued)

Table **Page**

LIST OF FIGURES

LIST OF FIGURES
(Continued)

NOMENCLATURE

A	Impeller blade angle (degree)
A'	Impeller blade angle (radian)
A_p	Impeller pitch (m)
C	Impeller off-bottom clearance, distance from the lowest point of the impeller to the tank bottom (m)
C'	Impeller off-bottom clearance, distance from the impeller centerline to the tank bottom (m)
CBS	Complete off-bottom suspension, as defined by Zwietering (1958)
D	Impeller diameter (m)
dp	Particle size (m)
e_t	Local energy dissipation rate (watts/kg)
$[e_t]_b$	Local energy dissipation rate at the bottom (watts/kg)
H	Liquid height (m)
k	Blade thickness (m)
K	Calibration constant for strain gages (kg_f-m/mV-s)
L	Blade length (m)
N	Impeller speed (rpm)
n	Number of impellers
n_B	Number of baffles
n_b	Number of blades
Njs	Minimum agitation speed (rpm)

NOMENCLATURE
(Continued)

Njs'	Minimum agitation speed (rps)
P	Power drawn by impeller (watts)
Pjs	Power dissipation at minimum agitation speed (watts)
S	Spacing between impellers (m)
T	Vessel diameter (m)
u_s	Relative vertical velocity between particle and fluid in turbulent region (m/s)
v_l	Liquid fraction based on vessel volume (dimensionless)
Vt	Volume of vessel (m^3)
W_B	Baffle width (m)
W_b	Blade width (m)
X	Weight percentage of solids, 100g/g (wt/wt%)

Dimensionless number

Ar	Archimedes number, $dp^3g\Delta\rho/\nu\rho$ (dimensionless)
Fr	Froude number, N^2D/g (dimensionless)
Npo	Power number, $P/\rho N'^3D^5$ (dimensionless)
Re	Reynolds number, $Njs'D^3\rho_l/\mu$ (dimensionless)
Rem	Modified Reynolds number, $Njs'D^3\rho_l/\mu T$ (dimensionless)
S'	Zwietering correlation parameter (dimensionless)
Z	Baldi *et al.* theoretical model parameter, $dp^{1/6}(g\Delta\rho/\rho_l)^{1/2}/Npo^{1/3}D^{5/3}Njs'$ (dimensionless)

NOMENCLATURE
(Continued)

Impeller Type

CHEM Chemineer HE-3

6FBT Six-blade flat-blade turbine

6FDT Six-blade flat-disk turbine

6FPT Six-blade flat (45°) pitched-blade turbine

Symbols

μ Dynamic viscosity (kg/m-s)

ν Kinematic viscosity (m^2/s)

ρ_l Density of liquid (kg/m^3)

ρ_s Density of solid (kg/m^3)

$\Delta\rho$ Solid-liquid density difference, $\rho_s - \rho_l$ (kg/m^3)

Subscripts

l Liquid phase

s Solid phase

Constants

g Gravitational constant (9.81 m/s^2)

g_c Conversion factor (9.81 $kg\text{-}m/kg_f\text{-}s^2$)

CHAPTER 1

INTRODUCTION

Solid-liquid mixing is one of the most common operations in the chemical process industry. Mechanically agitated vessels are frequently used to bring about adequate solid-liquid contact.

Depending on the application — such a promoting a chemical reaction or mass transfer between the phases, or obtaining a uniform particle concentration in an effluent stream — the suspension can be classified as either complete off-bottom suspension (CBS) or relatively uniform suspension. The former is the most important state for the design of solid-liquid agitation apparatus in which no particle rests on the tank base for longer than one or two seconds. This level of agitation often represents an optimum value for operating conditions relative to the capital investment and operating costs to achieve desired rates of mass transfer and chemical reaction. Until such a condition is reached, the total solid-liquid interfacial area is not completely or efficiently utilized and above this speed, the rate of mass transfer typically increases very slowly. Therefore, any additional energy beyond that required for this minimum agitation or just-suspended speed (Njs), also called critical impeller speed, is not typically useful. Consequently, the knowledge of Njs is very important.

A study of solids suspension in liquid by mechanical agitation includes several basic considerations: vessel dimensions and geometry, impeller type, dimensions and geometry, solids and liquid properties, and solids loading.

The impeller clearance (often expressed in relative terms as the impeller off-bottom clearance to tank diameter ratio, C'/T) significantly influences the minimum agitation or just-suspended speed. Two hydrodynamic regimes can typically be observed depending on the impeller clearance. At high values of this variable, large vortices above and below the impeller are present. At low values, the lower vortices are absent. In the latter case, the minimum agitation is lower. Also, the decrease of the power consumption in this region can be noticeable, since a considerable amount of power dissipated is caused by the vortices below the impeller. The value of the impeller clearance, at which this hydrodynamic change occurs, depends on the impeller type and size.

Because of its practical importance for industrial applications, in this research *the effect of very small impeller clearances off the tank bottom, on the minimum agitation speed and power dissipation, for complete off-bottom suspension, was investigated using different types of impellers*. The specific objectives of this work are:

- Quantify the effect of small off-bottom clearances on the minimum agitation speed and power dissipation at this state;
- Quantify the effect of the impeller diameter, tank diameter, and solids loading at low off-bottom impeller clearances, and examine the effects of scale-up;
- Analyze the effect of the presence of two impellers with the lower impeller being located very near to the tank bottom;
- Extend some of the empirical correlations for solids suspension, available in the literature, to the region very near to the tank bottom, for different types of impellers;
- Produce a mathematical model to correlate the experimental results obtained.

CHAPTER 2

LITERATURE SURVEY

2.1 Effect of Impeller Clearance

Although, solids suspension have been studied extensively, the effect of positioning the impeller very near to the tank bottom has received little attention. The most relevant information about this effect will be presented in this section.

2.1.1 Minimum agitation Speed (Njs) and Power Dissipation (Pjs)

Zwietering (1958) found that for propeller, paddle, and vaned disk turbine the minimum agitation speed (Njs), became smaller as the impeller off-bottom clearance to tank diameter ratio (C'/T), was reduced. For six-blade flat-disk turbines, Njs was found to be independent of C'/T in the range of $1/7 < C'/T < 1/2$.

Zwietering also found from a graphical analysis of his experimental data, that the influence of the impeller off-bottom clearance (C') could not be expressed in a power law form. He considered to be more appropriate to use the ratio C'/T as a constant parameter in his correlation. Chudacek (1986) also expressed doubts on the suitability of the power law form to quantify the clearance effect in the overall range examined.

Kolar (1961) found the six-blade flat-disk turbines to be unsuitable for solids suspension when such an impeller was positioned one-half of the tank diameter above the bottom. Nienow (1968), contrary to Zwietering and Kolar, found that Njs for this impeller decreases with the impeller clearance.

Conti *et al.* (1981) and Chapman *et al.* (1983) also found that the impeller clearance has a significant effect on Njs for disk turbines.

Chudacek (1985) reported that for maximum suspension efficiency, the impeller should be positioned with minimum clearance, as governed either by the settled solids height or by the given tank geometry in all the cases, except for a profiled bottom tank at high concentration (24.4 v/v%) of finer and coarser slurries. In the last case, the optimum clearance was one-third of the tank diameter. However, at this high solids concentration the impeller was essentially embedded in the slurry.

Chudacek (1986) found that 98% complete suspension and complete off-bottom suspension (CBS) are more sensitive to the impeller position than homogeneous suspensions. In most geometries, a reduction in clearance typically lead to a reduction in the impeller speed for complete suspension. Some exceptions were found for cone-and-fillet tank due to bypass of liquid into the suction side of the impeller.

Raghava Rao *et al.* (1988b) found that the value of the critical impeller speed decreases with a decrease in the impeller clearance for all the impellers. However, the extent of reduction is greater for disk turbines and pitched-blade upflow impellers than for pitched-blade dowflown impellers.

Oldshue and Sharma (1992) defined three distinct regions where C'/T has an effect on Njs. Their data suggest that there is a relation between C'/T and D/T in the determination of these regions. Myers *et al.* (1994a) reported that the effect of C'/T is much less than that of D/T, and that the effects of these two geometric parameter are not entirely independent of each other.

Weisman and Efferding (1960) attempted a theoretical analysis of the process based on a kinetic energy balance, in order to show the consistency of their experimental data. Although a firm correlation could not be advanced on the basis of the two T/D ratios studied (2.375 and 2.75), the following tentative equation was suggested:

$$\frac{1.74\ g_c\ Pjs}{g\left(\pi\ T^3/4\right)\ u_1\ \Delta\rho}\sqrt{\frac{v_1}{1-v_1}}\left(\frac{D}{T}\right) = 0.16\ \exp\left(5.3\ C'/T\right) \qquad (2.1)$$

Gray (1987) investigated the effect of the impeller clearance on the power dissipation at the just suspended state (Pjs) in the lower region for flat bottom tanks. Similarly to Myers (1994a), Gray found Pjs to be independent of the impeller size for axial-flow impellers in the range of D/T investigated. He also found an exponential dependence of Pjs on C'/T similar to that obtained by Weisman and Efferding (1960):

$$Pjs \propto \exp\left(a\ C'/T\right) \qquad (2.2)$$

For the "single-eight" regime ($C'/T < 0.35$), it was found that $a = 1.2$, and for the "double-eight" regime ($C'/T > 0.35$), $a = 5.3$ was found. For a 0.102 m radial-flow impeller, Gray found similar values. For the "single-eight" regime ($C'/T < 0.17$), he reported that $a = 1.2$, and for the "double-eight" regime ($C'/T > 0.17$), $a = 5.3$. This last value is in agreement with Weisman and Efferding (1960) who found $a = 5.3$ for flat paddle blade impellers, however, they did not report any observed change in the flow pattern over their range of impeller clearance studied. The dependence of Pjs to the impeller clearance was highly dependent upon the flow pattern observed. For the same flow pattern, the dependence was found to be the same regardless of the type of impeller (radial- or mixed axial-flow) or shape of the tank bottom (flat or round bottom).

2.1.2 Power Number (Npo)

Rushton *et al.* (1950) and Bates *et al.* (1963) reported a general power relationship as a function of physical and geometrical parameters:

$$Npo = K(Re)^n(Fr)^m\left(\frac{T}{D}\right)^t\left(\frac{H}{D}\right)^h\left(\frac{C'}{D}\right)^c\left(\frac{L}{D}\right)^l\left(\frac{W_b}{D}\right)^w\left(\frac{A_p}{D}\right)^p\left(\frac{W_B}{D}\right)^q(n_b)^r(n_B)^s \quad (2.3)$$

This relationship contains three basically different parameters: those defining the boundary conditions and the geometry of the system (T/D, H/D, C'/D, L/D, W_b, A_p, W_B, n_b, n_B); that pertaining to the action of viscosity and gravity (Re); and that which characterizes the general flow pattern (Fr). This full form is seldom used in practical power calculation. For the turbulent region, if geometrical similarity is assumed and if no vortex is present, the Equation (2.3) reduces to:

$$Npo = \left(\frac{P}{\rho N^3 D^5}\right) = \text{constant} \quad (2.4)$$

This dimensionless group of the power number (Npo) represents an important parameter in the design of mixing operation.

O'Okane (1974) demonstrated that it was not possible to find values of the exponents in the generalized power relationship which could be applied to all types of impellers.

Nienow and Miles (1971) pointed out the considerable effect that minor dimensions have on the power number, particularly the disk thickness-to-blade height ratio. As this ratio increases, the friction loss from the inside edge of the blade of the disk turbine would tend to decrease and therefore so would Npo.

Gray *et al.* (1982) proposed a power correlation for six-blade flat-disk turbine. The result was a constant power number of 5.17 representing the data for C'/D > 1.1, and varied with $(C'/D)^{0.29}$ for C'/D < 1.1. The baffling effect was found to be negligible over the range of standard size baffling, $1/12 \leq W/T \leq 1/10$. The effect of D/T was small under these conditions.

Rewatkar *et al.* (1990) found that Npo for the standard disk turbine (D/T = 1/3, C' = D) and pitched-blade turbine was 5.18 and 1.67, respectively. The Npo was observed to have a strong dependence on the flow pattern generated by the impellers. In general, Npo increased for pitched-blade turbine and decreased for disk turbine with a decrease in clearance. However, in practice, Npo decreased when the clearance was more than T/4 because of surface aeration. Without the effect of surface aeration, the liquid height was found to have little effect on power consumption. Rewatkar *et al.* (1990) obtained an overall correlation for the impeller power number for a pitched-blade turbine:

$$Npo = 0.653 \left(T/D \right)^{0.11} (C'/T)^{-0.23} (n_b)^{0.68} (A')^{1.82} \qquad (2.5)$$

for: $6 \leq T/D \leq 3$, W/D = 0.3, H/T = 1, $0.25 \leq C'/T \leq 0.33$, $0.5 \leq A' \leq 1.05$, $4 \leq n_b \leq 8$

Chang (1993) in his master thesis, conducted an extensive study on the effect of the impeller clearance on Npo for four types of impellers: six-blade flat-disk turbines (6FDT), six-blade flat-blade turbines (6FBT), six-blade flat (45°) pitched-blade turbine (6FPT), and six-blade curve-blade turbine. The agitation system was very similar to the present work. He studied over a wide range of impeller clearance, including the "single-eight" and "double-eight" regime. No effect of the D/T (0.264-0.352) and H/T (1-2) ratios was observed.

For the case of the 6FDT, at low impeller clearances ($1/6 < C'/D < 1/3$) a step increase in Npo was observed (from 3.34 to 4.30). This was explained as due to the reduction in the bottom circulation of the disk turbines at low clearances. In the range $1/3 < C'/D < 1$, there was a moderate increase in the power number. The reason for this could be the transition state of flow pattern around in the impeller blades. At $C'/D = 1$, the power number increased to 4.9, while it increased to 5.10 at $C'/D = 2$.

For the case of the 6FBT, Npo moderately decreased with an increase in the impeller clearance between $1/6 < C'/D < 1/2$. Beyond this range, the rate of decrease was lower. Furthermore, for $C/D = 5/6$, Npo reached the minimum value of 2.09.

Similar to the 6FBT, the power number in the 6FPT decreased from $C/D = 1/6$ to $C/D = 2$, values of 1.90 and 1.34 were found, respectively. The higher values of Npo at low impeller clearance was due to the throttling effect of the bottom tank.

2.1.3 Change of Flow Pattern

Conti *et al.* (1981) noted that by lowering C', the hydrodynamic regime changed from one with large vortices above and below the impeller (the so-called double-eight figure) to that where the lower vortices were absent (single-eight). The value of C' at which the change occurred was always equal to about 0.22 T in the various systems examined, this value was practically independent of either Njs or D/T ($0.22 < D/T < 0.37$). The power decrease at $C'/T = 0.22$ was very considerable. The results showed that the dissipated power and the minimum impeller velocity, for complete suspension of the solids, were strongly dependent on the hydrodynamic regime.

Gray (1987) also found that the dependence of the power on the type of impeller was highly dependent upon the pattern observed. For the same flow pattern, the dependence was found to be similar for each type of impeller (radial or axial). The change in the flow pattern was found to be independent of the D/T ratio over the limited range studied. For disk impellers, the pattern change was found to occur at C'/T = 0.22 as found by Conti *et al.* (1981) for eight-blade flat-blade disk turbine agitating in flat bottom tanks. For six-blade flat-blade impellers, the flow pattern changed at C'/T = 0.17, similarly to that observed by Nienow (1968), for six-blade flat-disk impellers. Axial-flow impellers maintained the "single-eight" flow pattern for propellers up to C'/T = 0.35 in a flat bottom tank. Zwietering (1958) observed the "single-eight" flow pattern for propellers up to C'/T = 0.4. Round bottom tanks help to promote the "single-eight" pattern and for this study, the "single-eight" pattern was observed at C'/T values as high as 0.67.

Armenante and Li (1993) noted that for the case of one radial-flow impeller the flow pattern below the impeller was a function of the impeller clearance off the tank bottom. For low C'/T values (corresponding to C'/T < 0.21), the flow pattern was observed to be swirling outwards so that the particle suspension occurred from the periphery of the tank. For high values of C'/T (corresponding to C'/T > 0.26), the swirling action turned inward, and solid suspension occurred from the center of the tank bottom. For intermediate values of C'/T, a transition region consisting of an unstable flow pattern was noticed. The range in which the presence of the transition region occurred (0.21 < C'/T < 0.26) was independent of the presence of additional impellers, at least if the distance between impellers was kept equal to the impeller diameter.

2.2 Effects of Impeller Diameter, Tank Diameter, and Solids Loading

There has been a number of publications dealing with solids-suspension during the past 40 years. Unfortunately, the results obtained on the effect of the impeller diameter(D), tank diameter (T), and solids loading (X) are different and can be confusing.

The exponent on the impeller diameter (constant tank diameter) found in the literature varies between -1.16 (Raghava Rao *et al.*, 1988b, mixed axial-flow impellers) to -2.45 (Zwietering, 1958, radial-flow impellers), depending on the type of impeller and the experimental conditions used. Baldi *et al.* (1978) reported a theoretical value of -1.67, for disk turbines, using Kolmogoroff's theory of isotropic turbulence.

Raghava Rao *et al.* (1988b) presented an explanation on a rational basis, to understand the effect of impeller diameter on the solid suspension for different designs of impellers. For the case of radial-flow impellers, the solids suspension occurs because of the liquid velocity and turbulence. The turbulence intensity decays along the length of the flow path [(T/2) - (D/2) + C']. With an increase in the impeller diameter, less decay in the turbulence will occur and the liquid velocity ($\sim D^{7/6}$) will increase. The overall effect of increased liquid velocity and the lesser decay in turbulence makes the dependence on impeller diameter very strong. For the case of a pitched-blade turbine downflow impeller, the solids suspension occurs mainly because of the liquid flow generated by the impeller. The average liquid velocity is proportional to ND. Therefore, Njs should be inversely proportional to D. In this case, it is obvious that the length of the liquid path will not change appreciably with changes in the impeller diameter, because the liquid flow is downward directly from the impeller.

The dependence of the tank diameter is also expressed in a power form. For the minimum agitation speed reported values of the dependence at constant impeller diameter-to-tank diameter ratio lies between those reported by Baldi *et al.* (1978): -0.5 (C/D = 0.5) to -0.89 (C/D = 1).

Chudacek (1986) reported values between -0.56 to -0.86, depending of the type of impeller, tank bottom shape, and suspension criterion. Raghava Rao *et al.* (1988b) reported an exponent of 0.31 for the case of constant impeller diameter for 6FPT. They also explained on a rational basis the effect of the tank diameter.

Einenkel (1980) reported values of the exponent for the power per unit volume dependence on the tank diameter, scale-up parameter. These values vary between -0.7 to 0.5. For a scale-up factor of 10, these extreme values represent a difference in power per unit volume by a factor of 15.8. Chudacek (1986) investigated the relationship between solids suspension criteria, mechanism of suspension, tank geometry, and this exponent. The results indicated that this scale-up parameter is not constant and depends on the mechanism of suspension.

Values of the exponent in the dependence of the minimum agitation speed on the solids concentration fall into two groups: in the range 0.13 to 0.18 for low and moderately concentrated suspensions, and zero for highly concentrated suspensions. (Chudacek, 1986). The reason for the discrepancy at lower concentration can be explained from the statistical chance factor involved. The probability, for the suspension of the solids is less, for lower concentrations, and is higher for higher concentrations. This probability factor must be a function of solids concentration (Narayanan *et al.*, 1969).

2.3 Effects of Other Variables

Liquid level exhibits a negligible effect on the minimum agitation speed (Zwietering, 1958), and on the power requirements (Weisman and Efferding, 1960), unless impeller placement is such that the flow pattern is significantly affected by phenomena such as air entrainment (Myers *et al.*, 1994a).

Installing baffles destroys the vortices and promotes a flow pattern conductive to good mixing (Oldshue, 1983). The standard baffles, four vertical baffles (1/12 to 1/10 the tank diameter in width), provide conditions which are conductive to top-to-bottom turnover, and the elimination of vortices. Based on the suspended slurry height, Weisman and Efferding (1960) recommended to set the baffle off-bottom clearance one-half of the impeller diameter (BC = 0.5 D), for six-blade paddle impellers. Myers and Fasano (1992) suggested that all highly tangential flow impellers would particularly benefit setting the baffle off-bottom clearance, one-fourth to one-half of the baffle width. The change in baffle design would have a negligible effect on power draw characteristics.

Increasing the number of blades produces an increase in efficiency. Chapman *et al.* (1983) reported that increasing the number of blades from four to six on an mixed flow impeller pumping down (D/T = 0.25), slightly lowered the power (~ 13%) and speed (~ 9%) to just suspend a 1% concentration of soda glass ballotini.

Raghava Rao *et al.* (1988b) studied the effects of blade width and thickness, for pitched-blade downflow turbines. For the blade width, they found a minimum value of Njs at 0.35 D. The value of Njs slightly decreased with an increase in the blade thickness; while keeping the other design parameter constant the power increased.

Inclination of blades also plays an important role in solids suspension. For a blade inclination angle (α) of 30°, the radial flow rate may be considered insignificant. For a blade inclination of 45°, however, radial volumetric flow rate becomes significant (Musil *et al.*, 1984).

The effect of the particle size (dp) on the minimum agitation speed seems to depend of the hydraulic regime and the range of the particle size. The value of the exponent on the particle size lies between the theoretical values of 0.66 for laminar settling of particle and 0.16 for turbulent settling (Chudacek, 1986). Myers *et al.* (1994b), for all the data in the range examined (85-19100 μm), found an exponent of 0.20 similar to that of Zwietering (1958).

Myers *et al.* (1994b), similarly to Zwietering, also found that for mixed axial-flow and axial-flow impellers, the dependence on the dimensionless density was :

$$Njs \propto (\Delta\rho / \rho_l)^{0.45} \qquad (2.6)$$

The dimensionless density was varied over three-hundred fold, from 0.0060 to 1.91. This dependence seems to be the most accepted. Nienow (1968) reported an exponent of 0.43, and Narayanan *et al.* (1969) an exponent of 0.5.

The experiments in the turbulent region confirm the negligible effect of viscous forces. The dependence of the minimum agitation speed on the viscosity (ν) is reported as exponents in the range of 0.1-0.2.

The exponents of the variables: liquid viscosity, solids-liquid density difference, particle size, and solids concentration have been found to be independent of impeller clearance (Zwietering, 1958; Raghava Rao *et al.*, 1988b).

2.4 Mechanisms of Suspension

A comparison of the suspension ability on the basis of suspension mechanism has been reported in the literature. For the case of the radial impellers, the suspension is attributed to random turbulent bursts (Baldi *et al.*, 1978, Chapman *et al.*, 1983). Raghava Rao *et al.* (1988b) state that a decrease in clearance results in the decrease of the path length; this decrease causes a dual effect: decay of turbulence along the flow pattern reduces and the liquid velocity is increased. Open impeller types (without the disk) do not normally pump in a truly radial direction, since there is a pressure difference between each side of the impeller. They tend to pump upward or downward while discharging radially (Oldshue, 1983). Because of the more uniform radial flow pattern, disk impellers tend to draw more power than open impellers, which affect the economy of their application.

Since the axially discharging impellers are more efficient than radially discharging impellers, producing higher flow but lower turbulence intensity, Chudacek (1985) speculated that the flow and not the shear rate controls the suspension of solids for this type of impeller. An alternative explanation might be that the path length between the impeller and the point from which particles are last suspended is less for an axial-flow impeller, reducing the probability of the turbulent eddies decaying (Chapman *et al.*, 1983). This type of impellers produces a flow that leaves the impeller tip, hits the vessel, scours the bottom, and lifts the particles from the periphery. At very low impeller clearance, the impeller stream hits the vessel bottom with higher velocity causing a sharp change in flow direction, which dissipates more energy, increasing the power consumption and power number (Raghava Rao and Joshi, 1988a).

2.5 Effect of Multiple Impellers

Very little effort has been directed towards understanding the effect of multiple impellers on solid-liquid agitation. Weisman and Efferding (1960) attempted to study the effect of two impellers, and recently Armenante *et al.* (1992) and Armenante and Li (1993) conducted experiments to study the effect of two and three radial-flow impellers. They found that in many situations the presence of multiple impellers reduced the minimum agitation speed requirement to produce the just suspended state, but the power consumption required for this purpose was significantly higher than that measured for single impellers.

Armenante *et al.* (1992) found that the dependence of Njs on the impeller diameter does not change too significantly with the number of impellers mounted on the shaft. However, the clearance of the lowest impeller off the tank bottom plays a major role. Later, Armenante and Li (1993) found that the region in which the change of flow pattern occurred is not influenced by the presence of multiple impellers. They also observed that a near linear relationship exists between Njs and the ratio C'/D (constant T), for the case in which one impeller is used. However, the same does not apply when two impellers were present. The lower impeller consumes slightly less power than the top one, but this difference disappeared as C'/D increased. Njs was only a weak function of the spacing between the impellers. The results obtained led to the following conclusions:

- The impeller closer to the bottom is primarily responsible for generating a suspension.
- The presence of additional impellers may result in a flow pattern interfering with the primary low pattern of a single impeller, thus demanding higher agitation requirements.

CHAPTER 3

CORRELATIONS AND THEORIES AVAILABLE

3.1 Zwietering (1958) Correlation

The pioneering work of Zwietering (1958) still represents the most complete investigation of the minimum agitation speed (Oldshue, 1983; Chapman *et al.*, 1983; Nienow, 1985; Janson and Theliander, 1994), for the complete off-bottom suspension criterion (CBS, or 1-2 seconds criterion), in terms of both the variety and range of variables studied. He investigated the marine propellers, paddles, and turbine impellers in flat, dished (radius = vessel diameter), and conical (120°) bottom tank, fully baffled. He completed over a thousand experiments and analyzed the results using dimensional analysis to yield a purely empirical expression for Njs (standard deviation = ±10%):

$$Njs = \frac{S' \nu^{0.1} dp^{0.2} \left(g\Delta\rho/\rho_l\right)^{0.45} X^{0.13}}{D^{0.85}} \qquad (3.1)$$

for: T = 0.15-0.6 m, H = T, D = 0.06-0.224 m, $\Delta\rho$ = 560-1810 kg-m^{-3}, dp = 125-850 μm, X = 0.5-20 wt/wt%, ν = 0.39-11.1.3x10^{-6} m^2/s.

In this equation S' is a dimensional constant which is presented in graphs of S' against D/T and C'/T as parameters for each type of impeller.

The above expression is the most widely recommended basis for design. Later studies often followed Zwietering's approach, typically presenting the results in the form of dimensionless correlations. Some authors extended the Zwietering correlation in terms of the range of variables or impeller type.

Nienow (1968) extended the range covered for the density difference, particle size, and concentration, for the disk turbines. Chapman *et al.* (1983) used two criteria (CBS and concentration measurements near the base) to investigate the effects of particles and liquid properties, tank diameters, and impeller type (radial and mixed-flow).

Chudacek (1985) analyzed phenomenologically in detail the solids suspension in the classical flat bottom tank. A fully profiled bottom and a "cone and fillet" bottom tanks were used as alternatives geometries. Chudacek (1986) made an extensive experimental work showing the relationship between solids suspension criteria, mechanism of suspension, tank geometry, and scale-up parameters.

Raghava Rao *et al.* (1988b) studied systematically the critical impeller speed for solid suspension using pitched-blade turbines. They extended the number of variables investigated by including the effect of blade width and blade thickness. Myers *et al.* (1992) using an innovative video technique investigated the influence of baffle off-bottom clearance on the solids suspension of pitched-blade and high efficiency impellers. Later, Myers *et al.* (1994b) studied the influence of solid properties on the just suspended agitation requirements of the above impellers. The general trends found in these studies confirmed the results obtained by Zwietering and the validity of his correlation.

None of these published correlations predicts the effect of impeller position from the tank bottom. Only recently, Aravinth *et al.* (1996) proposed a new correlation for 6FBT, in which the power form was used to quantify the effect of the impeller clearance. However, the maximum deviation between experiments and the regression curve was 19.2%.

3.2 Baldi *et al.* (1978) Theoretical Model

Published suspension theories can be divided into six groups according to the presumed suspension mechanism (Rieger and Ditl, 1992):

1. The first group is composed of those theories based on the balance between energy dissipated by the settling particles and the energy dissipated in the fluid by the agitator. The theories presented by Kolar (1961) and by Musil and Vlk (1978) were based on this hypothesis. However, these models are based on an energy balance which is not complete and assumed that the agitation tank is hydrodynamically homogeneous (Chudacek, 1986). They also assumed that all power is consumed only for solids suspension (for suspension of low concentration, this assumption is not satisfied). Not all of the energy terms can be satisfactorily described at present and, even if they could, their solution would be fairly complex. The energy balance model would therefore appear to have only a slim chance of success.
2. Another group is composed of those theories based on the presumption that the energy needed to suspend the particle from the bottom is proportional to that of turbulent vortices. This group involves the theories presented by Baldi *et al.* (1978).
3. The third group is composed of theories based on a balance between the upward fluid velocity and the particle's settling velocity. Narayanan *et al.* (1969) assumed that the velocity of ascendant fluid to be equal to the mean fluid velocity, whereas Wichterle (1988) assumed that the ratio of the velocity within the boundary layer and the settling velocity of the particles is constant (simplified momentum balance). However, Janson and Theliander (1994) showed that this ratio is not a constant.

4. The fourth group includes the paper published by Molerus and Latzel (1987a). Their theory concerning the suspension of fine particles (Ar < 40) also rests on the boundary layer theory, mainly on the balance between the force of a fluid affecting the particles and the gravity force reduced in buoyancy.
5. The fifth group consists of theories based on the presumption that the agitator must overcome the pressure difference caused by the differences in particle concentrations in upward and downward flow. The theory of Molerus and Latzel (1987b) for large particles (Ar > 40) are based on this presumption.
6. Rieger and Ditl (1992) also report a theory presented for relatively large particle forms. This theory balances the potential energy necessary to achieve suspension with the kinetic energy of fluid flow being discharged from the agitator.

Perhaps the most successful attempt to model solids suspension is due to Baldi *et al.* (Chapman *et al.*, 1983; Nienow, 1985; Rieger and Ditl, 1992). However, since it is linked to mean energy dissipation rates and Kolmogoroff's theory of isotropic turbulence, it is somewhat less realistic from the fluid mechanics point of view (Nienow, 1985). They assumed that the particles being suspended are picked up by turbulent eddies of a critical size. In general, these eddies are much larger than the Kolmogoroff scale of turbulence. This size would be of the order of the particle size because smaller ones would be insufficiently energetic to achieve suspension; and the low frequencies of arrival of larger eddies would reduce their chance of achieving it. An energy balance could then be performed on the basis that the kinetic energy imparted by the eddies was proportional to the potential energy gained by the particle.

This energy balance led to the specification of a dimensionless group (Z), which was related to the ratio of the energy dissipated on the tank base ($[e_T]_B$), responsible for suspension, to the average energy dissipation in the tank (e_T), i.e., for cylindrical vessels of liquid height equal to the tank diameter:

$$Z = \frac{dp^{1/6} T (g\Delta\rho/\rho_l)^{1/2}}{Npo^{1/3} D^{5/3} Njs} \tag{3.2}$$

If $[e_T]_B$ is proportional to e_T, then it implies that Z is a constant. However, Baldi *et al.* also considered that $[e_T]_B/e_T$ ratio actually depends on the fluid properties especially viscosity and on the impeller size, position, and type. Therefore:

$$Z = f\,(Rem,\ T/D,\ C/D,\ \text{impeller type}) \tag{3.3}$$

where, by analogy with the decay of turbulence downstream from a grid so that:

$$Re\,m = \frac{D^3 Njs}{\nu T} \tag{3.4}$$

Experimental data obtained with eight-blade flat-disk turbine, at constant C'/D and independently from the ratio D/T, showed Z to follow the relation:

$$Z \propto Rem^n \tag{3.5}$$

The dependence of Njs on solids loading (X), was not accounted for in the model, but was obtained empirically from experiments ($Z \propto X^{-m}$), and agreed very close with Zwietering's relationship. Nevertheless, assuming that the above relationship is known, an expression for Njs can be deduced from their work:

$$Njs \propto \frac{\nu^{n/(n+1)} (g\Delta\rho/\rho_l)^{1/(2n+1)} dp^{1/(6n+6)} T X^{m/(n+1)}}{D^{(5+9n)/(3n+3)} Npo^{1/(3n+3)}} \tag{3.6}$$

Two examples of their results were presented by Chapman *et al.* (1983):

(a) For an eight-blade flat-disk turbine, C'/D = 0.5:

$$Z = \text{constant} \approx 2 \tag{3.7}$$

so that:

$$Njs = \frac{1.03\left(g\Delta\rho/\rho_l\right)^{1/2} dp^{1/6} TX^{0.134}}{D^{0.85} Npo^{1/3}} \tag{3.8}$$

(b) For an eight-blade flat-disk turbine, C'/D = 1:

$$Z \propto Rem^{0.2} \tag{3.9}$$

so that:

$$Njs \propto \frac{\nu^{0.17}\left(g\Delta\rho/\rho_l\right)^{0.14} dp^{0.14}\left(T/D\right)X^{0.11}}{D^{0.89} Npo^{0.28}} \tag{3.10}$$

Thus, the model suggests that the exponents on the various exponents vary slightly with geometry, but they are nonetheless still very close to those proposed by Zwietering (1958). Chapman *et al.* (1983) showed that this approach works well for disk turbines, confirming the experimental results of Baldi *et al.* However, it was less successful for other geometries.

This model indicates much more the significance of the particle and fluid physical properties (Nienow, 1985). However, this approach has its limitations: the energy is not dissipated uniformly throughout the vessel and there is no satisfactory knowledge of the dissipation intensity very near to the bottom. Moreover, the validity of Kolmogoroff's theory in a mechanically agitated vessel is still questionable (Wichterle, 1988).

3.3 Conti *et al.* (1981) Correlation

Extending the theoretical model of Baldi *et al.*, Conti *et al.* (1981) proposed empirical correlations for eight-blade flat-disk impellers in which the dimensionless grouping Z, was found to increase in value linearly with increasing impeller clearance. Two correlations were given dependent upon the flow pattern observed.

Following the approach of Baldi *et al.*, the experimental results by Conti *et al.* were interpreted on the basis of the dimensionless numbers Z, Rem, Npo, C/D, T/D, and X. When all the other parameters were constant, they found that the relation between Z and X could be expressed as:

$$Z\, X^{0.134} \propto \text{constant} \tag{3.11}$$

Further, $Z\, X^{0.134}$ was found to be independent of D. Hence they proposed the following relation:

$$Z\, X^{0.134} = f(\text{Rem}*\text{Npo}, C'/T) \tag{3.12}$$

Using the experimental values for Njs and Npo, they found that the following expression gave the best correlation:

$$Z\, X^{0.134} = a\,(\text{Rem}*\text{Npo}) + b \tag{3.13}$$

where: for $C'/T < 0.22$ (Npo = 5.5):

$$\begin{aligned} a &= 2.08\text{E-}5 - 6\text{E-}5\ C'/T \\ b &= 0.575 - 1.25\ C'/T \end{aligned} \tag{3.14}$$

and for $C'/T > 0.22$ (Npo = 8):

$$\begin{aligned} a &= 1.70\text{E-}5 - 4.55\text{E-}5\ C'/T \\ b &= 0.21 \end{aligned} \tag{3.15}$$

CHAPTER 4

EXPERIMENTAL EQUIPMENT AND PROCEDURE

4.1 Experimental Set-Up

The experimental set-up is shown in Figure 1. The solids suspension experiments were carried out in open, flat bottomed, cylindrical vessels. Four tank sizes were used: 0.188 m, 0.244 m, 0.292 m, and 0.584 m. The material of construction of these tanks was Plexiglass. All the tanks were equipped with four baffles of standard width and equally spaced. Since the main aim was to analyze the effect of the impeller clearance very near to the tank bottom, the baffles were extended until the bottom. The vessels were located on a tank support system that could be moved vertically so as to change the distance between the (fixed) shaft with the impellers mounted on it and the tank bottom. Table 1 gives the details of the vessel dimensions.

Table 1 Dimensions of Vessels

Vessel Diameter T (m)	**Liquid Height H (m)**	**H/T**	**Bottom Shape**	**Baffle Number n_B**	**Baffle Width W_B**	**Material of Construction**
0.188	0.188	1	Flat	4	T/10	Plexiglass
0.244	0.244	1	Flat	4	T/10	Plexiglass
0.292	0.292	1	Flat	4	T/10	Plexiglass
0.584	0.584	1	Flat	4	T/10	Plexiglass

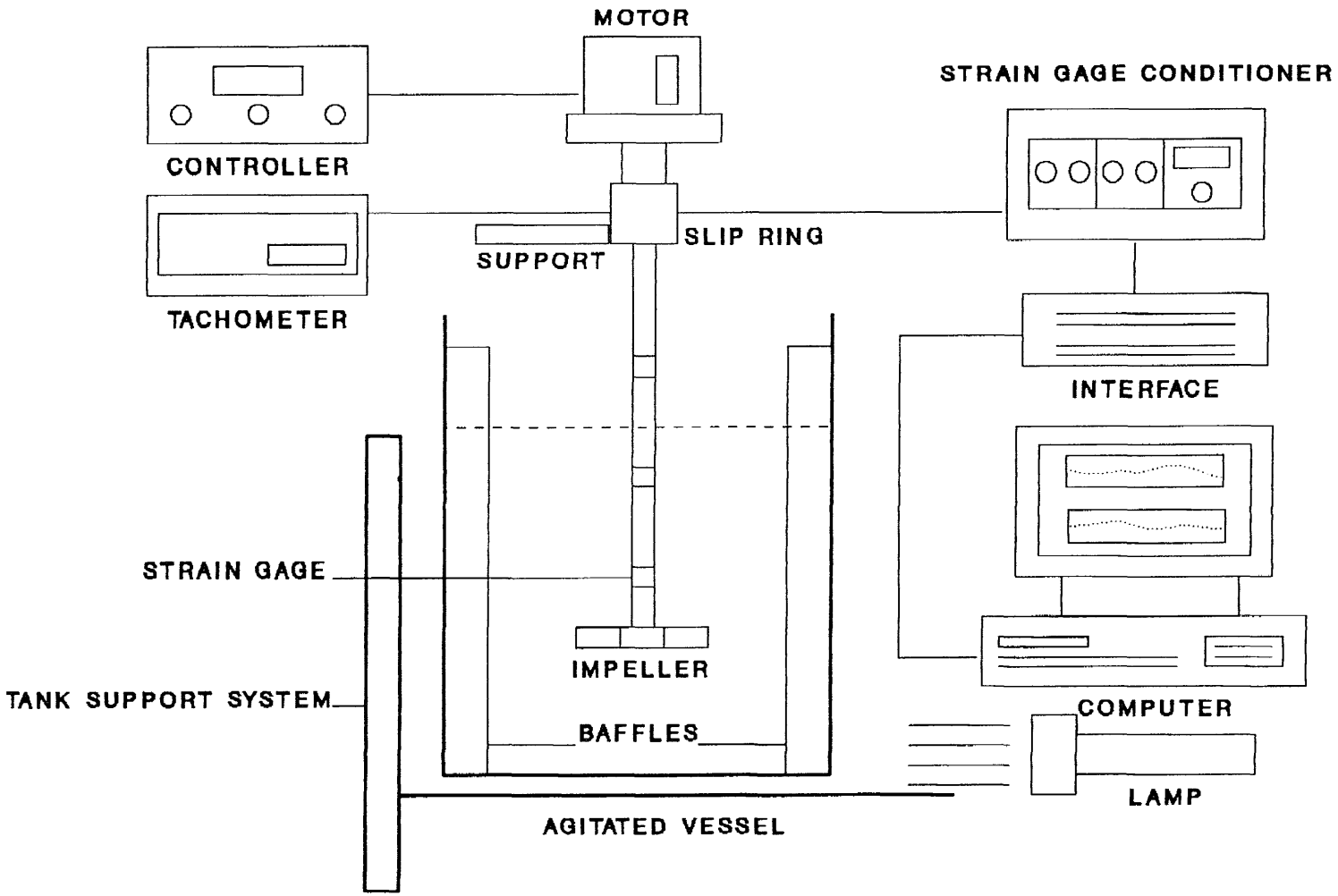

Figure 1 Experimental Set-Up

The tanks were filled with tap water up to a liquid height equal to the tank diameter. The air bubbles were eliminated by agitating the water and cleaning inside the wall of the tanks. The temperature was measured in each experimental run, the average value being 22±0.5 °C. The solid phase was made of glass beads (Superbrite, 110-5005), having a particle size of 110 μm, and density of 2500 kg/m^3. A concentration of 0.5 wt/wt% was used in the majority of the experiments. Additionally, the effect of the solids loading was studied using 1.0 and 1.5 wt/wt% of concentration in the 0.292 m tank, for each type of impeller (0.102 m impeller size). The solid and liquid phases were changed frequently to maintain them "clean", at least after three experimental runs.

Four types of impellers were investigated, namely, six-blade flat-disk turbine (6FDT), six-blade flat-blade turbine (6FBT), six-blade flat (45°) pitched-blade turbine (6FPT), and the high efficiency impeller Chemineer HE-3 (CHEM). For the radial-flow impellers (6FDT and 6FBT) and the mixed axial-flow impeller (6FPT), four sizes were used: 0.0635 m, 0.0762 m, 0.102 m, and 0.203 m. For the axial-flow impeller (CHEM), five sizes were used: 0.102 m, 0.114 m, 0.178 m, 0.203 m, and 0.229 m. All the impellers present standard design, except for the 0.0635 m 6FPT impeller. This impeller was made from a 0.0762 m 6FPT impeller by reducing the length of the blades. The dimensions of the impellers used in the tank of 0.188 m, 0.244 m, and 0.292 m diameter are shown in Table 2(a), and those used only in the tank of 0.584 m are shown in Table 2(b). Figure 2 shows schematically the geometry of the impellers. From the tables, it can be observed that strict geometrical similarity could be kept only for the major dimensions due to the techniques of manufacture. Some minor dimensions change can be noticed.

Table 2(a) Impeller Types and Dimensions
T = 0.188 m, 0.244 m, and 0.292 m

Impeller Type	Blade Number n_b	D (m)	L (m)	W_b (m)	k (mm)	A
Six-Blade Flat- Disk Turbine						
6FDT	6	0.0635	D/4	D/5	1.6	-
6FDT	6	0.0762	D/4	D/5	1.6	-
6FDT	6	0.102	D/4	D/5	2.0	-
Six-Blade Flat-Blade Turbine						
6FBT	6	0.0635	0.021	D/8	1.6	-
6FBT	6	0.0762	0.027	D/8	1.6	-
6FBT	6	0.102	0.038	D/8	2.0	-
Six-Blade Flat (45°) Pitched-Blade Turbine						
6FPT	6	0.0635	0.021	0.01	1.6	45°
6FPT	6	0.0762	0.027	D/8	1.6	45°
6FPT	6	0.102	0.038	D/8	2.0	45°
Chemineer (HE-3) Impeller						
CHEM	3	0.102	0.038	0.015	1.6	-
CHEM	3	0.114	0.044	0.018	1.6	-

D = Impeller diameter, L = Length of blade, W_b = Width of blade, k = Disk and blade thickness, A = Angle of blade

Table 2(b) Impeller Types and Dimensions
T = 0.584 m

Impeller Type	Blade Number n_b	D (m)	L (m)	W_b (m)	k (mm)	A
6FDT	6	0.203	D/4	D/5	3	-
6FBT	6	0.203	0.088	D/8	3	-
6FPT	6	0.203	0.083	D/8	3	45°
CHEM	3	0.178	0.075	0.027	1.6	-
CHEM	3	0.203	0.088	0.030	1.6	-
CHEM	3	0.229	0.100	0.036	1.6	-

D = Impeller diameter, L = Length of blade, W_b = Width of blade, k = Disk and blade thickness, A = Angle of blade

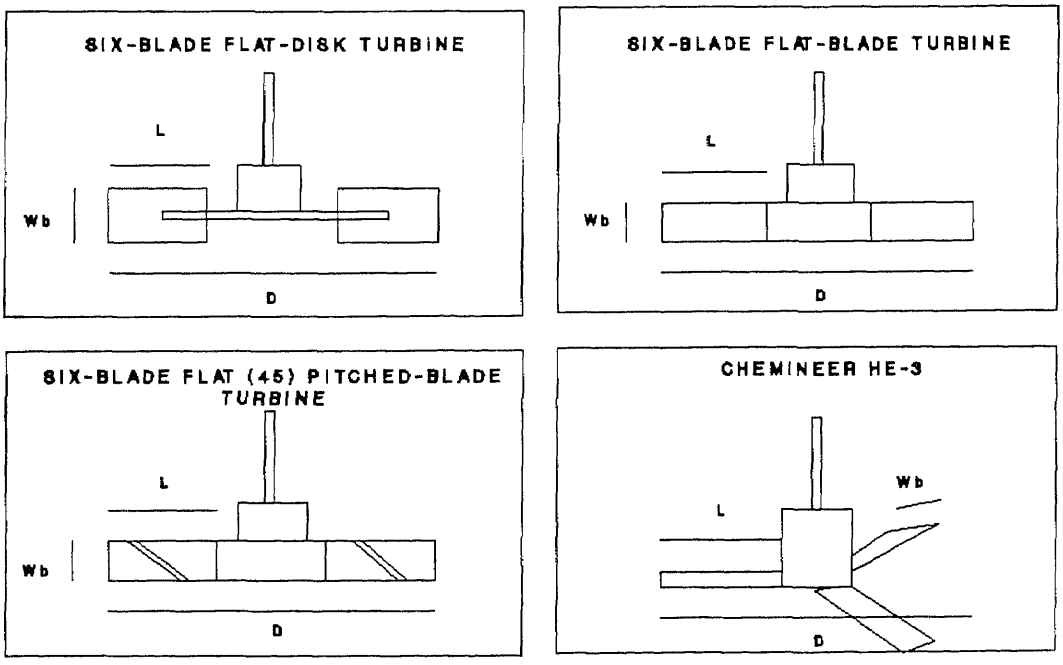

Figure 2 Impeller Geometry

The rotational speed was measured with an optical tachometer with a light sensor (Cole Parmer Instrument Co.), accurate within ±1 rpm. The power was provided to the impeller by a 2.0 HP variable speed motor (G. K. Heller Corp.) with a maximum speed of 1,800 rpm, which rotated a centrally mounted hollow aluminum shaft (length of 83.8 cm). To avoid lateral motion, the stationary slip ring was supported by a metal frame.

The hollow shaft was equipped with strain gages (Measurements Group Co., Raleigh, NC, CEA-06-187UV-350), which allowed the use of one or multiple impellers (up to three). Metal collars having a length of 2.54 cm, an internal diameter equals to O.D. of the shaft and an external diameter equal to the bore diameter of the impellers were mounted onto the shaft. These collars could be moved along the shaft between two strain gages. The arrangement allows the impellers to be mounted on the shaft without touching the protruding strain gages, and enabled the impeller collar assemblies to be moved along the shaft, thus permitting to vary the distances between them. A sketch of the agitation vessel is shown in Figure 3. The system is very similar to those used by Armenante *et al.* (1992), Chang (1993) and Armenante and Li (1993).

The strain gages were connected to a slip ring assembly (Electronics Co., Bayonne, NJ) with insulated lead wires passing through the hollow core of the shaft. The gage signal was picked-up by an external gage conditioner and amplifier system (2120A system, Measurement Group, Co.). A data acquisition system (Labtech Notebook, Version # 6.3.0, 1991) installed in a computer was used to analyze the gage signal (mV) from the conditioner, receive the signal from the tachometer, and calculate the power drawn by each impeller from the product of angular velocity and torque.

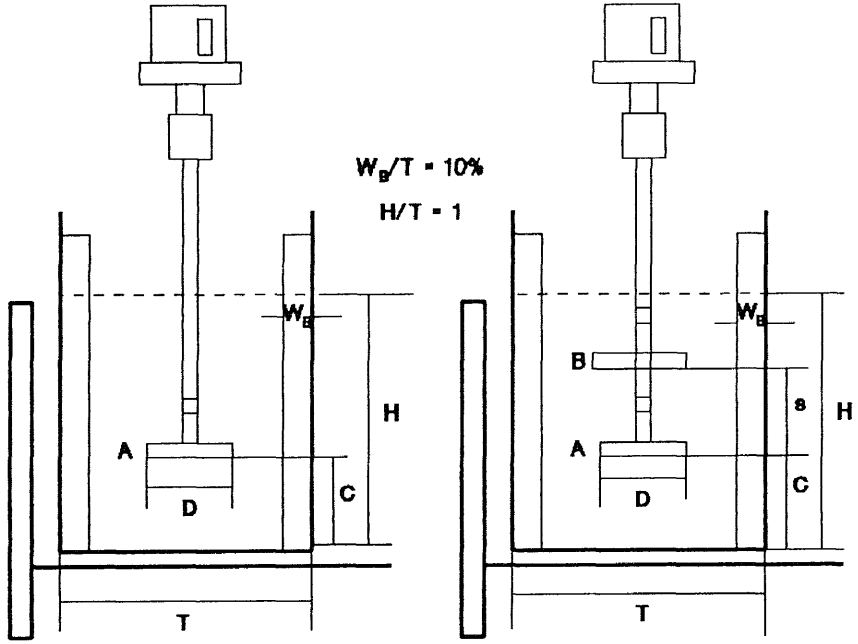

Figure 3 Sketch of Agitated Vessels

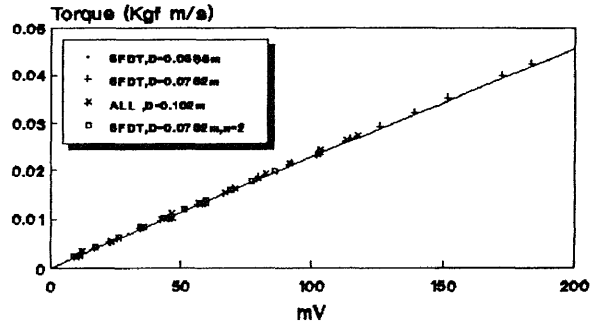

Figure 4(a) Calibration Curves for Strain Gages (T=0.188-0.292 m)

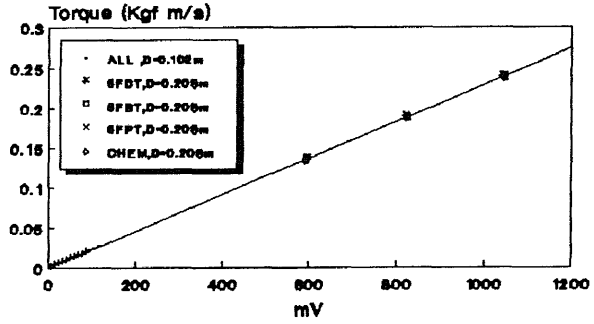

Figure 4(b) Calibration Curves for Strain Gages (T=0.584 m)

The sampling frequency of the data acquisition was 30 times/60 seconds and the representative power drawn was determined by calculating the average of 30 readings. When two impellers were used, the upper strain gage gave the torque associated with the two of them. Thus the power consumption of each impeller could be calculated. The corresponding Npo was calculated using the Equation 2.4 (Rushton expression).

Before using each impeller type or size, the system was calibrated for torsional measurements under static conditions. The shaft was placed horizontally, supported by two strands. An impeller was mounted on the shaft, closed to each strain gage and a known weight (50g to 800g) was suspended from the edge of impeller blade so as to create a torque of known intensity, similar to those obtained in the experiments. The torque was measured by the strain gage conditioner which gave a reading in mV. The signals from the strain gages (in mV) were sent to the same data acquisition system used in the actual experiments. Torque-mV calibration curves were constructed (12 to 16 points), the slope or proportionality constant (K) was calculated by linear regression. Examples of calibration curves for the strain gages are given in Figure 4. The reproducibility of the results for the proportionality factors K's, was within ±3.48% and ±2.63% in the first and second set of experiments, respectively, and ±3.24% and ±3.72 for each strain gage in the third set of experiments.

The distance between the impeller and the strain gage, did not affect the value of the proportionality factor, K. This was experimentally shown by Chang (1993) and confirmed in this work by measuring the response of the strain gage # 2, when using only one impeller and comparing the results with those of the calibration curve.

4.2 Experimental Procedure

In the first set of experiments, solids suspension experiments were carried out in the 0.292 m and 0.584 m tanks. In the first of these tanks, three types of impellers, each one having three possible sizes (0.0632 m, 0.0762 m, and 0.102 m) were used: six-blade flat-disk turbine (6FDT), six-blade flat-blade turbine (6FBT), and six-blade flat (45°) pitched-blade turbine (6FPT). Also the Chemineer HE-3 impeller (CHEM) was used. In the 0.584 m tank three sizes (0.178 m, 0.203 m, and 0.229 m) of the CHEM were investigated. In all cases, the concentration of the solid phase was 0.5 wt/wt%.

The impeller clearance, C, as measured from the lowest part of the impeller to the tank bottom, was varied in the range $1/48 \leq C/T \leq 1/4$. This definition of the impeller clearance was used to yield correlations that could be the extrapolated to $C/T = 0$. The usual definition of the impeller clearance, C', as measured from the impeller centerline to the tank bottom , was also used in this work in the range $1/24 \leq C'/T \leq 1/4$. In the tank of 0.292 m, values for the C'/D ratio of 1/2, 1/4, and 1/5 were also used.

The upper limit in the range of the impeller clearances was defined by the point at which a change in the flow pattern occurred. The lower limit was set by the settled solids bed height. To define the upper limit the impeller clearance was increased until the change of flow pattern was observed. In the "single-eight" regime, the last particles are suspended from around the periphery. On the other hand, in the "double-eight" regime, the last particles are suspended from annulus around the center of the tank bottom, particularly at the four points in line with the baffles. Between these regimes, a transition region is present, in which the flow is unstable, switching from one regime to the other.

Each run always began at low agitation speed. At each agitation speed, the system was allowed to reach the steady state (~ 10 min.). The speed was increased after each observation until the point of complete off-bottom suspension was reached.

At a particular speed, some solids are suspended from the tank bottom after moving vigorously. Increasing the speed the amount of solids suspended increases. When a particular impeller speed is reached, all the particles move vigorously on the tank bottom before being suspended. However, they momentarily stop for a while (which is prominent enough to be noticed) before becoming suspending. With a slight increase in the impeller speed, this momentarily stoppage of solid particles is eliminated. A similar observation was described by Raghava Rao *et al.* (1988b). The position of the suspension of the last particles depends on the impeller off-bottom clearance as mentioned before.

The complete off-bottom criterion used in the determination of the minimum agitation speed, was those defined by Zwietering (1958), as the speed at which no particle was visually observed at rest on the tank bottom for more than one or two seconds. A mirror placed at 45° under the tank was used for the visual observation. A lamp of 150 watts was used to illuminate laterally the tank bottom.

For some experimental runs, the solids suspension for one value of the impeller clearance was repeated (ten times), either by decreasing or increasing the agitation speed. The reproducibility of Njs was less than ±4.22%. While keeping Njs constant, the measurement of the power dissipation was also repeated. The reproducibility of the power dissipation was approximately ±6.18%, although occasionally within ±12.79% for gage signal readings less than 10 mV (accuracy within ±1 mV).

The power number (Npo) was calculated using the Equation (2.4), and the experimental values of Njs and Pjs obtained in the solids suspension. For each value of impeller off-bottom clearance used, Npo was also calculated using water only (without solids), at different Reynolds numbers. In this case, the power number was calculated by taking the average of the values measured at two different speeds (out of the range of Njs). The objective in this calculation was twofold. First, the value obtained in the solids suspension was compared with the value obtained using water only. Second, for the case of using water only, the relation of the power and the agitation speed was also calculated. Table 3 gives the rotational speeds (N) and the range of Reynolds number (Re) used in the experimental determination of the power number (Npo) using water only.

Table 3 Experimental Determination of the Power Number (Npo) Using Water Only

Impeller Type	**D (m)**	**N (rpm)**	**Re**
6FDT, 6FBT, 6FPT	0.0635	500-600	$3.4x10^4$-$4.0x10^4$
6FDT, 6FBT, 6FPT	0.0762	400-500	$3.9x10^4$-$4.8x10^4$
6FDT, 6FBT, 6FPT	0.102	300-400	$5.2x10^4$-$6.9x10^4$
CHEM	0.102	500-600	8.710^4-$10.4x10^4$
CHEM	0.114	400-500	$8.7x10^4$-$10.9x10^4$
CHEM	0.178-0.229	200-300	$10.6x10^4$-$26.2x10^3$
ALL	0.203	200-300	$13.7x10^4$-$20.6x10^3$

In the second set of experiments, the effects of the tank diameter and solids loading were investigated. The effect of the tank diameter was studied in two ways. First, the D/T ratio was kept constant (D/T = 0.348). For the 6FDT, 6FBT, and 6FPT, the 0.0635m, 0.102 m, and 0.203 m impeller sizes were used in the tanks having a diameter of 0.188 m, 0.292 m, and 0.584 m, respectively. In this case, the conclusions drawn are applicable for both constant C/T and constant C'/T. Additionally, experiments were conducted in which the impeller diameter (D = 0.0762 m) was kept constant in the 0.188 m, 0.244 m, and 0.292 m diameter tanks. The conclusions drawn in this case are only applicable for constant C/T .

The effect of the solids loading was investigated in the 0.292 m diameter tank, and using different types of impellers all having a 0.102 m diameter. Three values of concentration were used: 0.5%, 1.0%, and 1.5%. Similarly to the first case of the effect of tank diameter the results are applicable to both constant C/T and constant C'/T.

In the third set of experiments, the effect of the presence of two impellers was investigated. The lower impeller was always positioned very close to the tank bottom. The comparison with the case of using one impeller was performed positioning the lower impeller of the dual-impeller system at the same impeller off-bottom clearance. This set of experiments was carried out in the 0.292 m tank, using two 0.0762 m impellers of the same type. The impellers were two 6FDTs, two 6FBTs, or two 6FPTs.

Table 4 summarizes the sets of experimental runs carried out in this work. In each set the tank size, the impeller type and size, the range of C/T, and the values of C'/T and C'/D used are shown.

Table 4 Experimental Sets

T (m)	Impeller Type	D (m)	C/T	C'/T	C'/D
FIRST SET OF EXPERIMENTAL RUNS					
0.292 X = 0.5%	6FDT,6FBT,6FPT	0.0635	1/4-1/48	1/5[+],1/8,1/16,1/24	1/2,1/4,1/5
	6FDT,6FBT,6FPT	0.0762	1/4-1/48	1/5[+],1/8,1/16,1/24	1/2,1/4,1/5
	6FDT,6FBT,6FPT	0.102	1/4-1/48	1/5[+],1/8,1/16,1/24	1/2,1/4,1/5
	CHEM	0.102	1/4-1/48	1/4-1/48	-
	CHEM	0.114	1/4-1/48	1/4-1/48	-
0.584 X = 0.5%	CHEM	0.178	1/4-1/48	1/4-1/48	1/2,1/4,1/5
	CHEM	0.203	1/4-1/48	1/4-1/48	1/2,1/4,1/5
	CHEM	0.229	1/4-1/48	1/4-1/48	1/2,1/4,1/5
SECOND SET OF EXPERIMENTAL RUNS					
0.188 X = 0.5%	6FDT,6FBT	0.0635	1/8,1/16,1/24,1/48	-	-
	6FDT,6FBT,6FPT	0.0762	1/8,1/16,1/24,1/48	-	-
0.244 X = 0.5%	6FDT,6FBT,6FPT	0.0762	1/8,1/16,1/24,1/48	-	-
0.292 X = ALL	ALL	0.102	1/8,1/16,1/24,1/48	-	-
0.584 X = 0.5%	ALL	0.203	1/8,1/16,1/24,1/48	-	-
*THIRD SET OF EXPERIMENTAL RUNS**					
0.292 X = 0.5%	6FDT,6FBT,6FPT	0.102	1/8,1/16,1/24,1/48	-	-

[+] Only for 6FBT and 6FPT

* Two impellers of the same type were used in each experiment

CHAPTER 5

RESULTS AND DISCUSSION

5.1 Effect of Impeller Clearance

In the first set of experiments, the effect of the impeller clearance (including very small clearances) on the minimum agitation speed (Njs), power dissipation at the minimum agitation speed (Pjs), and power number (Npo) was investigated. The solids suspension experiments were carried out in the 0.292 m tank, and three type of impellers were used: six-blade flat-disk turbine (6FDT), six-blade flat-blade turbine (6FBT), and six-blade flat (45°) pitched-blade turbine (6FPT). In addition, the high efficiency impeller Chemineer HE-3 (CHEM) was also studied in the 0.584 m tank. In all cases, the power number (Npo) was also calculated using water only (without solids) at two different Reynolds numbers. The highest value of the impeller clearance was defined by the region in which the change of flow pattern occurred. As low as possible impeller clearances, as allowed by the system geometry or by the settled solids bed height were also used. The impeller clearance range was $1/48 < C/T < 1/4$.

Njs and Pjs were expressed as a function of impeller clearance (C/T), defined as the distance from the lower part of the impeller to the tank bottom. This definition was chosen to compare the values of Njs, Pjs, and Npo (calculated using the Rushton expression) at $C/T = 0$. When necessary the impeller clearance was expressed as C'/T ($= C/T + W_b/2T$). A comparison of the effect of C/T on Njs, Pjs, and Npo at constant D/T ratio, between the different impellers used, is also presented.

5.1.1 Minimum Agitation Speed (Njs)

In Figure 5(a, b, c, d), the values of Njs have been plotted against C/T, for each type of impeller. In general, it can be seen that the value of Njs decreases with a decrease in C/T, for all the impellers. However, for the 6FPT and CHEM impellers with small D/T values, there is a minimum clearance below which an increase in Njs with lower C/T values is observed. This phenomenon has been attributed to a "throttling effect" resulting from the sharp change in flow direction just below the impeller. When D/T is large this effect is not appreciable, since the wider blades of these impellers produce a higher flow which is not significantly hindered by the presence of the tank bottom (Chudacek, 1985). In Table 5, the minimum clearances for Njs, also called optimum clearances, are shown.

Table 5 Optimum Clearances for Minimum Agitation Speed (Njs)

Impeller Type	D (m)	C/T	C'/T	C'/D
6FPT	0.0635	0.05	0.066	0.31
T = 0.292 m	0.0762	0.05	0.066	0.25
	0.102	-	-	-
CHEM	0.102	0.063	0.063	0.18
T = 0.292 m	0.114	-	-	-
CHEM	0.178	0.083	0.083	0.27
T = 0.584 m	0.203	0.083	0.083	0.24
	0.229	-	-	-

Njs was correlated as a function of the impeller clearance. Only the range of C/T in which Njs decreases with a decrease of C/T was used. Three types of correlation were analyzed: linear, exponential, and power law. In all cases, the correlation with the power law was the poorest. This is in agreement with Zwietering (1958) and Chudacek (1986). Recently, Aravinth *et al.* (1996) proposed a new correlation for 6FBT, in which the power law was used to account the effect of the impeller clearance. A maximum deviation of 19.2% was reported. In general, the correlations based on the linear and exponential forms were similar, the exponential form being slightly superior.

In the literature, there are different opinions about the form of the impeller clearance dependence on Njs. Conti *et al.* (1981) proposed empirical correlations for eight-blade flat-disk turbine, in which Njs can be found as a quadratic function of the impeller clearance. Musil and Vlk (1978) for conical and truncated cone bottom tanks, defined two different regions for the effect of the impeller clearance on Njs. The first one where the impeller clearance had no effect upon Njs, and the second one where a linear dependence of Njs upon the impeller clearance was observed. According to Baldi *et al.* (1978), the influence of the impeller clearance on Njs is more complex. The data reported by Oldshue and Sharma (1992) indicate a constant value for Njs ($0.05 < C'/T < 0.10$), for radial-flow and mixed axial-flow impellers. Armenante *et al.* (1992) suggested a near lineal relationship between Njs and the C'/D ratio ($0.5 < C'/D < 0.83$), for six-blade flat-blade turbines. The data presented by Myers *et al.* (1994a) suggested an exponential dependence of Njs upon C'/T, for mixed axial-flow and axial-flow impellers. The selection of the exponential form was based on the best correlation over the positive range of Njs.

Table 6 Correlations for Minimum Agitation Speed (Njs)

Impeller Type	D (m)	C/T	Njs (rpm)	r
6FDT	0.0635	1/48 < C/T < 1/8	Njs = 656 exp (2.07 C/T)	0.9978
T = 0.292 m	0.0762	1/48 < C/T < 1/8	Njs = 418 exp (2.23 C/T)	0.9757
	0.102	1/48 < C/T < 1/8	Njs = 226 exp (2.19 C/T)	0.9875
6FBT	0.0635	1/48 < C/T < 1/5	Njs = 693 exp (2.05 C/T)	0.9967
T = 0.292 m	0.0762	1/48 < C/T < 1/5	Njs = 479 exp (1.99 C/T)	0.9966
	0.102	1/48 < C/T < 1/5	Njs = 265 exp (1.89 C/T)	0.9976
6FPT	0.0635	1/20 < C/T < 1/4	Njs = 619 exp (0.67 C/T)	0.9972
T = 0.292 m	0.0762	1/20 < C/T < 1/4	Njs = 466 exp (0.58 C/T)	0.9941
	0.102	1/48 < C/T < 1/4	Njs = 283 exp (0.68 C/T)	0.9899
CHEM	0.102	1/16 < C/T < 1/4	Njs = 399 exp (0.79 C/T)	0.9525
T = 0.292 m	0.114	1/48 < C/T < 1/4	Njs = 340 exp (0.64 C/T)	0.9459
CHEM	0.178	1/12 < C/T < 1/4	Njs = 286 exp (0.84 C/T)	0.9741
T = 0.584 m	0.203	1/16 < C/T < 1/4	Njs = 233 exp (0.80 C/T)	0.9626
	0.229	1/48 < C/T < 1/4	Njs = 195 exp (0.79 C/T)	0.9597

From Table 6, it can be observed that the dependence of Njs with C/T is stronger depending on the impeller type according to the following progression:

$$6FPT < CHEM < 6FBT < 6FDT \qquad (5.1)$$

5.1.2 Power Dissipation at Minimum Agitation Speed (Pjs)

In Figure 6(a, b, c, d), the values of the power dissipation at minimum agitation speed (Pjs) have been plotted against the impeller clearance for each type of impeller. Similarly to Njs, the value of Pjs decreases when the impeller clearance decreases. For the case of the mixed axial-flow (6FPT) and axial-flow (CHEM) impellers, Figures 6(c) and 6(d), respectively, Pjs seems to be independent of the impeller sizes, as found by Gray (1987) and Myers (1994a). For the 0.0635 m 6FPT impeller an increase (10%) of the power dissipation can be seen as compared with the other sizes. This can be attributed to changes in minor dimensions as will be explained later (See section 5.1.3, Power Number).

From Figures 6(c) and 6(d), it can also be observed that the throttling effect in the power dissipation is more noticeable than in the case of Njs (the change in flow direction dissipates more energy). Table 7 shows the minimum clearances for Pjs, also referred as the optimum suspension efficiencies (Chudacek, 1985). Since the throttling effect is not significant for the case of the radial-flow (6FDT and 6FBT) impellers, they must be positioned as low as possible for the task of maximum suspension efficiency. For the cases of the mixed axial-flow (6FPT) and axial-flow (CHEM) impellers, they should be positioned with minimum clearance, as governed either by the presence of the throttling effect or by the agitation system geometry. These results support the observation given by Chudacek (1985), using the complete off-bottom suspension criterion, for three blade propellers, in different tank bottom geometry. Furthermore, the values shown in Table 7 do not support the current practice of universally positioning the impeller at 0.33 D, for the task of complete off-bottom suspension.

Table 7 Optimum Clearances for Power Dissipation (Pjs)

Impeller Type	D (m)	C/T	C'/T	C'/D
6FPT	0.0635	0.063	0.079	0.37
T = 0.292 m	0.0762	0.063	0.079	0.30
	0.102	0.05	0.072	0.21
CHEM	0.102	0.083	0.083	0.24
T = 0.292 m	0.114	0.063	0.063	0.16
CHEM	0.178	0.083	0.083	0.27
T = 0.584 m	0.203	0.083	0.083	0.24
	0.229	0.063	0.063	0.16

Pjs was also correlated using the three forms: linear, exponential, and power law. Similar to the case of Njs, only the positive range of impeller clearance was used. The correlation using the power form was the poorest, and the exponential form was superior when correlating Pjs as a function of C/T. Weisman and Efferding (1960) and Gray (1987) suggested an exponential dependence of Pjs with the impeller clearance. Similarly to the case of Njs, the selection of the exponential form was based on the best correlation.

For the 6FDTs the value of Pjs to C/T dependence was found to be between 6.72 to 8.39. As observed for Npo in Figure 7(a), for the case of the 6FDT, there is a change in the slope of the dependence at approximately C/T = 1/28, below which the bottom recirculation is reduced producing a smaller power consumption.

For the 6FBTs this value was found to be between 4.74 to 5.30, i. e., in agreement with Weisman and Efferding (1960) who found a value of 5.3, for flat paddle impellers. However, Gray (1987) found a value of 1.2 for a six flat-blade impeller in the region of the "single eight" (C'/T < 0.17), and a value of 5.3 in the region of the "double-eight" (C'/T > 0.17), only one size was investigated in his work.

For the case of the 6FPTs, the exponent of C/T in the expression for Pjs was found to be between 0.99 to 1.06 in agreement with Gray (1987), who found a value of 1.2, for flat (45°) pitched-blade impellers. As mentioned before, Pjs for the 0.0635 m 6FPT impeller shows an unusual increase as compared with the other sizes. However, the dependence with C/T is similar for all the sizes used, the difference being due to the experimental error. This suggests that changes in minor geometrical dimensions do not affect the dependence of C/T on each type of impellers.

For the CHEMs, the exponent of C/T in the expression for Pjs was found to be between 1.82 to 1.89 in the tank of 0.292 m diameter, and between 1.65 to 1.73 for the tank of 0.584 m diameter.

The correlations for Pjs are shown in Table 8, for each type of impeller. The 6FDTs present two correlations, depending on the region in which the breakdown on Npo was observed. For the 6FPT and CHEM impellers, in the region in which the throttling effect is significant, no attempt was made to find a correlation. From Table 8, the dependence of Pjs with C/T, follows a relation similar to Equation (5.1) for the case of Njs (in both comparisons, the presence of only three blades for the CHEM must be noticed):

$$6FPT < CHEM < 6FBT < 6FDT \qquad (5.2)$$

Table 8 Correlations for Power Dissipation (Pjs)

Impeller Type	D (m)	C/T	Pjs (watts)	r
6FDT	0.0635	1/28 < C/T < 1/8	Pjs = 5.02 exp (6.72 C/T)	0.9987
T = 0.292 m		1/48 < C/T < 1/28	Pjs = 3.52 exp (16.40 C/T)	0.9993
	0.0762	1/28 < C/T < 1/8	Pjs = 3.53 exp (7.14 C/T)	0.9771
		1/48 < C/T < 1/28	Pjs = 2.07 exp (19.67 C/T)	0.9997
	0.102	1/28 < C/T < 1/8	Pjs = 2.05 exp (8.39 C/T)	0.9902
		1/48 < C/T < 1/28	Pjs = 1.77 exp (11.29 C/T)	0.9204
6FBT	0.0635	1/48 < C/T < 1/5	Pjs = 4.01 exp (5.31 C/T)	0.9956
T = 0.292 m	0.0762	1/48 < C/T < 1/5	Pjs = 3.38 exp (4.99 C/T)	0.9868
	0.102	1/48 < C/T < 1/5	Pjs = 2.47 exp (4.74 C/T)	0.9973
6FPT	0.0635	1/20 < C/T < 1/4	Pjs = 2.23 exp (1.05 C/T)	0.9918
T = 0.292 m	0.0762	1/20 < C/T < 1/4	Pjs = 2.14 exp (0.99 C/T)	0.9896
	0.102	1/48 < C/T < 1/4	Pjs = 2.10 exp (1.06 C/T)	0.9973
CHEM	0.102	1/16 < C/T < 1/4	Pjs = 1.31 exp (1.82 C/T)	0.9301
T = 0.292 m	0.114	1/48 < C/T < 1/4	Pjs = 1.27 exp (1.89 C/T)	0.9208
CHEM	0.178	1/12 < C/T < 1/4	Pjs = 6.92 exp (1.65 C/T)	0.9256
T = 0.584 m	0.203	1/16 < C/T < 1/4	Pjs = 6.93 exp (1.68 C/T)	0.9164
	0.229	1/48 < C/T < 1/4	Pjs = 6.90 exp (1.73 C/T)	0.9046

5.1.3 Power Number (Npo)

In Figure 7(a, b, c, d), the values of the power number (Npo) calculated using the Equation (2.4), and the experimental values of Njs and Pjs, have been plotted against the impeller clearance, for each type of impeller. Npo was also calculated using water only (without solids). In Figure 7, the values of Npo using water only (calculated by taking the average of the power numbers at two different rotational speed) are also included. A good agreement between the values obtained can be observed.

For the 6FDTs, Figure 7(a), the power number is nearly constant from C/T = 1/8 to C/T = 1/28. A steep decrease was observed from C/T = 1/28 to C/T = 1/48. This can be due to the reduction in the bottom recirculation as mentioned before. For the case of 0.0762 m and 0.102 m impellers, the power number seems to be independent of the D/T ratio. The 0.0625 m impeller shows a decrease in the power number. This could be attributed to the higher disk thickness-to-blade width ratio (1/8 for this size against 1/10 for the other sizes), which reduces Npo (Nienow and Miles, 1971). Although, all these observations have been drawn from the plot of Npo against the impeller clearance (C/T) as defined in this work, similar behavior can be observed by plotting Npo against C'/T (= $C/T + W_b/2T$).

For the case of the 6FBTs, Figure 7(b), the power number shows a slight increase between C/T = 1/5 to C/T = 1/16. Then a steep increase is observed from C/T = 1/16 to C/T = 1/48. A minimum value (2.14-2.16), for each impeller size, was observed in the transition region (C/T > 1/5). In this case, the effect of the D/T ratio is more insignificant. Again, these observations can also be drawn from a plot of Npo against C'/T .

The 6FPTs plot in Figure 7(c) shows the same behavior of the 6FBT, i. e., a slight increase between C/T = 1/5 to C/T = 1/16 and a steep increase from C/T = 1/16 to C/T = 1/48. The power number seems to be independent of the D/T ratio for the 0.0762 m and 0.102 m impellers. However, contrary to the 6FDT, the 0.0635 m 6FPT shows an increase in the power number. This could also be attributed to the considerable effect that minor dimensions have on the power number. In this case, the blade height-to-impeller diameter ratio is higher for the 0.0635 m 6FPT. A similar increase in the power number has been reported by Bates *et al.* (1968) for the 6FBT. An increase of this ratio from 1/8 to 1/5 produce an increase of the power number of approximately 40%.

From Figure 7(d), the CHEMs also show a slight increase in Npo between C/T = 1/4 to C/T = 1/16 and then a steep increase from C/T = 1/16 to C/T = 1/48. In this case, a slight decrease of the power number with the impeller diameter can be appreciated. All the impellers present a similar blade thickness (1.6 mm, see Table 2). If the explanation given above for the case of the disk turbine is applied in this situation, the power number must increase with the impeller diameter since the blade thickness-to-impeller diameter ratio decreases. However, this is not the case for this type of impeller, Npo decreases with a decrease of the blade thickness-to-impeller diameter ratio. This must be due to the different orientation of the blades (approximately 90° with respect to the disk turbine blades), the effect of the blade length-to-impeller diameter ratio on the friction loss seems to be most significant. For this reason, the power number decreases with an increase of the blade length-to-impeller diameter ratio (L/D = 0.37, 0.39, 0.42, 0.43, and 0.43 for D = 0.102 m, 0.114 m, 0.178 m, 0.203 m, and 0.229 m, respectively).

Table 9 shows the maximum difference between the two resulting power numbers using water only, for each type of impellers. Also, the maximum difference between the average value of the power number using water only and the power number obtained in the solids suspension experiments is shown. In both cases, the maximum difference was observed at low impeller clearances due to instability of the flow in this region, which makes the measurement of the power dissipation very difficult. From the two values obtained for the case of water only, the relation between the power dissipation (P) and the rotational speed (N) was calculated, this relation was expressed as the slope in a log-log plot of P and N. The values of the slope are also shown in Table 9 (the values must be interpreted as the average values in the range of C/T investigated). These values indicate a good agreement with the Rushton expression, defined in Equation (2.4), since the power dissipation is proportional to the agitation speed raised to the power of 3.

Table 9 Comparison between Experimental Values for Power Number (Npo)

	Water only		**Solids Suspension**
Impeller Type	**Maximum difference**	**Slope**	**Maximum difference**
6FDT	±4.40%	3.06±0.16	±5.31
6FBT	±5.10%	3.05±0.09	±3.94
6FPT	±3.98%	2.99±0.11	±3.66
CHEM	±4.63%	2.92±0.08	±3.33

The power number was also correlated as a function of the impeller clearance. In this case, the power law gave the best correlation. Following the Rushton equation ($P \sim N^3$), the exponent of C/T for the expressions of Pjs (Table 8) must be three times the values of the exponent of C/T found for Njs (Table 6). This relation is not followed for these exponents. The difference can be attributed to the C/T dependence of Npo.

The correlations for constant C'/T follow a similar pattern. Since these correlations will be used later, they are shown in Table 10. The experimental values of Npo obtained in the 0.188 m and 0.244 m tank sizes were included in these correlations. For the 6FDT, 6FBT, and 6FPT, the values of Npo obtained in the 0.584 m tank size were always higher.

For the 6FDTs, two set of correlations are shown, one for the 0.0635 m impeller size, and the other for the 0.0762 m and 0.102 m impeller sizes. This is due to the difference in the disk thickness-to-impeller diameter ratio. Each set of correlation also presents two ranges of impeller clearance, depending upon the region in which the change in slope was observed. The correlations in the lower region show a very similar dependence with C'/T (0.30-0.33) for both sets. The major difference in Npo is observed in the region in which a constant value for Npo was found (3.92 and 4.21 for the lower and the higher sizes, respectively). For the 6FPTs, due to the difference in the blade width-to-impeller diameter, a different correlation for the 0.0635 m impeller was calculated. However, the dependence with C'/T was similar in both cases. This supports the idea that minor dimension differences do not affect the dependence with C'/T. Although there is a slight decrease of Npo with the impeller diameter for the CHEMs, two sets of correlations are shown depending on the tank size. Graphical comparison is shown in Figure 8.

Table 10 Correlations for Power Number (Npo)

Six-Blade Flat-Disk Turbine:

$$Npo = 3.92 \qquad \text{(maximum deviation = } \pm 3.62\%) \qquad (5.3)$$

T = 0.188-0.292 m, D = 0.0635 m, $0.07 < C'/T < 0.19$, k/D = 1/40

$$Npo = 9.35\,(C'/T)^{0.33} \qquad \text{(maximum deviation = } \pm 6.19\%) \qquad (5.4)$$

T = 0.188-0.292 m, D = 0.0635 m, $C'/T < 0.07$, k/D = 1/40

$$Npo = 4.21 \qquad \text{(maximum deviation = } \pm 2.38\%) \qquad (5.5)$$

T = 0.188-0.292 m, D = 0.0762-0.102 m, $0.107 < C'/T < 0.17$, k/D = 1/50

$$Npo = 8.16\,(C'/T)^{0.30} \qquad \text{(maximum deviation = } \pm 9.36\%) \qquad (5.6)$$

T = 0.188-0.292 m, D = 0.0762-0.102 m, $C'/T < 0.11$, k/D = 1/50

Six-Blade Flat-Blade Turbine:

$$Npo = 1.92\,(C'/T)^{-0.09} \qquad \text{(maximum deviation = } \pm 5.23\%) \qquad (5.7)$$

T = 0.188-0.292 m, D = 0.0635-0.102 m, $C'/T < 0.2$

Six-Blade Flat (45°) Pitched-Blade Turbine:

$$Npo = 1.23\,(C'/T)^{-0.13} \qquad \text{(maximum deviation = } \pm 3.45\%) \qquad (5.8)$$

T = 0.188-0.292 m, D = 0.0762-0.102 m, $C'/T < 0.26$

$$Npo = 1.34\,(C'/T)^{-0.13} \qquad \text{(maximum deviation = } \pm 3.41\%) \qquad (5.9)$$

T = 0.188-0.292 m, D = 0.0635 m, $C'/T < 0.10$

Chemineer HE-3 Impeller:

$$Npo = 0.25\,(C'/T)^{-0.12} \qquad \text{(maximum deviation = } \pm 5.45\%) \qquad (5.10)$$

T = 0.584 m, D = 0.178-0.229 m, $C'/T < 0.25$

$$Npo = 0.32\,(C'/T)^{-0.07} \qquad \text{(maximum deviation = } \pm 6.01\%) \qquad (5.11)$$

T = 0.292 m, D = 0.102-0.114 m, $C'/T < 0.10$

5.1.4 Change of Flow Pattern

To define the upper limit of the "single-eight" regime, the impeller clearance was increased until the change of the flow pattern was observed. For instance, the position of the last particles was carefully observed. As described in Section 4.2, in the "single-eight" regime, the last particles are suspended from the periphery of the tank bottom, while, in the "double-eight" regime, the last particles are suspended from an annular space around the center of the tank bottom.

In general, for the 6FDTs, the change of flow pattern occurred between $0.13 < C/T < 0.19$ ($0.16 < C'/T < 0.21$), and for the 6FBTs, this change was observed between $0.19 < C/T < 0.24$ ($0.21 < C'/T < 0.25$). In the present work, the range in which the transition region occurred was a function of the impeller type and size. This is in contrast with previous authors who found the flow pattern change independently of the D/T ratio. Nienow (1968) observed the flow pattern change at $C'/T = 0.17$ for a six flat disk turbine. Conti *et al.* (1981) reported the flow pattern change at $C'/T = 0.22$ for an eight-blade flat-disk turbine. For a six-blade flat-blade turbine, Gray (1978) reported the flow pattern change at $C'/T = 0.17$, and Armenante *et al.* (1993) found that the transition region occurred between $0.21 < C'/T < 0.26$, independently of the number of impellers.

For the 6FPT and CHEM impellers, the "single-eight" regime was observed up to $C/T = 0.25$ ($C'/T = 0.26$ and $C'/T = 0.25$, respectively). Zwietering (1958) observed the "single-eight" flow pattern for propellers up to $C'/T = 0.4$, and Gray (1978) found that the mixed axial-flow (6FPT) impellers maintained the "single-eight" flow pattern up to $C'/T = 0.35$ in a flat bottom tank.

Table 11 gives the range of C/T (C'/T), within which the change of flow pattern was observed for each type and size of impellers. In general, the flow pattern change occurred earlier for the 6FDT, followed by the 6FBT, and no change occurred up to C/T = 0.25 for the mixed axial-flow (6FPT) and axial-flow (CHEM) impellers. A similar sequence (6FDT-6FBT-6FPT, CHEM) has been observed for the minimum agitation speed (Njs), the power dissipation (Pjs), and the power number (Npo):

Table 11 Change of Flow Pattern Observed in this Work

Impeller Type	D (m)	D/T	C/T	C'/T
6FDT	0.0635	0.217	0.16-0.19	0.18-0.21
T = 0.292 m	0.0762	0.261	0.14-0.17	0.16-0.20
	0.102	0.348	0.13-0.16	0.17-0.19
6FBT	0.0635	0.217	0.22-0.24	0.23-0.25
T = 0.292 m	0.0762	0.261	0.19-0.21	0.21-0.22
	0.102	0.348	0.19-0.21	0.22-0.23
6FBT	0.0635	0.217	>0.25	>0.26
T = 0.292 m	0.0762	0.261	>0.25	>0.26
	0.102	0.348	>0.25	>0.27
CHEM	0.102	0.348	>0.25	>0.25
T = 0.292 m	0.114	0.39	>0.25	>0.25

5.1.5 Comparison of Njs and Pjs at Constant D/T

In Figures 9, 10 and 11, the comparison of Njs, Pjs, and Npo between the different impellers at D/T ratios of 0.217, 0.261, and 0.348 m are shown, respectively. The comparison at D/T = 0.348 will be discussed here, since, in this impeller size, the four types of impellers could be compared. The conclusions drawn at this D/T ratio are also applicable to the others D/T ratios.

From Figure 9(a), the minimum agitation speed is lower for the 6FDT as compared with the 6FBT in the "single-eight" flow pattern regime. Njs for the 6FPT is lower than for the 6FBT until the point in which the throttling effect increases the value of Njs. This conclusion can be also drawn by comparing Njs for the 6FPT with that for the 6FDT. In both cases, the value of the impeller clearance in which the tendency is reverted depends of the impeller size. Similar results can be drawn when the experimental data of Raghava Rao *et al.* (1988b) are analyzed. In all the range of impeller clearance investigated, Njs for the CHEM was higher than for the other impellers. This impeller presents only three blades against six blades for the other impellers. Chapman *et al.* (1983) found that increasing the number of blades reduces both Njs and Pjs.

From Figure 9(b), it can be observed that the power dissipation (Pjs) for the 6FDT is higher than for the other radial-flow impeller in the major part of the range of impeller clearances. However, at the point (C/T = 1/28) at which the change in slope for Pjs occurred, this value is lower than for the 6FBT. The power dissipation for the mixed-axial flow (6FPT) and axial-flow (CHEM) impellers are lower than those of the radial-flow impellers. The power dissipation for the 6FPT being higher than that of CHEM.

As shown in Figure 9(c), Npo is higher for the 6FDT, followed by the 6FBT. Npo for the mixed axial-flow and axial-flow impellers are lower than for the radial-flow impellers. Npo for the CHEM being lower than for the 6FPT.

At very small impeller clearances, 6FDT produces a flow pattern that scours the base and is efficient for suspension (Nienow and Miles, 1978). For this type of impeller the suspension is due to the random turbulent bursts (Baldi *et al.*, 1978; Chapman *et al.*, 1983). Since the path length is reduced, the performance improves at very low impeller clearance (Raghava Rao *et al.*, 1988b). However, it seems that only a part of the energy supplied by the lowest half part of the impeller is available for the solids suspension, the power consumption is higher than the mixed-axial flow and axial-flow impellers power consumption. The behavior of the 6FBT seems to be between the 6FDT (radial-flow) and the 6FPT (mixed axial-flow). Because of the more uniform radial-flow pattern, 6FDT tend to draw more power than 6FBT (Oldshue, 1983).

The 6FPT produces a flow that leaves the impeller tip, hits the vessel, scours the bottom, and lifts the particles from the periphery. At very low impeller clearances, the impeller stream hits the vessel bottom with higher velocity causing a sharp change in flow direction which dissipates more energy (throttling effect), increasing the power consumption and power number (Raghava Rao and Joshi, 1988a). The same mechanism can be applied for the CHEM. As observed by Myers (1994a) the much lower torque requirement of the high-efficiency impeller represents a substantial decrease in capital investment for new equipment, , although the difference in power requirement of these two impellers can not be overwhelming.

5.2 Effect of Impeller Diameter

The effect of the impeller diameter was investigated for three cases: constant C/T (Figure 12), constant C'/T (Figure 13), and constant C'/D (Figure 14).

In Figures 12(a) and 13(a), the values of Njs for the 6FDT have been plotted against the impeller diameter for constant C/T and constant C'/T, respectively. In both cases, the effect of the impeller diameter seems to be independent of the impeller clearance. These dependencies can be expressed as:

$$Njs \propto D^{-2.25\pm0.03} \qquad (1/48 < C/T < 1/8) \qquad (5.12)$$

$$Njs \propto D^{-2.29\pm0.03} \qquad (1/24 < C'/T < 1/8) \qquad (5.13)$$

These values are lower than -2.35 found by Zwietering (1958) and -2.45 found by Chapman *et al.* (1983). Figure 14(a) shows the dependence of the Njs at constant C'/D . For C'/D = 1/4 and 1/5, values of the exponent of -2.16 and -2.20 were found, respectively; within the experimental error, the value of the exponent seems to be independent of the D/T ratio (-2.18±0.03). At C'/D = 1/2 a value of -1.65 was found, this value is in agreement with Baldi *et al.* (1978) who found -1.67, however, in this work at C'/D = 1/2 the 0.102 m impeller was found in the region of the "double-eight".

From Figures 12(b) and 13(b), the dependence of Njs with the impeller diameter for the 6FBT can be expressed as:

$$Njs \propto D^{-2.07\pm0.03} \qquad (1/48 < C/T < 1/5) \qquad (5.14)$$

$$Njs \propto D^{-2.05\pm0.03} \qquad (1/24 < C'/T < 1/5) \qquad (5.15)$$

At constant C'/D, Figure 14(b), values of -1.83 (C'/D = 1/2), -1.95 (C'/D = 1/4) and -1.97 (C'/D = -1.97) were found. The average value being -1.91±0.07.

From Figures 12(c) and 13(c), the dependence for the 6FPT can be expressed as:

$$Njs \propto D^{-1.66\pm0.01} \qquad (1/20 < C/T < 1/28) \qquad (5.16)$$

$$Njs \propto D^{-1.67\pm0.03} \qquad (1/16 < C'/T < 1/4) \qquad (5.17)$$

For this impeller, only the positive range of the impeller clearance was used (in which Njs decreases with a decrease of the impeller clearance). At constant C'/D, Figure 14(c), values between -1.60 (C'/D = 1/2) to -1.63 (C'/D = 1/4) were found (-1.62±0.02). At C'/D = 1/5, when the throttling effect was present a value of 1.71 was found

From Figure 12(d), the dependence for the CHEM can be expressed as:

$$Njs \propto D^{-1.62\pm0.02} \qquad (1/12 < C'/T < 1/4) \qquad (5.18)$$

Again, only the positive range was used for T = 0.584m. At constant C'/D, values between 1.47 (C'/D = 1/2) to 1.56 (C'/D = 1/4) were found (-1.52±0.06), Figure 14(d). At C'/D = 1/5, the value of the exponent found was -1.69, in this value the throttling effect was present. Table 12 shows the comparison of the exponents found in each case.

Table 12 Comparison of Exponents Found for Impeller Diameter (D)

	Exponent on D		
Impeller Type	**C/T**	**C'/T**	**C'/D**
6FDT	-2.25	-2.29	-2.18
6FBT	-2.07	-2.07	-1.91
6FPT	-1.66	-1.67	-1.62
CHEM	-1.62	-1.62	-1.52

An inspection of these values reveals that the effect of D on Njs at constant C/T (C'/T) are higher than the effect at constant C'/D. Armenante and Li (1993) observed that a review of the literature on solids suspension, for radial-flow impellers, reveals that those investigators that quantified the effect of D on Njs at constant C' reported values for the exponent for D significantly higher than those who kept C'/D constant. For example, for radial-flow impellers, Zwietering (1958), Nienow (1968), Narayanan *et al.*(1969), and Chapman *et al.* (1983) for constant C'/T, reported values of -2.35, -2.18, -2.00, and -2.45, respectively. Baldi *et al.* (1978) and Armenante and Li (1993), for constant C'/D, reported values of -1.67 and -1.77, respectively.

Raghava Rao *et al.* (1988b) explained on a rational basis, the effect of impeller diameter on the solids suspension, for different designs of impeller. For the case of radial-flow impellers, the effect of the length of the flow path [(T/2) - (D/2) + C'] in the decay of the turbulence, and the effect of the impeller diameter in the liquid velocity ($\sim D^{7/6}$) make the dependence on the impeller diameter very strong. In the case of axial-flow impellers, the solids suspension occurs mainly because of the liquid flow generated by the impeller; Chudacek (1986) also considered that it is the flow and not the shear rate that controls the suspension of solids for three blade square pitch propellers. Since the average liquid velocity is proportional to ND, Njs should be inversely proportional to D. In conclusion, the effect of the impeller diameter for the radial-flow impellers is stronger than for the mixed axial-flow and axial-flow impellers. The results obtained in this work, i.e., -2.29 and -2.07 for radial-flow impellers and -1.67 and -1.62 for axially discharging impellers, at constant C'/T, support this conclusion.

5.3 Effect of Tank Diameter

The effect of tank diameter was studied in two ways. First, D/T was kept constant at a value of 0.348 (T/D = 2.874), using the tanks of 0.188 m, 0.292 m, and 0.584 m. In the first tank, the impeller diameter used was 0.0635 m, since the D/T ratio was 0.337 (T/D = 2.961), a correction was performed. Njs was corrected using the expression $Njs \propto D^{-exp}$, using the exponents found in the Section 5.2. For the power number, an average value between those for the 0.0762 m and 0.102 m impeller sizes was used, and Pjs was calculated using the Equation (2.4).

In Figure 15(a, b, c), the effect of the tank diameter on Njs at constant D/T is shown, for each type of impeller. The following relationship was obtained:

$$Njs \propto T^{-0.82\pm0.01} \tag{5.19}$$

This relationship applies for the three impellers: 6FDT, 6FBT, and 6FPT, and for all values of the impeller clearance (C/T or C'/T). Again, the impeller clearance does not seem to affect this value. In the case of the CHEM, using only two tanks: 0.292 m and 0.584 m, and the same D/T ratio, the following expression was found:

$$Njs \propto T^{-0.78\pm0.01} \tag{5.20}$$

This value is applicable for all the values of the impeller clearance (C/T = C'/T) analyzed. However, for the cases of the mixed axial-flow and axial impellers, only the positive range for the impeller clearance was considered.

The values of exponent over T reported by Zwietering (1958) and Chapman *et al.* (1983) are -0.85 and -0.76, respectively. These values are comparable to that obtained in the present work.

In the second way, D = 0.0762 m was kept constant using the tanks of 0.188 m, 0.244 m, and 0.292 m. However, in this case the comparison was conducted only at constant C/T. The following expressions were found, Figure 16(a, b, c):

$$Njs \propto T^{1.40\pm0.01} \qquad (6FDT) \qquad (5.21)$$

$$Njs \propto T^{1.24\pm0.03} \qquad (6FDT) \qquad (5.22)$$

$$Njs \propto T^{0.87\pm0.03} \qquad (6FPT) \qquad (5.23)$$

In the first case, the overall effect of impeller diameter and tank diameter results in a negative exponent. In the second case, when the same impeller size was used in the three tanks, independent of the impeller clearance, the circulation path increased, resulting in a positive exponent over T (Raghava Rao *et al.*, 1988b). In Section 5.2, the exponent over D was obtained at constant T and varying D ($Njs \propto D^d$, at constant T), while in the second way in this section, D was kept constant and T was varied ($Njs \propto T^t$, at constant D). Therefore, when both D and T are varied simultaneously while scaling up to keep the D/T ratio constant, the exponent over T (at constant D/T) or D should be an overall effect of the above situations (since $Njs \propto [D/T]^d\ T^{t'}$, at constant D/T, then $t' = t + d$). In other words, from the values of the exponent on D (Table 12), and the results shown in Equations (5.21), (5.22), and (5.23), the exponents over T in the first way should be -0.85 (= 1.40 - 2.25) for the 6FDT, -0.83 (= 1.24 - 2.07) for the 6FBT, and -0.79 (= 0.87 - 1.66) for the 6FPT. The values obtained of -0.82 are very close to these values.

The exponents on T found at constant D/T and constant D are shown in Table 13. Only the C/T ranges are shown. However for constant D/T ratio, the value of the exponents is also applicable to constant C'/T.

5.4 Effect of Solids Loading

The effect of solids loading was investigated using the 0.102 m impeller in the tank of 0.292 m (D/T = 0.348). Three concentrations were used: 0.5, 1.0, and 1.5 wt/wt%.

In Figure 17(a, b, c, d), the values of Njs have been plotted against the solids loading, for each type of impeller. The following expressions were found:

$$Njs \propto X^{0.13\pm0.003} \qquad \text{(6FDT and 6FBT)} \qquad (5.24)$$

$$Njs \propto X^{0.11\pm0.001} \qquad \text{(6FPT and CHEM)} \qquad (5.25)$$

With an increase in solids loading, the liquid flow generated by the impeller decreases. This is because some of the impeller energy dissipates at the solid-liquid interface (Raghava Rao *et al.*, 1988b).

In Table 13, the exponents on the solids concentration are shown. As before, the exponents of the solids loading are applicable at both constant C/T and constant C'/T.

Table 13 Exponents of Njs Found in this Work
Constant C/T

			Exponent on			
Impeller Type	**D/T**	**C/T**	**D**	**T Const. D/T**	**T Const. D**	**X**
6FDT	0.217-0.348	1/48-1/8	-2.25	-0.82	1.40	0.13
6FBT	0.217-0.348	1/48-1/5	-2.07	-0.82	1.24	0.13
6FPT	0.217-0.348	1/20-1/4	-1.66	-0.82	0.87	0.11
CHEM	0.304-0.391	1/12-1/4	-1.62	-0.78	-	0.11

5.5 Comparison at C/T = 0

Table 14 shows the values of Njs and Pjs, extrapolated for C/T = 0 from the correlations presented in Tables 6 and 8, respectively. For the cases of the mixed axial-flow and axial-flow impellers, the throttling effect is not included in this extrapolation.

The values of Njs can be interpreted as the minimum value required for the impellers, when "touching" the bottom tank, to reach the periphery, and lift the particles. The same concept can be applied to the values of Pjs , without considering the friction loss between the impeller and the tank bottom. However, in the latter case, the values include those required to "overcome" the resistance to the movement presented by the static fluid.

When the effect of D on Njs is analyzed, the values of the exponent are very similar to those found in Section 5.2: -2.24, -2.03, -1.66, and -1.52, for the 6FDT, 6FBT, 6FPT (T = 0.292 m), and CHEM (T = 0.584 m), respectively. This suggests that the effect of C/T is not appreciable over the exponents found on D, in all the range investigated.

Npo was calculated from two experimental values: Njs and Pjs. Considering the experimental error and also the difference in the disk thickness-to-blade width ratio, Npo appears to be independent of D/T at C/T = 0 for the 6FDTs (2.66±0.3) and for the 6FBTs (2.57±0.04). The 6FPTs present two values: one for the 0.0762 m and 0.102 m impeller sizes (1.80±0.02), and other for the 0.0635 m impeller size (1.97). The CHEMs also present two values: one for the 0.292 m tank size (0.38±0.03), and other for the 0.584 m tank size (0.33±0.01). For the 6FPTs and CHEMs, the different values observed seems to be due to the difference in the blade width- and blade length-to-impeller diameter ratio between the impeller sizes, respectively.

Table 14 Comparison at C/T = 0

Impeller Type	D (m)	Njs (rpm)	Pjs (watts)	Npo
6FDT	0.0635	656	3.52	2.61
T = 0.292 m	0.0762	418	2.07	2.38
	0.102	226	1.77	3.00
6FBT	0.0635	693	4.01	2.52
T = 0.292 m	0.0762	479	3.38	2.59
	0.102	265	2.47	2.60
6FPT	0.0635	619	2.23	1.97
T = 0.292 m	0.0762	466	2.14	1.78
	0.102	283	2.10	1.81
CHEM	0.102	399	1.31	0.40
T = 0.292 m	0.114	340	1.27	0.36
CHEM	0.178	286	6.92	0.34
T = 0.584 m	0.203	233	6.93	0.34
	0.229	195	6.90	0.32

6FDT: $Njs \propto D^{-2.24}$ (T = 0.292 m, D = 0.0635-0.102 m)
$Npo = 2.66 \pm 0.3$ (T = 0.292 m, D = 0.0635-0.102 m)
6FBT: $Njs \propto D^{-2.03}$ (T = 0.292 m, D = 0.0635-0.102 m)
$Npo = 2.57 \pm 0.04$ (T = 0.292 m, D = 0.0635-0.102 m)
6FPT: $Njs \propto D^{-1.66}$ (T = 0.292 m, D = 0.0635-0.102 m)
$Npo = 1.80 \pm 0.02$ (T = 0.292 m, D = 0.0762-0.102 m)
CHEM: $Njs \propto D^{-1.52}$ (T = 0.584 m, D = 0.178-0.229 m)
$Npo = 0.33 \pm 0.01$ (T = 0.584 m, D = 0.178-0.229 m)
$Npo = 0.38 \pm 0.03$ (T = 0.292 m, D = 0.102-0.114 m)

5.6 Scale-Up

The results and discussion presented in the last sections were concerned with the effects of different variables (D, T, and X) on Njs at constant C/T. If the same procedure is followed for the power dissipation (Pjs) at constant C'/T, the results shown in Table 15 can be obtained. By comparison, the exponents of Njs found at constant C'/T are also shown. Figures 18, 19, and 20, show the effect of these variables on Pjs.

It is an accepted practice (Zwietering, 1958; Chapman *et al.* ,1983) to calculate the exponents of the power consumption using the simplified Rushton expression: $Pjs \propto \rho\ Npo\ Njs^3\ D^5$. If the effect of D, T (at constant D/T ratio) and X on Njs, are expressed by the following power law relations:

$$Njs \propto D^d \qquad Njs \propto T^{t'} \qquad Njs \propto X^x \tag{5.26}$$

and combined with the Rushton expression, the following expressions can be obtained:

$$Pjs \propto D^{5+3d} \qquad Pjs \propto T^{5+3t'} \qquad Pjs \propto X^{3x} \tag{5.27}$$

The values of the exponents calculated from the expressions in Equation (5.27) were compared with the experimental values. For the 6FPT and CHEM, Pjs are shown as independent of the impeller diameter. The comparison is also shown in Table 15.

From Table 15, it can be noticed that the experimental values of the exponent over T are always higher than those calculated from the Equation (5.27), for the 6FDT, 6FBT, and 6FPT. This is due to the increase in Pjs (and Npo) observed in the tank of 0.584 m. In the case of CHEM, the experimental value is lower. This seems to be due to the increase in the blade length-to-impeller diameter ratio in the 0.584 m tank size, which reduces the friction loss and therefore produces a decrease in Npo .

Table 15 Exponents of Njs and Pjs Found in this Work
Constant C'/T

			Exponent on Njs			Exponent on Pjs		
Impeller Type	**D/T**	**C'/T**	**D Const. T**	**T Const. D/T**	**X**	**D Const. T**	**T Const. D/T**	**X**
6FDT	0.217-0.348	1/24-1/8	-2.29	-0.82	0.13	-2.13	2.83	0.42
						(-1.87)*	(2.54)*	(0.42)*
6FBT	0.217-0.348	1/24-1/4	-2.05	-0.82	0.13	-1.11	2.84	0.41
						(-1.15)	(2.54)	(0.42)
6FPT	0.217-0.348	1/16-1/4	-1.67	-0.82	0.11	-	2.63	0.34
						(-0.01)	(2.54)	(0.33)
CHEM	0.304-0.391	1/12-1/4	-1.62	-0.78	0.11	-	2.39	0.34
						(0.14)	(2.66)	(0.33)

* Calculated values using the Equation (5.27)

All the tanks were geometrically similar. However, at high tank sizes induced recirculation loops which account for the formation of central and peripheral fillets of unsuspended solids can be present (Chudacek, 1985). These recirculation loops influence the attainment of the complete off-bottom suspension. These fillets are very persistent and required considerable increase in the power consumption to be eliminated. The "scale-up" rules obtained at lower sizes cannot represent the behavior of the bulk of higher sizes. The impact that minor differences in the geometry reflects in the power dissipation was described before. The 0.203 m impeller size presents some difference in the geometry, specially in both the blade width- and the blade length-to-impeller diameter ratio. Also, the rotating shaft could not be completely introduced in these impellers, allowing a center hole under the base. A combination of all these effects seems to explain the difference between the lower tank sizes and the tank of 0.584 m.

5.7 Dual-Impeller Systems

The results obtained by Armenante *et al.* (1992) and Armenante and Li (1993) for multiple radial-flow impellers system led to the conclusion that the phenomenon of solid suspension off the tank bottom is largely dominated by the lower impeller, and that any interference in the flow pattern generated by this impeller, such as those resulting from the presence of more impellers, can result in higher energy requirements to achieve the same result.

The data presented in these works, for the case of two impellers, suggests that when lowering the impeller clearance the minimum agitation speed remains constant or slightly reduces as compared with the case of one impeller. Furthermore, the increase in the power dissipation is lower. When the impellers are closer, at low impeller clearance, the flow pattern of the upper impeller can be switched to that of the "single-eight", and the detrimental effect of the interference between different flow patterns can be avoid. This can be the case for axial-flow impellers (Oldshue, 1983).

In the present work, this observation was investigated. Three types of impellers: 6FDT, 6FBT, and 6FPT (0.0762 m) were investigated in the tank of 0.292 m. In all the cases, impellers of the same type were used in the same shaft. The distance between impellers was equal to the impeller diameter. For the case of the radial-flow impellers, the lower impeller was always in the "single-eight" regime, and the upper impeller in the "double-eight". For the 6FPTs both impellers were positioned in the "single-eight" regime. The comparison with the single impeller was made by positioning the lower impeller at the same impeller clearance. Figures 21, 22, and 23 show the results obtained for each dual-impeller system, respectively.

For the dual-6FDT system, Figure 21(a), the minimum agitation speed and the power consumption always increased. These observations support the detrimental effect produced for the interference of the different flow patterns. The power consumption for the lower impeller was always reduced, while the upper impeller consumed more power (higher impeller clearance). For the lower impeller, the less power consumption seems to be due to the reduction in the resistance to the movement of the impeller.

For the dual-6FBT system, Figure 22(a), the minimum agitation speed showed a slight increase. The total power consumption was twice as compared with the single impeller. The power consumed for each impeller was almost the same. In this case, it seems that in the range of impeller clearance investigated, the interference of the different flow pattern generated is not significant.

In Figure 23(a), the results obtained for the dual-6FPT system are shown. The minimum agitation speed showed a slight decrease. The two impellers consume less power than the single impeller. The interference between different flow patterns was avoided in this system. However, the total power consumption was always higher. It was concluded (see section 5.5) that all the impellers require a minimum power dissipation (as found at C/T = 0) to overcome the resistance to the movement of the static fluid. The net effect for the two impellers is the higher power consumption in the system.

In Figures 21(b), 22(b), and 23(b), the power number have been plotted for each type of impeller. These figures support the conclusions obtained above. The values and tendency observed are very similar to that obtained by Chang (1993), using a system very similar to that used in this work.

CHAPTER 6

EXTENSION OF CORRELATIONS AND APPLICATION OF THEORETICAL MODEL

6.1 Extension of Zwietering (1958) Correlation

The Zwietering correlation was first compared to the experimental data obtained in the present work. Only the values of Njs of the six-blade flat-disk turbine in the "double-eight" regime could be compared, since the geometries of the others impeller are not included in the Zwietering correlation. After this comparison, the Zwietering correlation was extended to the region of very low impeller clearance, for all the type of impellers.

The comparison is shown in Table 16. Since Zwietering (1958) found not effect of the impeller clearance for the six-blade flat-disk turbine, the Njs value is the same for C'/T = 1/4 and 1/6. There is a good agreement between the experimental values and those calculated from the correlation (the difference being close to the experimental error presented by Zwietering: ±10%).

Table 16 Comparison of Njs Values with Zwietering Correlation
Six-Blade Flat-Disk Turbines (6FDT)

	Njs (rpm)								
	D = 0.0635 m D/T = 0.217			**D = 0.0762 m D/T = 0.261**			**D = 0.102 m D/T = 0.348**		
C'/T	**Present work**	**Zwie-tering**	**diffe-rence**	**Present work**	**Zwie-tering**	**diffe-rence**	**Present work**	**Zwie-tering**	**diffe-rence**
1/4	1217	1084	-10.93%	716	704	-1.68%	403	357	-11.41%
1/6	-	-	-	700	704	0.57%	374	357	-4.55%

Zwietering's correlation was extended to include the effect of the impeller clearance, C'/T. All the experimental data were used (when necessary the relationship between C' and C was used: $C'/T = C/T + W_b/2T$). Three types of correlations — linear, exponential, and power — were used:

$$\frac{Njs}{D^d T^t X^x \mu^e dp^f (g\Delta\rho/\rho_l)^g} = a_1(C'/T) + b_1 \tag{6.1a}$$

$$\frac{Njs}{D^d T^t X^x \mu^e dp^f (g\Delta\rho/\rho_l)^g} = a_2 \exp[b_2(C'/T)] \tag{6.1b}$$

$$\frac{Njs}{D^d T^t X^x \mu^e dp^f (g\Delta\rho/\rho_l)^g} = a_3(C'/T)^{b3} \tag{6.1c}$$

From the relation between Njs and D and T :

$$Njs \propto D^d T^t = (D/T)^d T^{t+d} = (D/T)^d T^{t'} \tag{6.2}$$

it follows that:

$$t = t' - d \tag{6.3}$$

where both t' and d (also x) can be obtained from Table 15. Hence, it was possible to calculate t for each of the (6.1) equations. For the case of the 6FDT, a value of 1.47 (= -0.82 + 2.29) was obtained for t. Similarly, values of 1.25 (= -0.82 + 2.07), 0.85 (= -0.82 + 1.67), and 0.84 (= -0.78 + 1.62) for t could be obtained for the 6FBT, 6FPT, and CHEM, respectively. These exponents were found for each type of impeller, whereas, Zwietering correlation is for both radial-flow and axial-flow impellers. It appears that the effects of impeller and tank diameter are different for different impeller designs (Raghava Rao *et al.*, 1988b).

For the exponent on ν, dp, and ($g\ \Delta\rho/\rho$), the values reported by Zwietering (1958) were assumed. These values are very similar to those reported by other authors. For the case of the viscosity (ν), a value of 0.1 is also reported by Raghava Rao *et al.* (1988b) and Aravinth *et al.* (1996) for 6FPT and 6FBT, respectively; Chapman *et al.* (1983) observed no significant effect of the viscosity for various type of impellers, and Baldi *et al.* (1978) model suggests an exponent of 0.23, for eight-blade flat-disk turbine (C'/D = 1). The value of 0.45 of the exponent on the dimensionless density ($g\ \Delta\rho/\rho$) seems to be the most accepted (Raghava Rao *et al.*, 1988b; Myers *et al.*, 1994b; Aravinth *et al.*, 1996); Nienow (1968) and Narayanan *et al.* (1969) reported values of 0.43 and 0.5, respectively. The effect of the particle size (dp) on Njs seems to depend of the hydraulic regime and the range of the particle size. A theoretical value of 0.16 for turbulent settling was reported by Chudacek (1986). Myers *et al.* (1994b) found an exponent of 0.2 in the range examined (85-19100 μm). Similar value is found in other works (Nienow, 1968; Aravinth *et al.*, 1996). In general, the exponents of these variables have been found to be independent of the impeller clearance (Zwietering, 1958; Raghava Rao *et al.*, 1988b).

For each type of correlation, the constants a's and b's and the standard deviation were determined. As found in the preliminary correlations for Njs and Pjs in the section 5.1, the power law form was very poor in all cases. The exponential form was slightly superior to the linear form. In Table 17, the final correlations are shown. The agreement between the experimental values and the correlations presented are good, the maximum deviation being of $\pm$5.44%, $\pm$2.72%, $\pm$3.43%, and $\pm$2.87%, for the 6FDT, 6FBT, 6FPT, and CHEM, respectively. Graphical comparison are shown in Figure 24(a, b, c, d).

Table 17 Extension of Zwietering Correlation

For flat-bottom tank, fully baffled[+]:

Six-Blade Flat-Disk Turbine:

$$Njs' = \frac{0.91\ \nu^{0.1}\, dp^{0.2}\, (g\Delta\rho/\rho_l)^{0.45}\, T^{1.47}\, X^{0.13} \exp(2.15\ C'/T)}{D^{2.29}} \qquad (6.4)$$

T = 0.188-0.584 m, D = 0.0635-0.203 m, C'/T < 0.16
Glass beads, dp = 110 μm, ρ_s = 2,500 Kg/m^3, X = 0.5-1.5 wt/wt%, Tap water at 22°C

Six-Blade Flat-Blade Turbine:

$$Njs' = \frac{1.40\ \nu^{0.1}\, dp^{0.2}\, (g\Delta\rho/\rho_l)^{0.45}\, T^{1.25}\, X^{0.13} \exp(1.96\ C'/T)}{D^{2.07}} \qquad (6.5)$$

T = 0.188-0.584 m, D = 0.0635-0.203 m, C'/T < 0.21
Glass beads, dp = 110 μm, ρ_s = 2,500 Kg/m^3, X = 0.5-1.5 wt/wt%, Tap water at 22°C

Six-Blade Flat (45°) Pitched-Blade Turbine:

$$Njs' = \frac{2.33\ \nu^{0.1}\, dp^{0.2}\, (g\Delta\rho/\rho_l)^{0.45}\, T^{0.87}\, X^{0.11} \exp(0.65\ C'/T)}{D^{1.67}} \qquad (6.6)$$

T = 0.188-0.584 m, D = 0.0635-0.203 m, C'/T < 0.26
Glass beads, dp = 110 μm, ρ_s = 2,500 Kg/m^3, X = 0.5-1.5 wt/wt%, Tap water at 22°C

Chemineer HE-3 Impeller:

$$Njs' = \frac{3.72\ \nu^{0.1}\, dp^{0.2}\, (g\Delta\rho/\rho_l)^{0.45}\, T^{0.84}\, X^{0.11} \exp(0.72\ C'/T)}{D^{1.62}} \qquad (6.7)$$

T = 0.292-0.584 m, D = 0.102-0.229 m, C'/T < 0.25
Glass beads, dp = 110 μm, ρ_s = 2,500 Kg/m^3, X = 0.5-1.5 wt/wt%, Tap water at 22°C

[+] Njs' in rps

6.2 Application of Baldi *et al.* (1978) Theoretical Model

The theoretical model developed by Baldi *et al.* (1978) was also applied to the experimental values obtained in this work. The experimental approach was similar and the expression given in Equation (3.5) was used:

$$Z \propto Rem^{n}$$

A log-log plot (Z against 1/Rem), for C'/D ratios of 1/2, 1/4, and 1/5, are shown in Figure 25(a, b, c, d), for each type of impellers. In each case (C'/D ratio and impeller type), the Z values were found to be independent of D/T (Baldi *et al.*, 1978; Chapman *et al.*, 1983).

For the case of the 6FDT, Figure 25(a), at C'/D = 1/2, the 0.102 m impeller size was found in the regime of the "double-eight". When this value is discarded, the relationship between the Z values and the Rem can be expressed as:

$$Z \propto Rem^{0.51} \qquad (C'/D = 1/2) \qquad (6.8)$$

$$Z \propto Rem^{0.56} \qquad (C'/D = 1/4) \qquad (6.9)$$

$$Z \propto Rem^{0.62} \qquad (C'/D = 1/5) \qquad (6.10)$$

This suggests a strong effect of the Rem on the Z values at very low impeller clearance.

From Figure 25(b), for the case of the 6FBT, the relationship between the Z values and the modified Reynolds number can be expressed as:

$$Z \propto Rem^{0.17} \qquad (C'/D = 1/2) \qquad (6.11)$$

$$Z \propto Rem^{0.29} \qquad (C'/D = 1/4) \qquad (6.12)$$

$$Z \propto Rem^{030} \qquad (C'/D = 1/5) \qquad (6.13)$$

The effect of the Rem on the Z values is lower than for the 6FDT.

For the 6FPT, Figure 25(c), the following expressions are found:

$$Z = 1.83 \pm 0.02 \qquad (C'/D = 1/2) \qquad (6.14)$$

$$Z \propto Rem^{0.04} \qquad (C'/D = 1/4) \qquad (6.15)$$

$$Z \propto Rem^{0.10} \qquad (C'/D = 1/5) \qquad (6.16)$$

For this case the Z values depend only slightly of the Rem.

For the case of the CHEM, for all the values of C/D, Z was found to be independent of the Rem:

$$Z = 2.36 \pm 0.06 \qquad (C'/D = 1/2) \qquad (6.17)$$

$$Z = 2.45 \pm 0.04 \qquad (C'/D = 1/4) \qquad (6.18)$$

$$Z = 2.43 \pm 0.06 \qquad (C'/D = 1/5) \qquad (6.19)$$

For this case, the Z values do not depend of the Rem.

The exponents found for each type of impellers are very close, independent of the C'/D ratio. A statistical analysis shows that there is no need to complicate the Equation (3.5) by considering individual C'/D ratios. In this case, the following relationships between the Z values and the Rem can be found:

$$Z \propto Rem^{0.56 \pm 0.06} \qquad (6FDT) \qquad (6.20)$$

$$Z \propto Rem^{0.24 \pm 0.06} \qquad (6FBT) \qquad (6.21)$$

$$Z = 1.84 \pm 0.03 \qquad (6FPT) \qquad (6.22)$$

$$Z = 2.41 \pm 0.06 \qquad (CHEM) \qquad (6.23)$$

These results show the insensitivity of the exponents on the different variables to variations of the impeller clearance as revealed by several authors (Zwietering, 1958; Nienow, 1968; Chapman *et al.*, 1983; Raghava Rao *et al.*, 1988b).

Although, only one tank size (0.292 m) and one solids loading (0.5 wt/wt%) were used, the results obtained in this work appear to be in disagreement with the experimental observations of Baldi *et al.* (1978) and Chapman *et al.* (1983). Baldi *et al.* (1978) found for eight-blade flat-disk turbines, that the dimensionless group Z (or the local dissipated power to average dissipated power) was not affected by the hydrodynamic conditions very near to the tank bottom (as low as C'/D = 0.5). Chapman *et al.* (1983) confirmed this experimental result at C'/D = 0.5 for 6FDT, and found that the Baldi *et al.* model was not successful for other geometries. The inadequacy of this model can be attributed to the complex flow, which cannot be described by a simple equation (Nienow, 1985). In this work, for the 6FDT in the 0.292 m tank, at C'/D = 0.5 ratio, the 0.102 m impeller size was found in the "double-eight" regime. For the other sizes, a value of 1.22±0.05 for Z can be found (1.18±0.08 for the three sizes) apparently in agreement with Baldi *et al.* (2 for eight-blade flat-disk turbine) and Chapman *et al.* (1.17±0.15 for 6FDT). However, at lower C'/D ratios (1/4 and 1/5), the effect of the hydrodynamic conditions is significant. It must be noticed that the description of the solids suspension given by Baldi *et al.* (1978) in their work corresponds to the "double-eight" regime, and the experimental observation of Chapman *et al.* (1983) was conducted using a value of C'/T = 1/4, corresponding also this value to the "double-eight" regime. Unlike these studies, in this work, the application of the model was performed in the "single-eight" regime, with the impeller very near to the tank bottom. Although this represents the best attempt at a theoretical analysis of the solids suspension, there are certain doubts on the application of the Baldi *et al.* model very near to the tank bottom (Witcherle, 1988).

A similar analysis was conducted using C'/T as the parameter for the impeller clearance, Figure 26(a, b, c, d), the following relationships were found:

$$Z \propto Rem^{0.91\pm0.15} \qquad (6FDT) \qquad (6.24)$$

$$Z \propto Rem^{0.40\pm0.03} \qquad (6FBT) \qquad (6.25)$$

$$Z \propto Rem^{0.05\pm0.01} \qquad (6FPT) \qquad (6.26)$$

$$Z = 2.37\pm0.09 \qquad (CHEM) \qquad (6.27)$$

From both results (at constant C'/D and constant C'/T), it seems that the effect of the Rem is stronger for the six-blade flat-disk turbines, lower for the six-blade flat-blade turbines, almost independent for the six-blade flat (45°) pitched-blade turbines, and of no importance for the Chemineer HE-3 impellers. In other words, this effect decreases from radial-flow impellers to axial-flow impellers:

$$6FDT > 6FBT > 6FPT > CHEM \qquad (6.28)$$

Using the exponents found for the Rem, Equation (3.6) was used to calculate the exponents on the different variables, for each type of impellers. The resulting exponents are shown in Table 18 and Table 19, for constant C'/D and constant C'/T, respectively.

An inspection of the exponents in Table 19 reveals that the major deviation with the experimental values obtained by Zwietering (1958) lies in the exponent over the viscosity: +380%. For the density difference and particle size, a maximum deviation of -42% and -55% can be observed, respectively. From Table 17 and Table 19, the exponents on the tank diameter (at constant D) show a maximum deviation of -40%. In all cases, the maximum deviation is observed for the 6FDT. The exponents on the solids loading was not accounted here, this calculation has been postponed to the following section.

Table 18 Application of Baldi *et al.* Model to Various Impeller Configurations Constant C'/D

			Exponent on						
Case	**Impeller Type**	**C'/D**	**Rem**	**ν**	**dp**	**X**	**Δρ**	**T Const. D**	**Npo**
This work	6FDT	1/5-1/2	0.56	0.36	0.11	-	0.32	-1.15	-0.22
	6FBT	1/5-1/2	0.24	0.19	0.13	-	0.40	-0.92	-0.27
	6FPT	1/4-1/2	0.00	0.00	0.17	-	0.50	-0.67	-0.32
	CHEM	1/4-1/2	0.00	0.00	0.17	-	0.50	-0.67	-0.33

Table 19 Application of Baldi *et al.* Model to Various Impeller Configurations Constant C'/T

			Exponent on						
Case	**Impeller Type**	**C'/T**	**Rem**	**ν**	**dp**	**X**	**Δρ**	**T Const. D**	**Npo**
This work	6FDT	1/48-1/8	0.91	0.48	0.09	-	0.26	-1.30	-0.17
	6FBT	1/48-1/5	0.40	0.29	0.12	-	0.36	-1.05	-0.24
	6FPT	1/16-1/4	0.05	0.05	0.16	-	0.48	-0.73	-0.32
	CHEM	1/16-1/4	0.00	0.00	0.17	-	0.50	-0.67	-0.33

6.3 Extension of Baldi *et al.* (1978) Theoretical Model

The theoretical model of Baldi *et al.* (1978) was extended to include the impeller clearance and solids loading effects. The experimental results were interpreted on the basis of the dimensionless numbers Z, Rem, C'/T, and X:

$$Z = f(Rem, C'/T, X) \tag{6.29}$$

Following the experimental approach of Baldi *et al.* (1978), Conti *et al.* (1981) interpreted their results using the dimensionless numbers Z, Rem, Npo, C'/D, T/D, and X, for eight-blade flat-disk turbine. Since Z was found to be independent of T/D, they used an expression similar to Equation (6.29). When the Conti *et al.* correlation, Equation (3.13), is used to calculate Njs for the 6FDT, the values are always higher than the experimental Njs, Table 20. This correlation was deduced for eight-blade flat-disk turbines. Since Njs increases with a decrease of the number of blades (Chapman *et al.*, 1983), and also with a decrease in the power number (deduced from the correlation), the agreement improves.

Table 20 Comparison of Njs Values with Conti *et al.* Correlation
Six-Blade Flat-Disk Turbine (6FDT)

	Njs (rpm)								
	D = 0.0635 m D/T = 0.217			**D = 0.0762 m D/T = 0.261**			**D = 0.102 m D/T = 0.348**		
C'/T	**Present work**	**Conti *et al.***	**diffe-rence**	**Present work**	**Conti *et al.***	**diffe-rence**	**Present work**	**Conti *et al.***	**diffe-rence**
1/8	815	655	-19.63%	524	439	-16.22%	275	232	-15.64%
1/16	719	572	-20.45%	455	397	-12.75%	241	204	-15.35%
1/24	682	550	-19.35%	426	370	-13.15%	234	196	-16.24%

From the observation of the experimental results, the following expression between Z an X can be obtained:

$$Z \propto X^m \tag{6.30}$$

This is in agreement with the experimental results obtained by Baldi *et al.* (1978) and Conti *et al.* (1981). When this expression is combined with the Equation (3.5), the following expression can be obtained:

$$Z = Rm^n X^m f(C'/T) \tag{6.31}$$

Similarly to the extension of the Zwietering correlation, three types of correlations were tested for the effect of C'/T — linear, exponential, and power. Previously, the correlation was conducted using only the experimental values of Njs and Npo obtained for the tank of 0.292 m. When the values obtained for the tanks of 0.188 m, 0.244 m, and 0.584 m were included, the agreement found was always poor. This suggests a disadvantage of these correlations when scaling-up. Conti *et al.* correlation was conducted using only one tank size (0.19 m). The values for T = 0.584 m were discarded since the Npo obtained in this tank were unusual high for the 6FDT, 6FBT, and 6FPT. For the same reason the 0.0635 m 6FPT was not considered in the correlations. Since $Njs \propto T^t$, at constant D, and based on the observation given above, the following scale-up rule was used:

$$Njs/T \propto T^{t-1} \tag{6.32}$$

From Section 6.1 the exponents (t-1) can be obtained: 0.47 (= 1.47 - 1), 0.25 (= 1.25 - 1), and -0.15 (= 0.85 - 1) for the 6FDT, 6FBT, and 6FPT, respectively. Hence, Z and Rem can be corrected in the following way:

$$Z^* = Z\,(\,T/0.292\,)^{1-t} \tag{6.33}$$

$$Rem^* = Rem\,(T/0.292)^{t-1} \tag{6.34}$$

Among the correlations tested, the exponential form gave the best results. The effect of C'/T on both Njs and Npo are included in the exponential form. The correlations obtained are shown in Table 21. For the CHEM, according to the observation given before, two separated set of correlations for each tank size are shown.

The results obtained support the conclusions drawn before. When the impeller is very near to the tank bottom, the hydrodynamic conditions affect more to the radial-flow impellers than the mixed axial- and axial-flow impellers.

From the correlations in Table 21, expressions for Njs can be deduced using Equation (3.6), These correlations are shown in Table 22, for 6FDT, 6FBT, and 6FPT, and in Table 23 for CHEM. Experimental Njs values have been plotted against calculated Njs values in Figure 27(a, b, c, d). The agreement between the experimental Njs and the correlations are good, the maximum deviation being of ±5.20%, ±4.81%, ±2.02%, and ±2.81% for the 6FDT, 6FBT, 6FPT, and CHEM, respectively. Similarly to Section 6.2, Table 22 and Table 23 show a big discrepancy in the exponent on the viscosity: +360%., when compared to the Zwietering correlation The maximum deviation for the density difference, particle size, and tank diameter (constant D) are -40%, -56%, and -40% respectively. Again, these maximum deviations occur for the 6FDT. The exponents on the solids loading show a good agreement with the experimental values obtained in this work (maximum deviation = ±15%). The effect of the impeller clearance are very similar to that found in the extension of the Zwietering correlation.

Table 21 Extension of Baldi *et al.* Model

For flat-bottom tanks, fully baffled[+]:

Six-Blade Flat-Disk Turbines: (t-1 = 0.47)

$$Z^* = 0.00050 \exp(-4.72\ C'/T)\ Rem^{*0.86}\ X^{-0.28} \quad (6.35)$$

T = 0.188-0.292 m, D = 0.0635-0.103 m, C'/T< 0.16
Glass beads, dp = 110 μm, ρ_s = 2,500 Kg/m^3, X= 0.5-1.5 wt/wt%, Tap water at 22°C

Six-Blade Flat-Blade Turbines: (t-1 = 0.25)

$$Z^* = 0.035 \exp(-2.42\ C'/T)\ Rem^{*0.40}\ X^{-0.18} \quad (6.36)$$

T = 0.188-0.292 m, D = 0.0635-0.103 m, C'/T < 0.21
Glass beads, dp = 110 μm, ρ_s = 2,500 Kg/m^3, X= 0.5-1.5 wt/wt%, Tap water at 22°C

Six-Blade Flat (45°) Pitched-Blade Turbine: (t-1 = -0.15)

$$Z^* = 2.07 \exp(-0.26\ C'/T)\ Rem^{*-0.016}\ X^{-0.10} \quad (6.37)$$

T = 0.188-0.292 m, D = 0.0635-0.102 m, 0.0625 < C'/T < 0.26
Glass beads, dp = 110 μm, ρ_s = 2,500 Kg/m^3, X= 0.5-1.5 wt/wt%, Tap water at 22°C

Chemineer HE-3 Impeller:

$$Z^* = 2.60 \exp(-0.66\ C'/T)\ Rem^{*-0.020}\ X^{-0.11} \quad (6.38)$$

T = 0.292 m, D = 0.103-0.114 m, 0.0125 < C'/T < 0.25

$$Z^* = 1.96\ X^{-0.11} \quad (6.39)$$

T = 0.292 m, D = 0.103-0.114 m, 0.0625 < C'/T < 0.125

$$Z^* = 2.62 \exp(-0.69\ C'/T)\ Rem^{*-0.0058}\ X^{-0.11} \quad (6.40)$$

T = 0.584 m, D = 0.217-0.348 m, 0.0125 < C'/T < 0.25

$$Z^* = 2.23\ X^{-0.11} \quad (6.41)$$

T = 0.584 m, D = 0.217-0.348 m, 0.0625 < C'/T < 0.125
Glass beads, dp = 110 μm, ρ_s = 2,500 Kg/m^3, X = 0.5-1.5 wt/wt%, Tap water at 22°C

[+] Npo calculated from correlations in Table 10, Njs' in rps

Table 22 Expressions for Njs deduced from Z* Correlations 6FDT, 6FBT, and 6FPT

For flat-bottom tanks, fully baffled[+]:

Six-Blade Flat-Disk Turbines:

$$Njs' = \frac{58.94\ \nu^{0.46}\, dp^{0.089}\, (g\Delta\rho/\rho_l)^{0.27}\, T\, X^{0.15} \exp(2.53\ C'/T)}{Npo^{0.18}\, D^{2.28}} \qquad (6.42)$$

T = 0.188-0.292 m, D = 0.0635-0.203 m, C'/T < 0.16
Glass beads, dp = 110 μm, ρ_s = 2,500 Kg/m^3, X = 0.5-1.5 wt/wt%, Tap water at 22°C

Six-Blade Flat-Blade Turbines:

$$Njs' = \frac{10.94\ \nu^{0.28}\, dp^{0.12}\, (g\Delta\rho/\rho_l)^{0.36}\, T\, X^{0.13} \exp(1.73\ C'/T)}{Npo^{0.24}\, D^{205}} \qquad (6.43)$$

T = 0.188-0.292 m, D = 0.0635-0.203 m, C'/T < 0.21
Glass beads, dp = 110 μm, ρ_s = 2,500 Kg/m^3, X = 0.5-1.5 wt/wt%, Tap water at 22°C

Six-Blade Flat (45°) Pitched Blade Turbine:

$$Njs' = \frac{0.48\ \nu^{-0.016}\, dp^{017}\, (g\Delta\rho/\rho_l)^{0.51}\, T\, X^{0.10} \exp(0.27\ C'/T)}{Npo^{0.34}\, D^{1.65}} \qquad (6.44)$$

T = 0.188-0.292 m, D = 0.0635-0.203 m, 0.0625 < C'/T < 0.26
Glass beads, dp = 110 μm, ρ_s = 2,500 Kg/m^3, X = 0.5-1.5 wt/wt%, Tap water at 22°C

[+] Npo calculated from correlations in Table 10, Njs' in rps

Table 23 Expressions for Njs deduced from Z* Correlations
CHEM

For flat-bottom tanks, fully baffled[+]:

Chemineer HE-3 Impeller:

$$Njs' = \frac{0.38\ \nu^{-0.02}\, dp^{0.17}\, (g\Delta\rho/\rho_l)^{0.51}\, T\, X^{0.12} \exp(\ 0.68\ C'/T\ )}{Npo^{0.34}\, D^{1.64}} \qquad (6.45)$$

T = 0.292 m, D = 0.103-0.114 m, $0.125 < C'/T < 0.25$

$$Njs' = \frac{0.51\ dp^{0.17}\, (g\Delta\rho/\rho_l)^{0.50}\, T\, X^{0.11}}{Npo^{0.33}\, D^{1.67}} \qquad (6.46)$$

T = 0.292 m, D = 0.103-0.114 m, $0.0625 < C'/T < 0.125$

$$Njs' = \frac{0.38\ \nu^{-0.006}\, dp^{0.17}\, (g\Delta\rho/\rho_l)^{0.50}\, T\, X^{0.11} \exp(\ 0.69\ C'/T\ )}{Npo^{0.34}\, D^{1.66}} \qquad (6.47)$$

T = 0.584 m, D = 0.217-0.348 m, $0.125 < C'/T < 0.25$

$$Njs' = \frac{0.45\ dp^{0.17}\, (g\Delta\rho/\rho_l)^{0.50}\, T\, X^{0.11}}{Npo^{0.33}\, D^{1.67}} \qquad (6.48)$$

T = 0.584 m, D = 0.217-0.348 m, $0.0625 < C'/T < 0.125$
Glass beads, dp = 110 μm, ρ_s = 2,500 Kg/m^3, X = 0.5-1.5 wt/wt%, Tap water at 22°C

[+] Npo calculated from correlations in Table 10, Njs' in rps

CHAPTER 7

CONCLUSIONS

- Mixed axial-flow and axial-flow impellers are more efficient than the radial-flow impellers for complete off-bottom suspension, when the impeller is positioned close to the tank bottom. However, in the range in which the throttling effect is significant, the efficiency of the mixed axial-flow and axial-flow impellers decreases.
- The exponents for the impeller diameter, tank diameter, and solids loading in the Njs equations are very similar to those reported in the literature, in particular, to those presented by Zwietering (1958). The impeller off-bottom clearance does not appear to affect these values.
- During scale-up, the effects of minor dimensions and minor differences in geometry are significant for power consumption. These effects are not significant for scaling-up the minimum agitation speed, for complete off-bottom suspension.
- Although, some improvement in the minimum agitation speed has been noticed, the presence of a second impeller — with the lower impeller positioned very near to the tank bottom — increases the total power consumption. This increase in the power consumption does not justify the use of two impellers for the task of complete off-bottom suspension.
- The extension of the Zwietering's correlation allows a prediction of the effect of the impeller clearance very near to the tank bottom. This effect was included in a modification of the Zwietering's equation using an exponential term.

The application of the Baldi *et al.* (1978) model, when the impeller is placed very close to the tank bottom, reveals that the effect of the hydrodynamic conditions is more significant for the radial-flow impellers than the mixed axial-flow and axial-flow impellers. The results obtained here are in disagreement with the experimental observations of Baldi *et al.* (1978) and Chapman *et al.* (1983). However, in their studies the application of the model was conducted in the "double-eight" regime, while in this work the model was applied to the "single-eight" regime. The extension of the model to include the effect of the impeller clearance was successful; although, corrections for the dimensionless group, Z, and the modified Reynolds number were required for scaling-up. The expressions for Njs deduced after this extension show a big discrepancy in the effect of the viscosity when compared to the Zwietering's correlation.

APPENDIX A

FIGURES FOR CHAPTER 5 AND 6

This appendix includes the figures described in Chapter 5 (Results and Discussion) and Chapter 6 (Extension of Correlations and Application of Theoretical Model). For the effect of the impeller clearance, these figures include:

Effect on Njs, Pjs, and Npo (Figure 5-Figure 7)

Npo correlation (Figure 8)

Comparison at constant D/T (Figure 9-Figure 11)

For the effects of impeller diameter, tank diameter, and solids loading, these figures include:

Effects of D, T, and X on Njs (Figure 12-Figure 17)

Effects of D, T, and X on Pjs (Figure 18-Figure 20)

For dual-impeller systems, these figures include:

Dual-6FDT System (Figure 21)

Dual-6FBT system (Figure 22)

Dual-6FPT system (Figure 23)

For the extension of correlations and application of theoretical model, these figures include:

Extension of Zwietering Correlation (Figure 24)

Effect of Rem on Z Values (Figure 25-Figure 26)

Extension of Baldi *et al.* model (Figure 27)

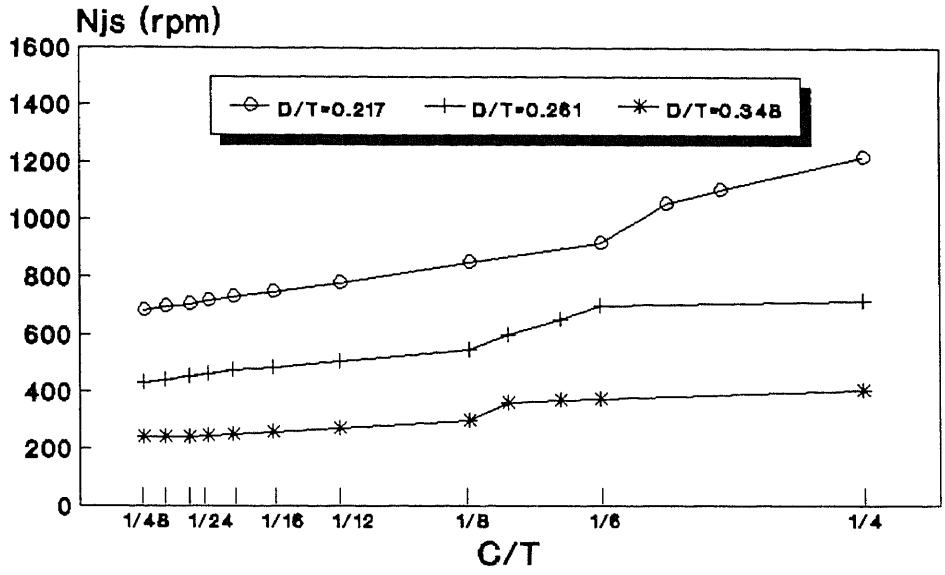

T=0.292 m, X=0.5 wt/wt%

Figure 5(a) Effect of C/T on Njs (6FDT)

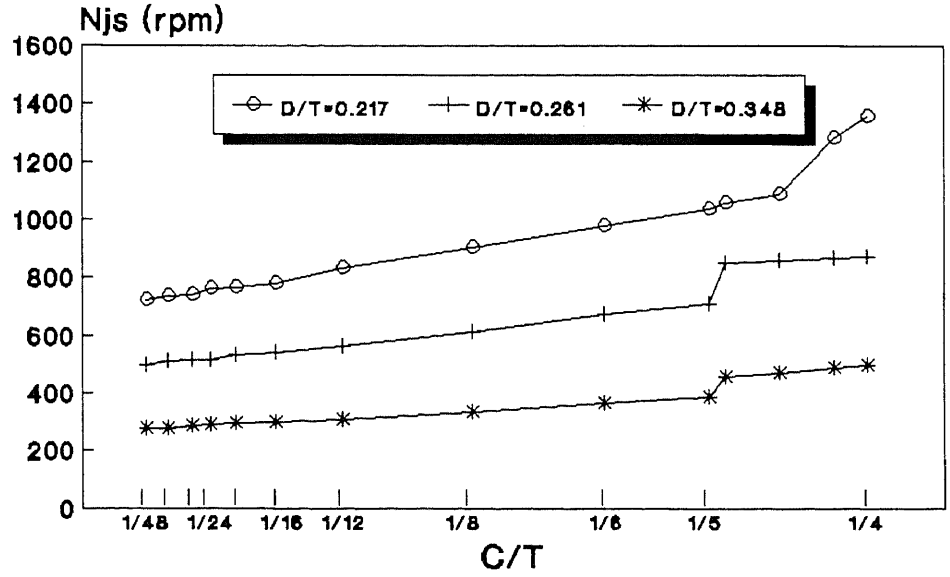

T=0.292 m, X=0.5 wt/wt%

Figure 5(b) Effect of C/T on Njs (6FBT)

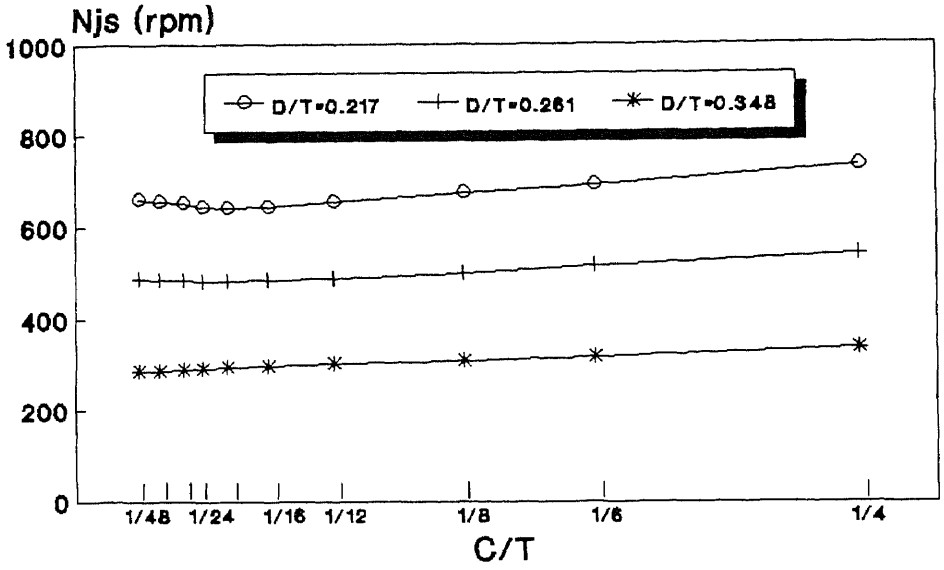

T=0.292 m, X=0.5 wt/wt%

Figure 5(c) Effect of C/T on Njs (6FPT)

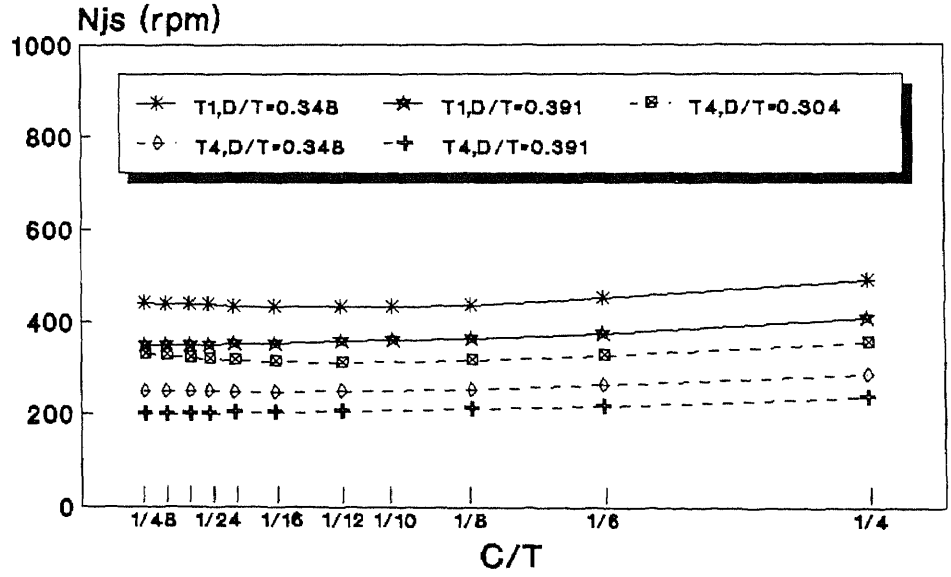

T1=0.292 m, T4=0.584 m, X=0.5 wt/wt%

Figure 5(d) Effect of C/T on Njs (CHEM)

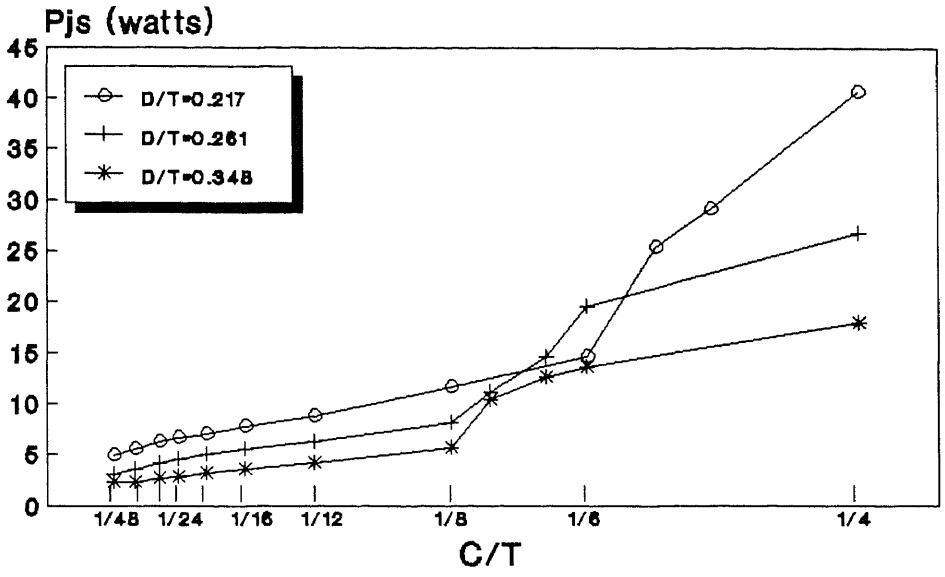

T=0.292 m, X=0.5 wt/wt%

Figure 6(a) Effect of C/T on Pjs (6FDT)

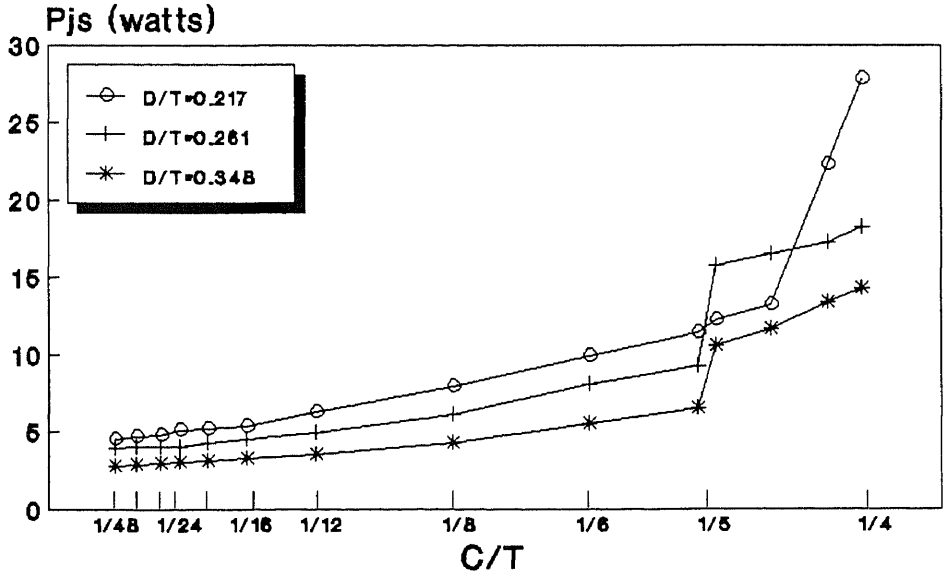

T=0.292 m, X=0.5 wt/wt%

Figure 6(b) Effect of C/T on Pjs (6FBT)

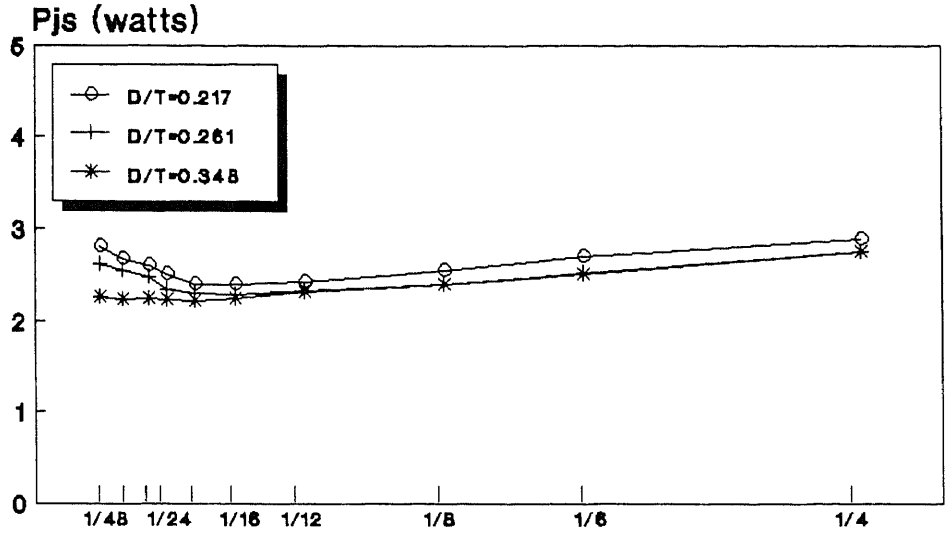

T=0.292 m, X=0.5 wt/wt%

Figure 6(c) Effect of C/T on Pjs (6FPT)

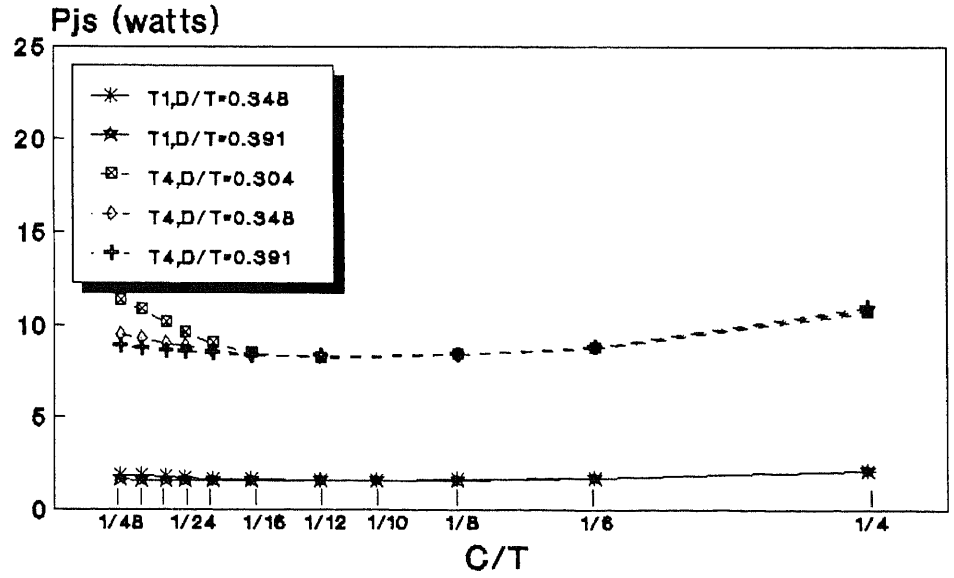

T1=0.292 m, T4=0.584 m, X=0.5 wt/wt%

Figure 6(d) Effect of C/T on Pjs (CHEM)

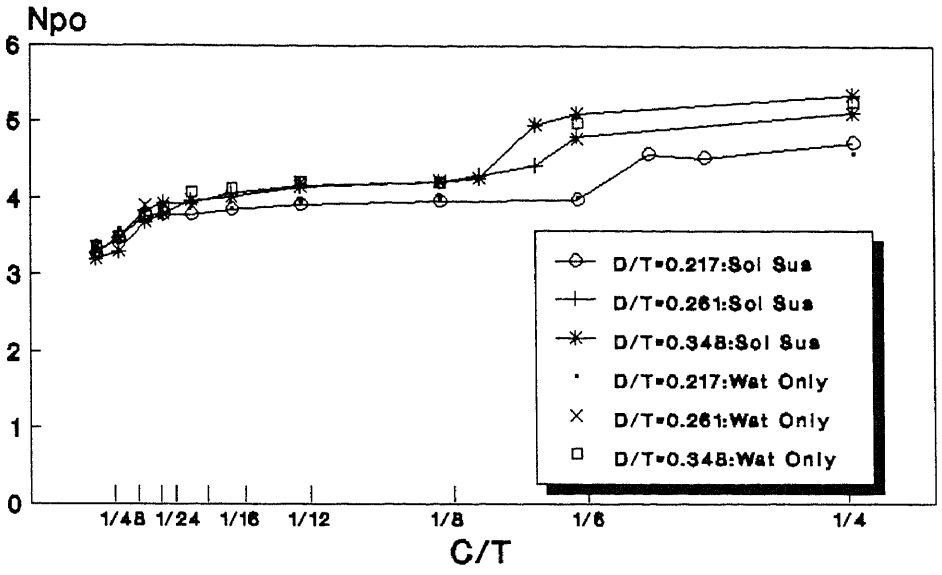

T=0.292 m, X=0.5 wt/wt%

Figure 7(a) Effect of C/T on Npo (6FDT)

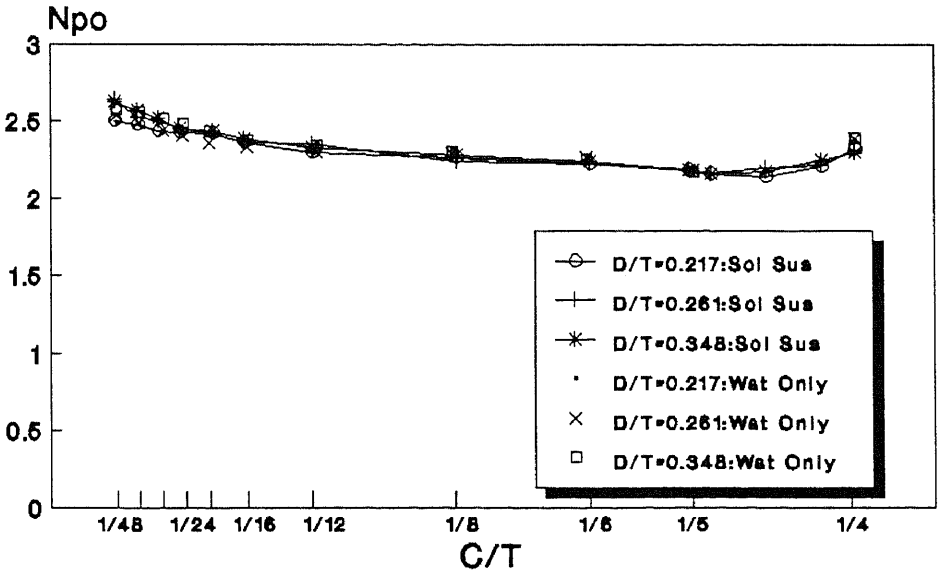

T=0.292 m, X=0.5 wt/wt%

Figure 7(b) Effect of C/T on Npo (6FBT)

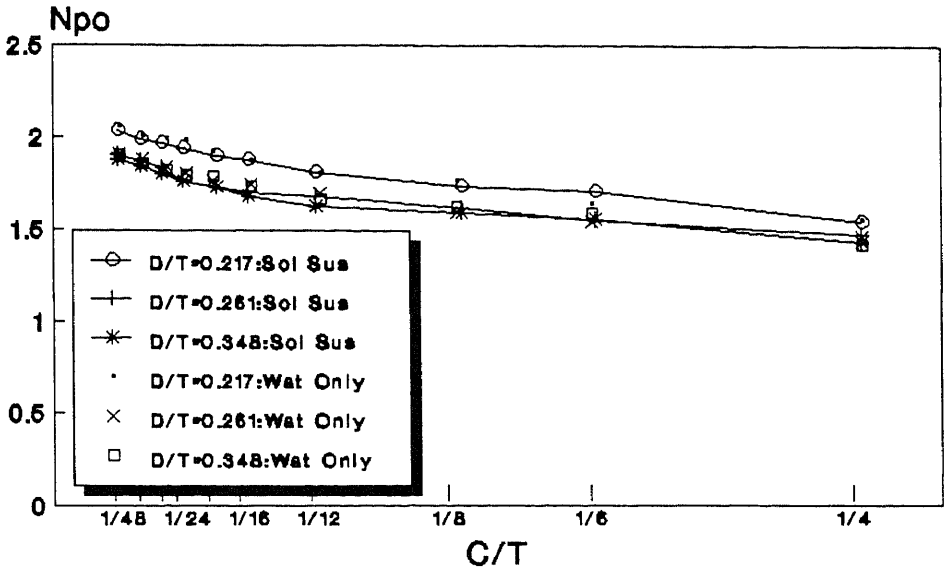

T=0.292 m, X=0.5 wt/wt%

Figure 7(c) Effect of C/T on Npo (6FPT)

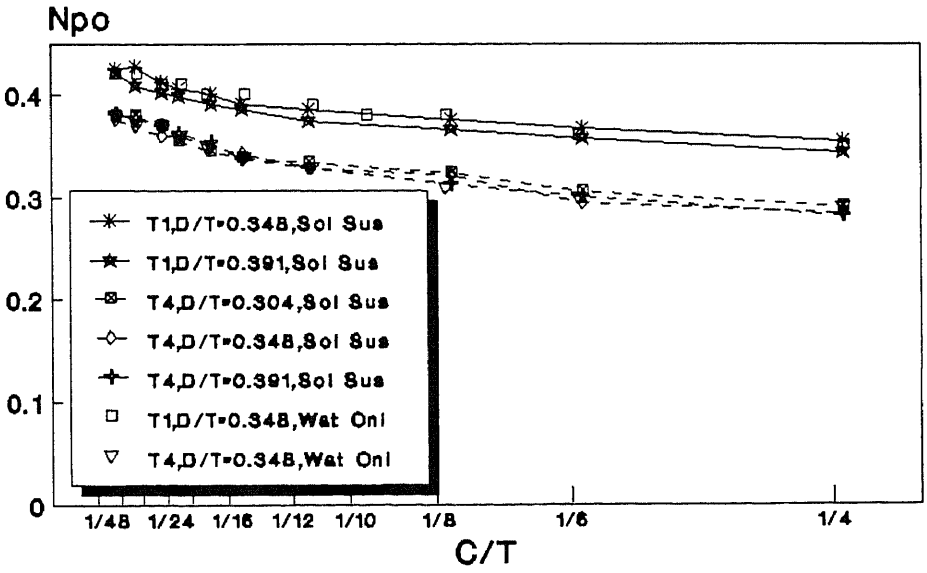

T1=0.292 m, T4=0.584 m, X=0.5 wt/wt%

Figure 7(d) Effect of C/T on Npo (CHEM)

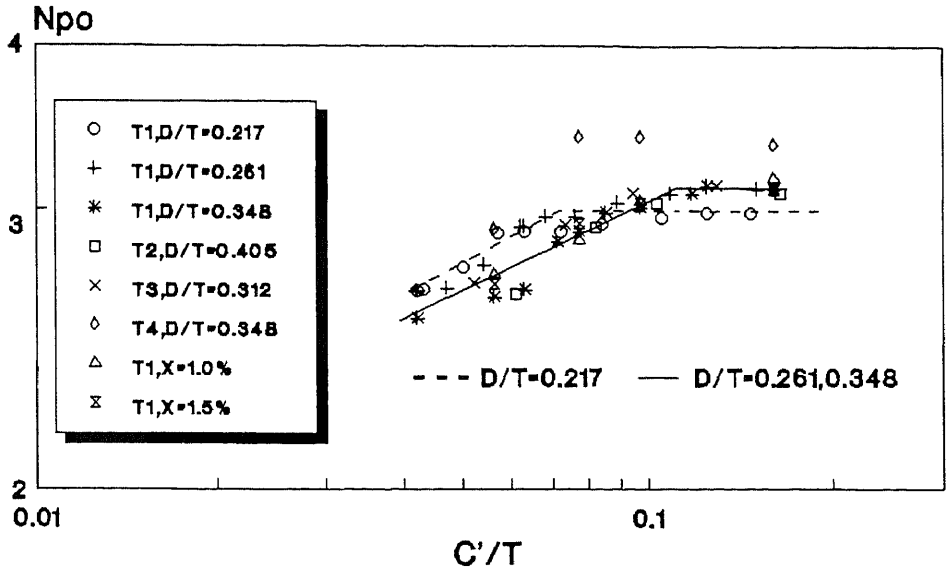

T1=0.292m,T2=0.188m,T3=0.244m,T4=0.584m

Figure 8(a) Power Number Correlation (6FDT)

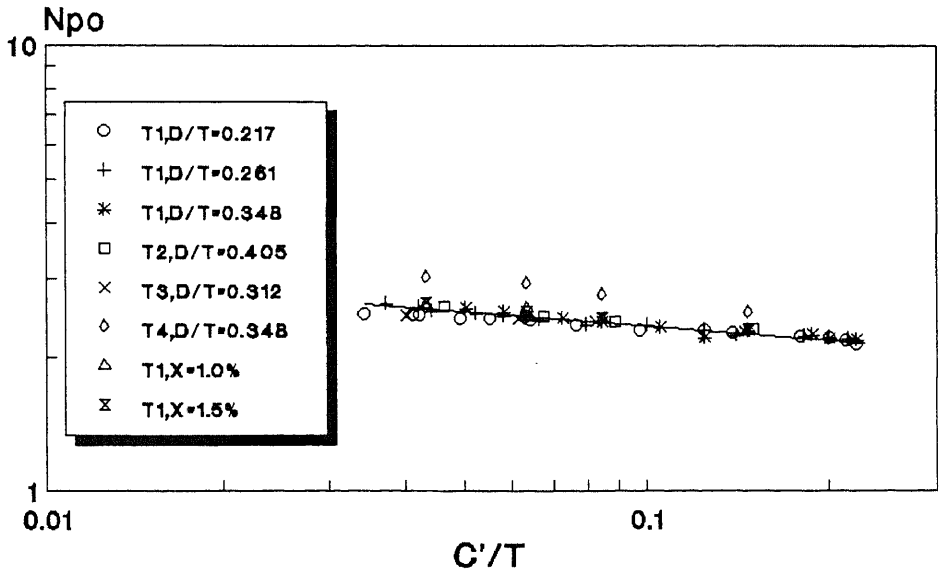

T1=0.292m,T2=0.188m,T3=0.244m,T4=0.584m

Figure 8(b) Power Number Correlation (6FBT)

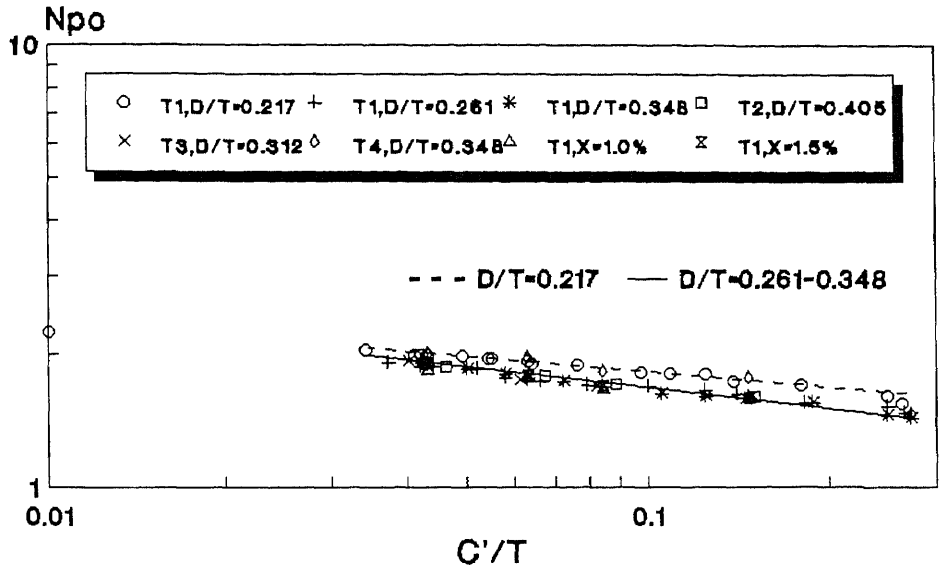

T1=0.292m,T2=0.188m,T3=0.244m,T4=0.584m

Figure 8(c) Power Number Correlation (6FPT)

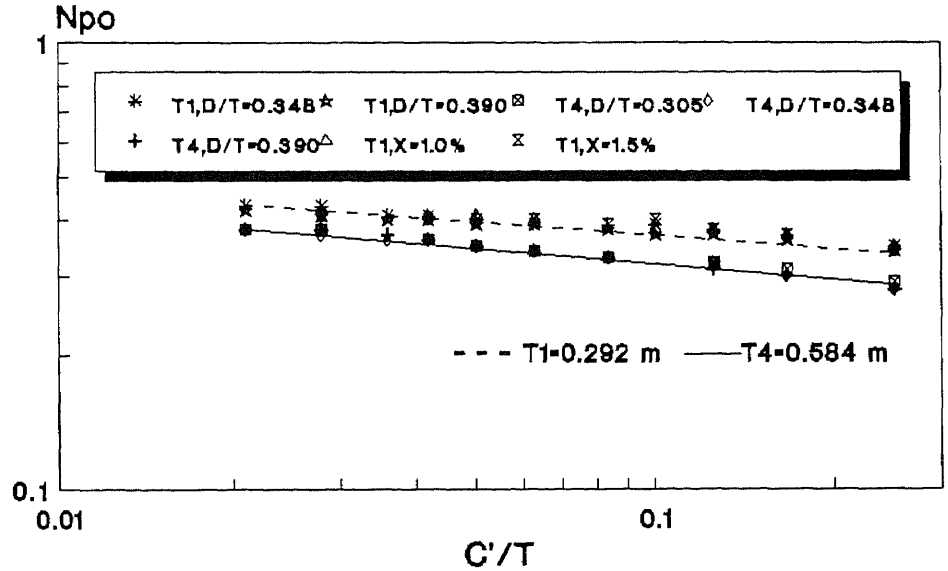

T1=0.292 m,T4=0.584 m

Figure 8(d) Power Number Correlation (CHEM)

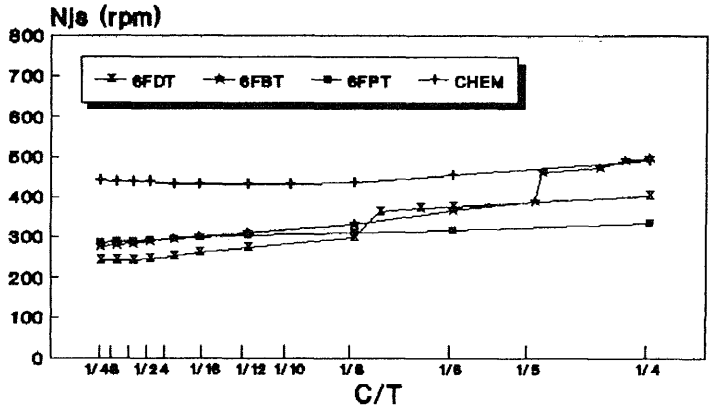

Figure 9(a) Comparison at D/T=0.348 (Njs)

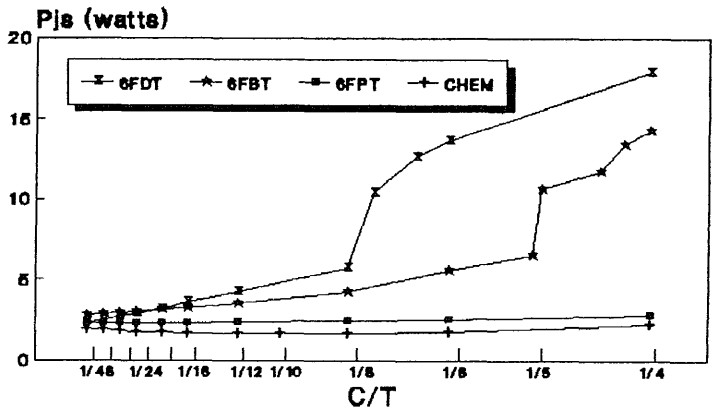

Figure 9(b) Comparison at D/T=0.348 (Pjs)

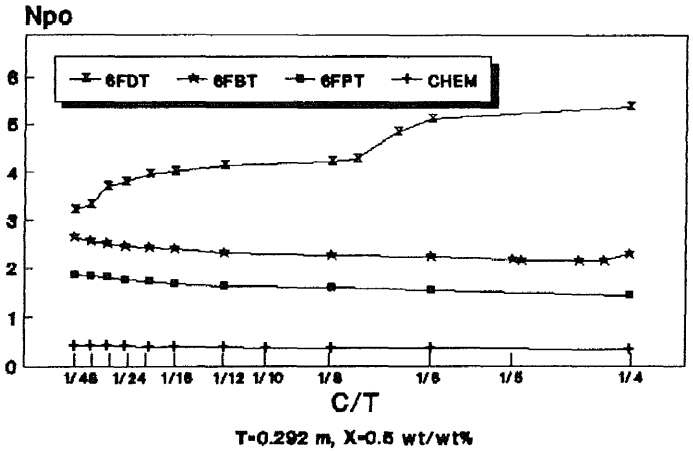

Figure 9(c) Comparison at D/T=0.348 (Npo)

Comparison for D=0.102 m, T=0.292 m, X=0.5 wt/wt%

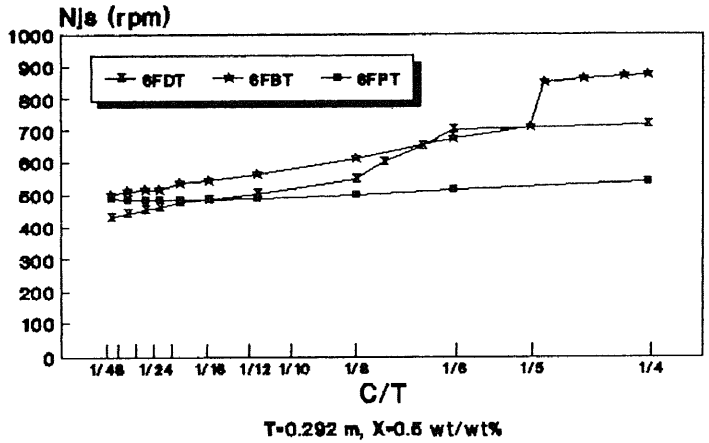

Figure 10(a) Comparison at D/T=0.261 (Njs)

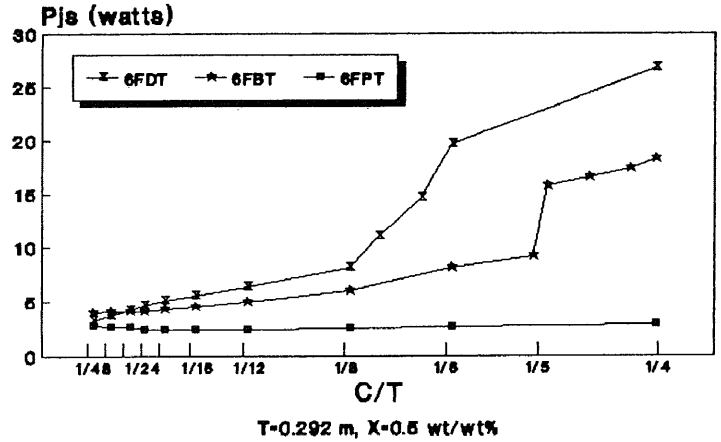

Figure 10(b) Comparison at D/T=0.261 (Pjs)

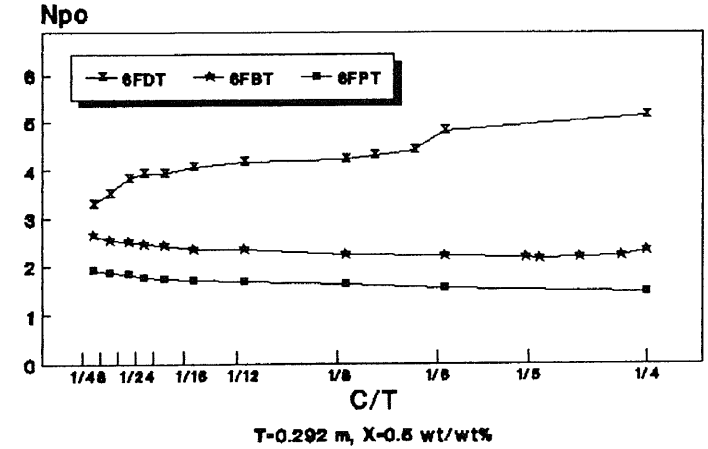

Figure 10(c) Comparison at D/T=0.261 (Npo)

Comparison for D=0.0762 m, T=0.292 m, X=0.5 wt/wt%

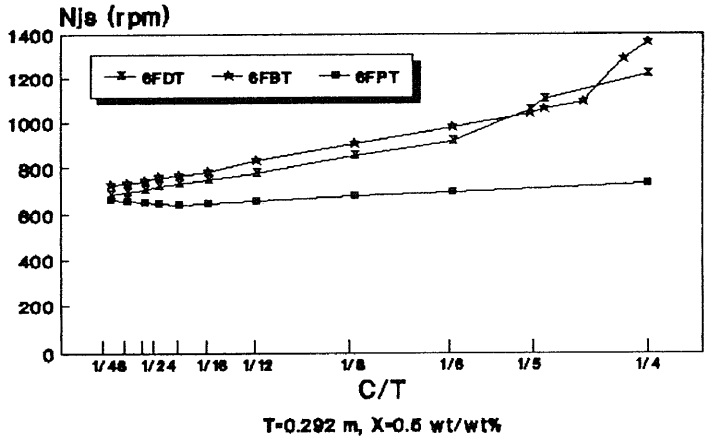

Figure 11(a) Comparison at D/T=0.217 (Njs)

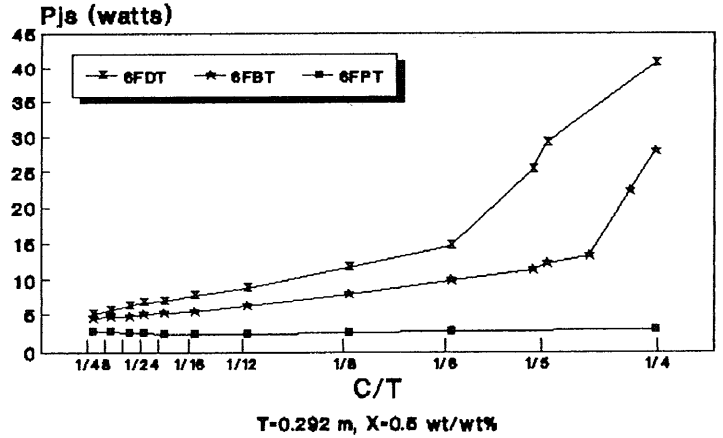

Figure 11(b) Comparison at D/T=0.217 (Pjs)

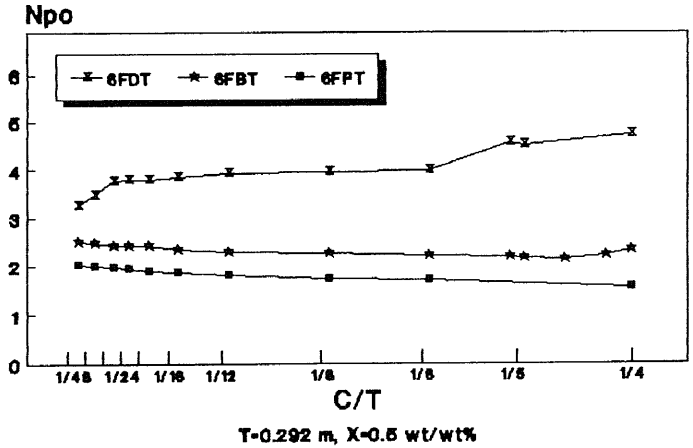

Figure 11(c) Comparison at D/T=0.217 (Npo)

Comparison for D=0.0635 m, T=0.292 m, X=0.5 wt/wt%

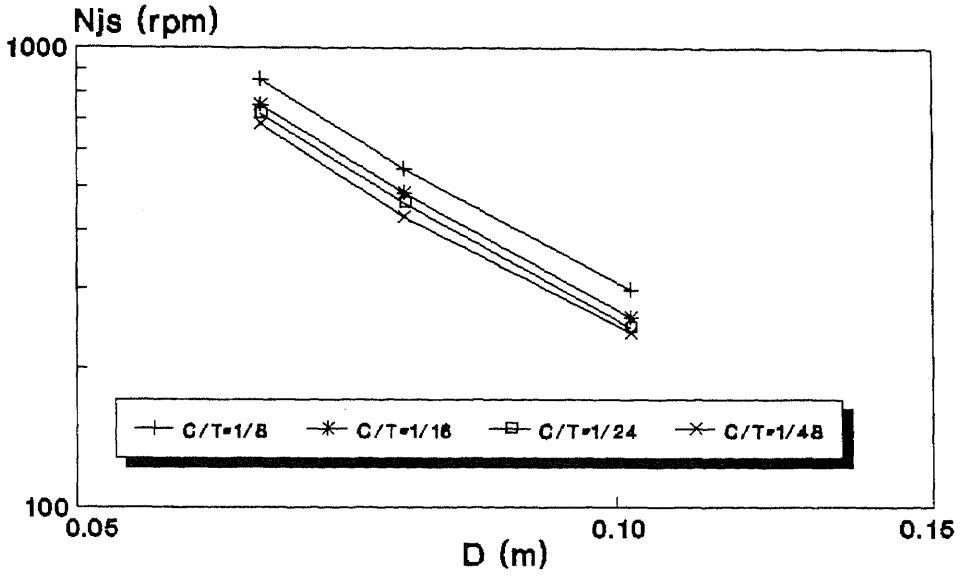

T=0.292 m, X=0.5 wt/wt%

Figure 12(a) Effect of D on Njs (C/T) (6FDT)

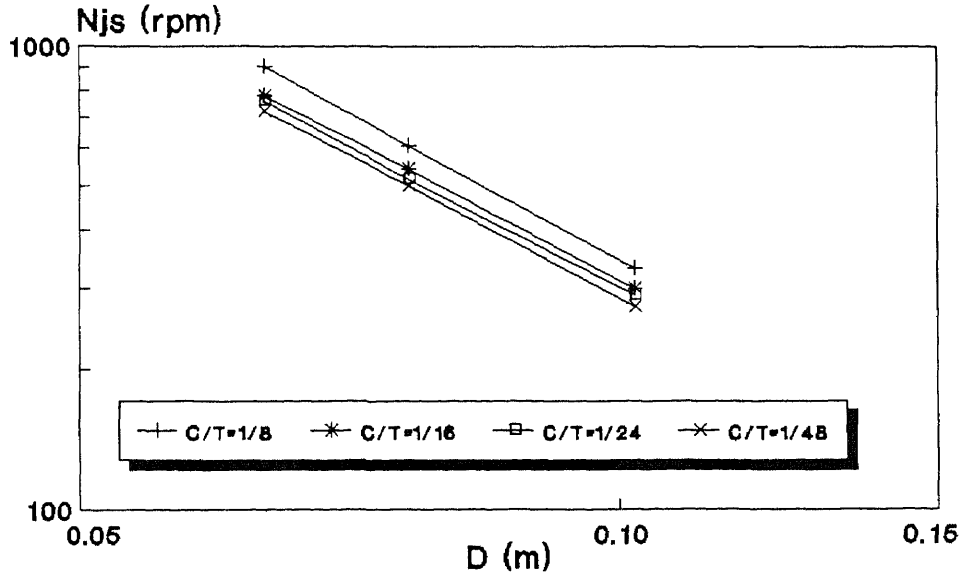

T=0.292 m, X=0.5 wt/wt%

Figure 12(b) Effect of D on Njs (C/T) (6FBT)

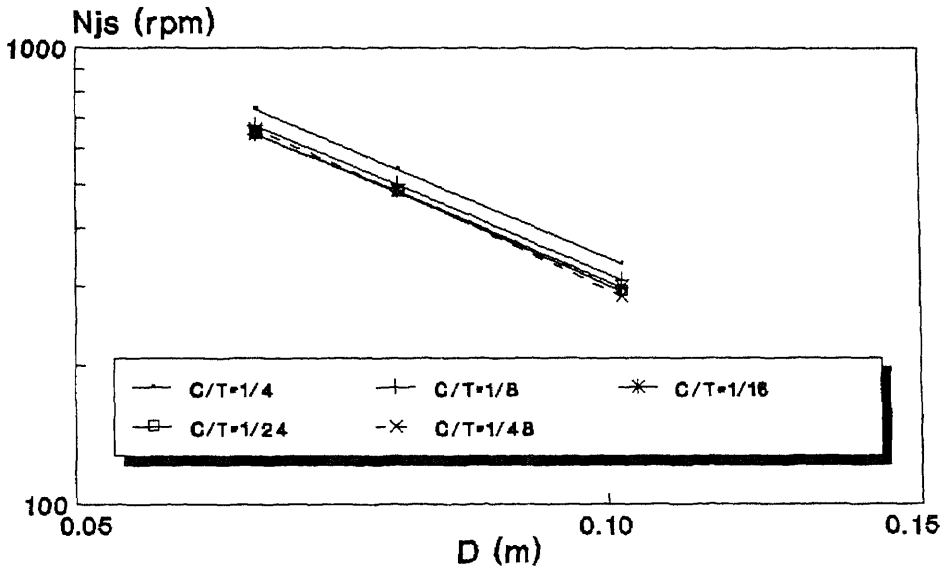

T=0.292 m, X=0.5 wt/wt%

Figure 12(c) Effect of D on Njs (C/T) (6FPT)

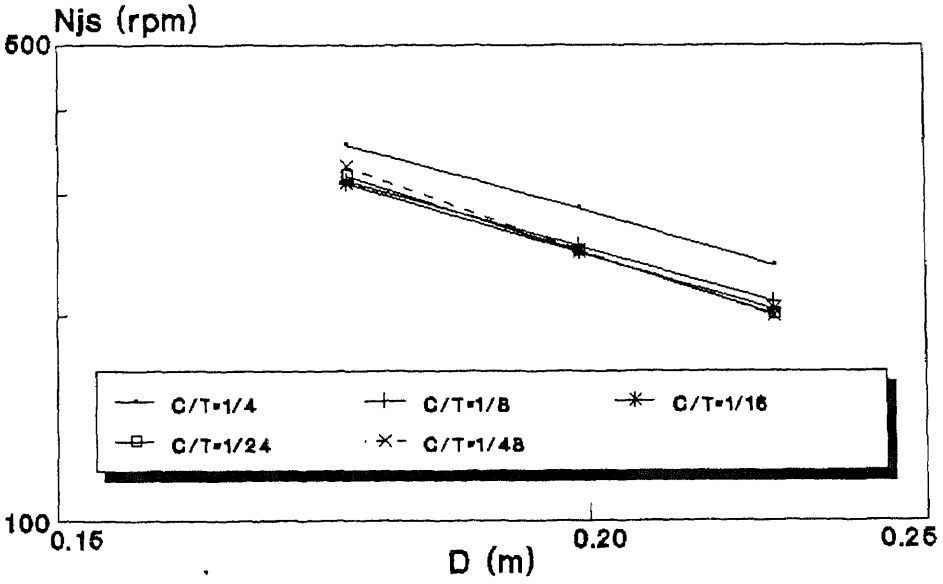

T=0.584 m, X=0.5 wt/wt%

Figure 12(d) Effect of D on Njs (C/T) (CHEM)

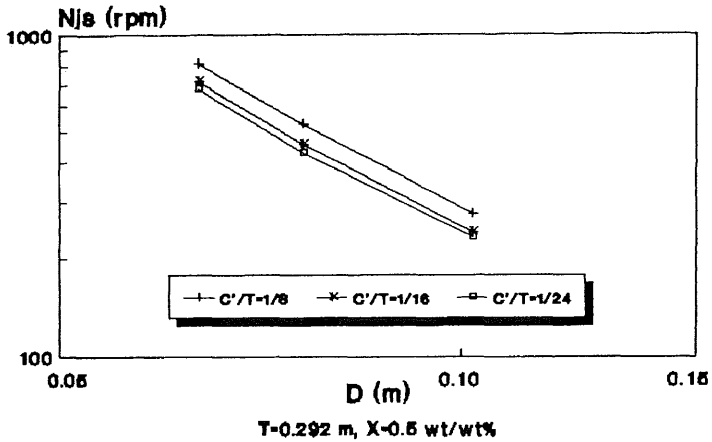

Figure 13(a) Effect of D on Njs (C'/T) (6FDT)

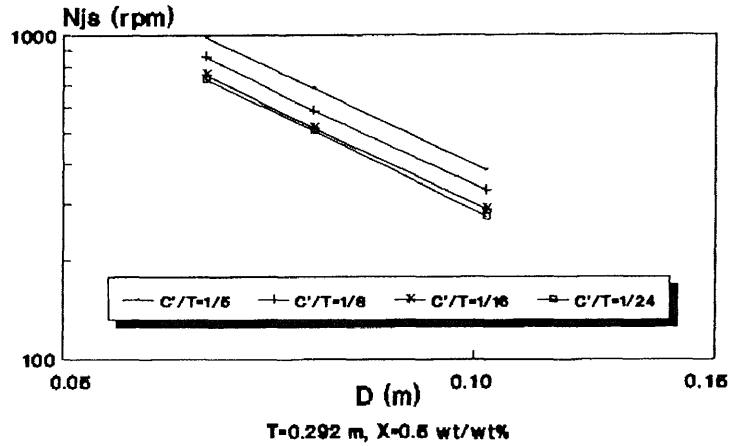

Figure 13(b) Effect of D on Njs (C'/T) (6FBT)

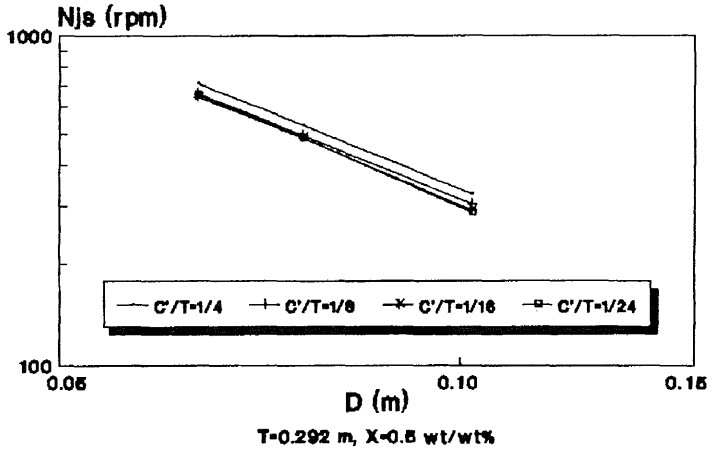

Figure 13(c) Effect of D on Njs (C'/T) (6FPT)

Effect of Impeller Diameter (D) on Minimum Agitation Speed (Njs) at Constant C'/T

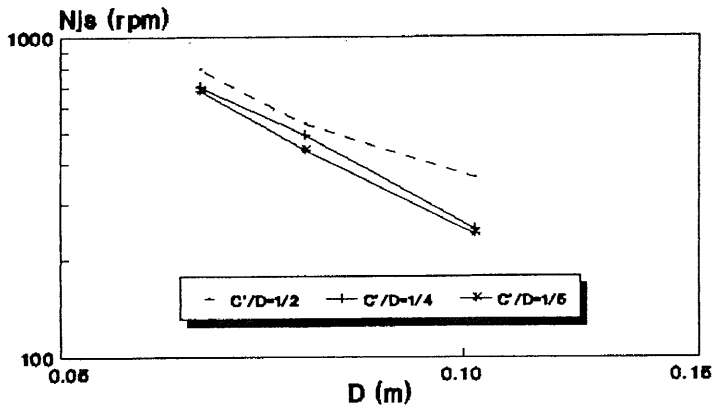

Figure 14(a) Effect of D on Njs (C'/D) (6FDT)

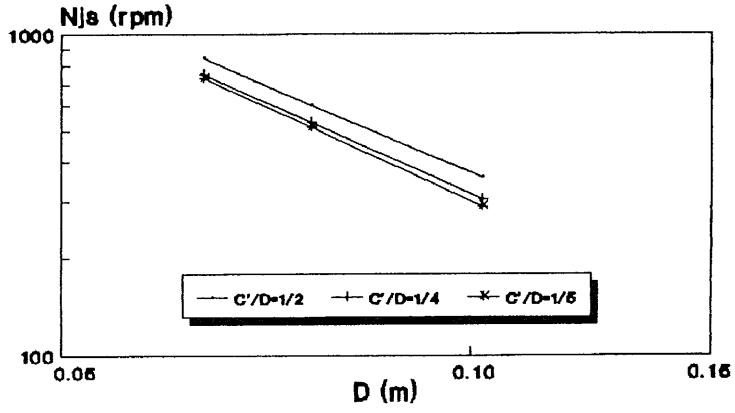

Figure 14(b) Effect of D on Njs (C'/D) (6FBT)

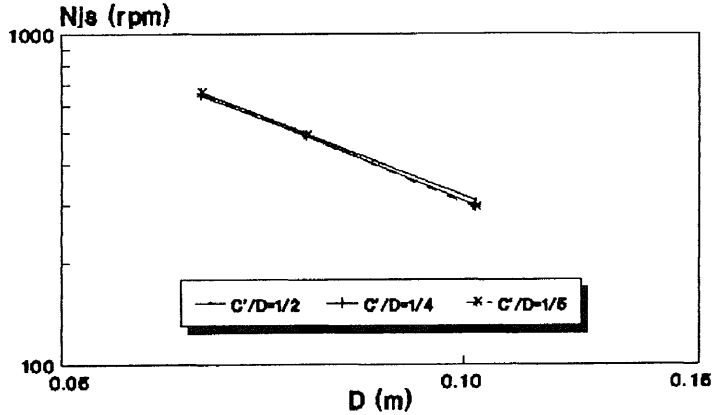

Figure 14(c) Effect of D on Njs (C'/D) (6FPT)

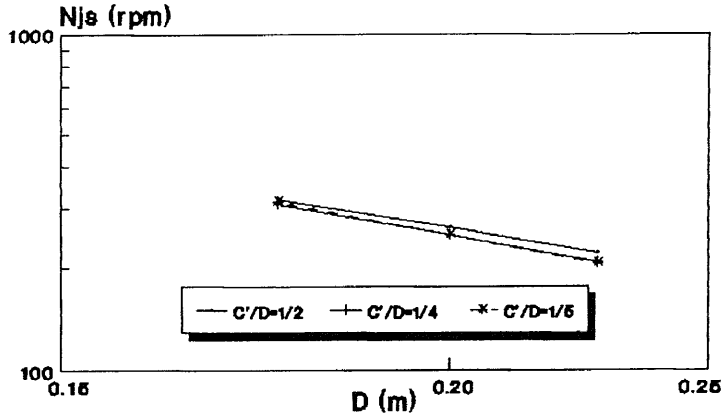

Figure 14(d) Effect of D on Njs (C'/D) (CHEM)

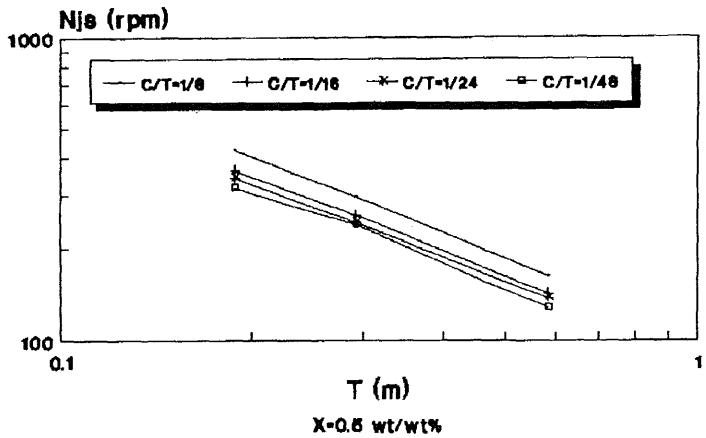

Figure 15(a) Effect of T on Njs (D/T) (6FDT)

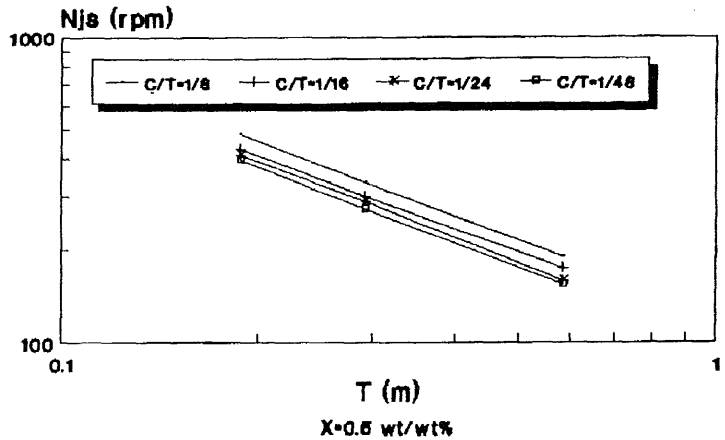

Figure 15(b) Effect of T on Njs (D/T) (6FBT)

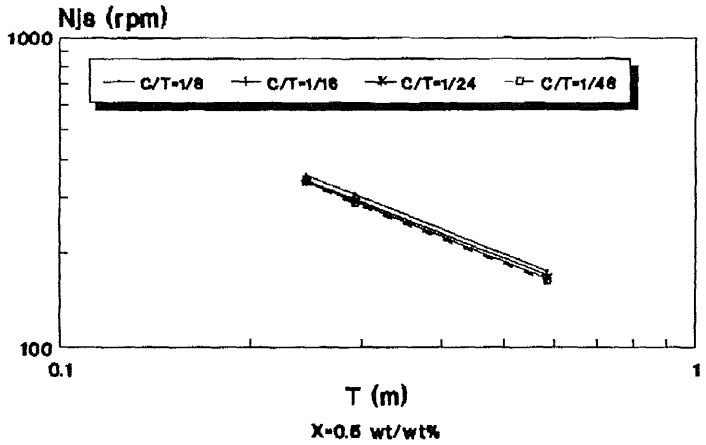

Figure 15(c) Effect of T on Njs (D/T) (6FPT)

Effect of Tank Diameter (T) on Minimun Agitation Speed (Njs) at Constant D/T (=0.348)

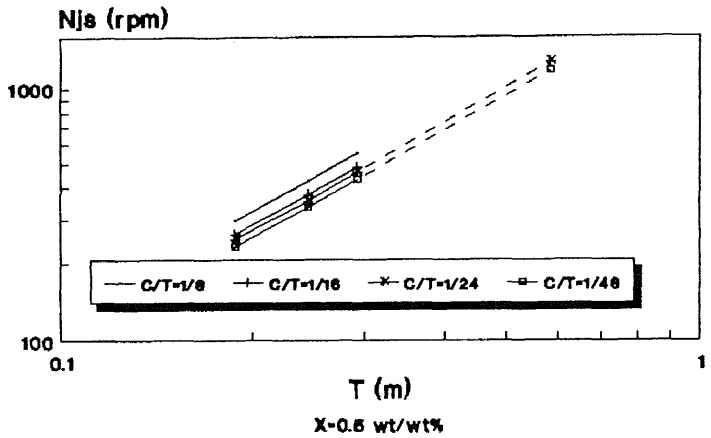

Figure 16(a) Effect of T on Njs (D) (6FDT)

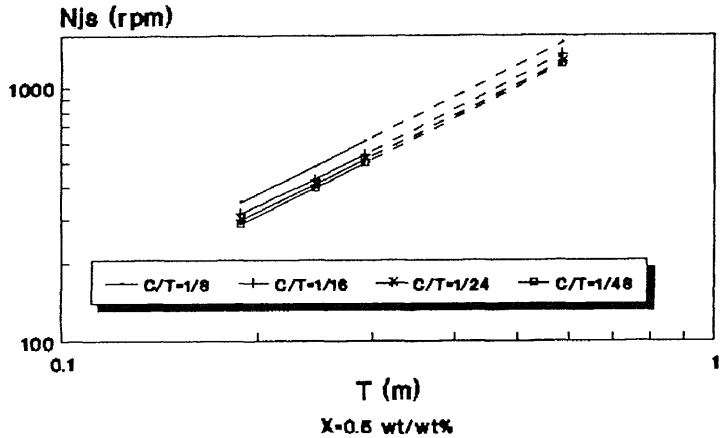

Figure 16(b) Effect of T on Njs (D) (6FBT)

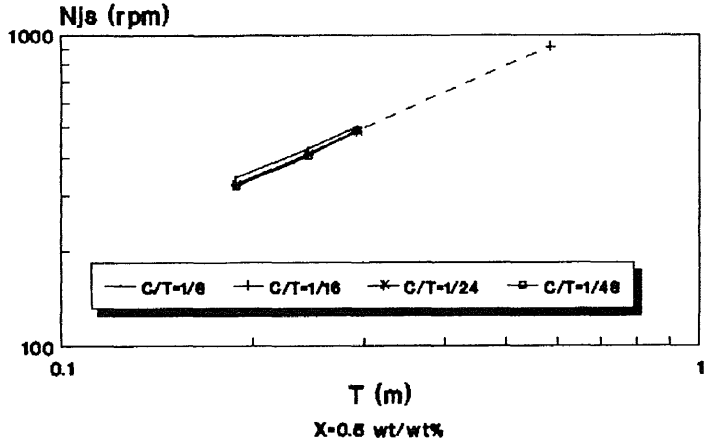

Figure 16(c) Effect of T on Njs (D) (6FPT)

Effect of Tank Diameter (T) on Minimun Agitation Speed (Njs) at Constant D (=0.0762 m)

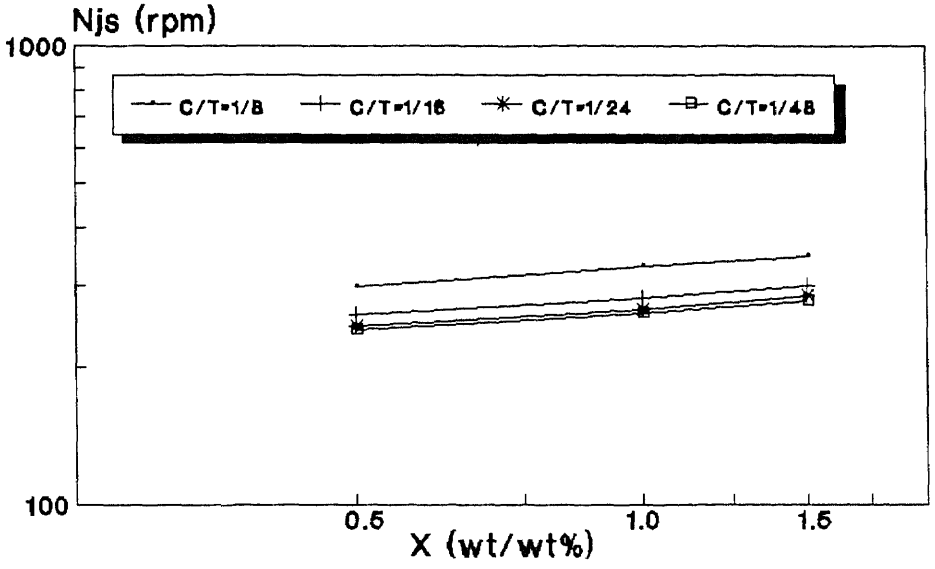

Figure 17(a) Effect of X on Njs (C/T) (6FDT)

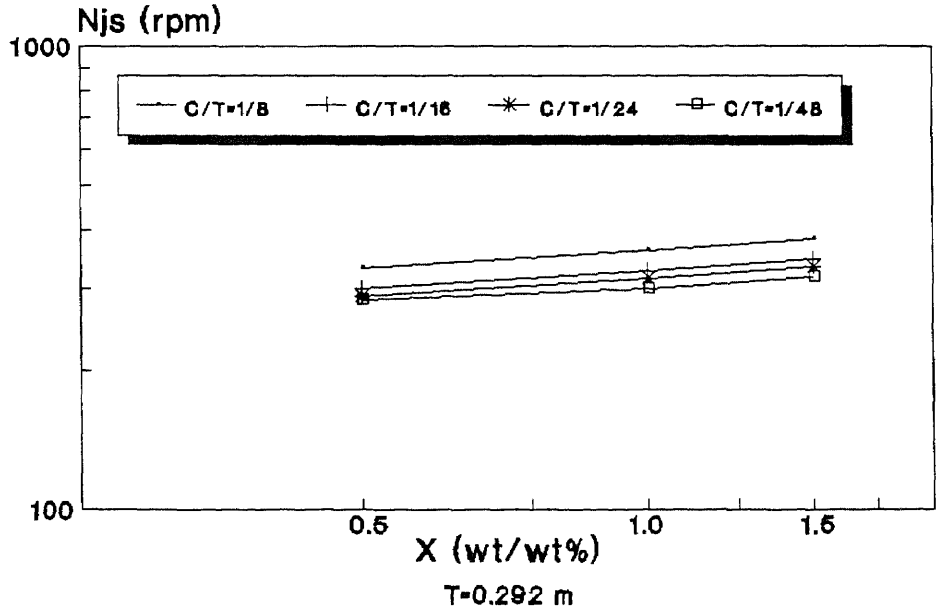

Figure 17(b) Effect of X on Njs (C/T) (6FBT)

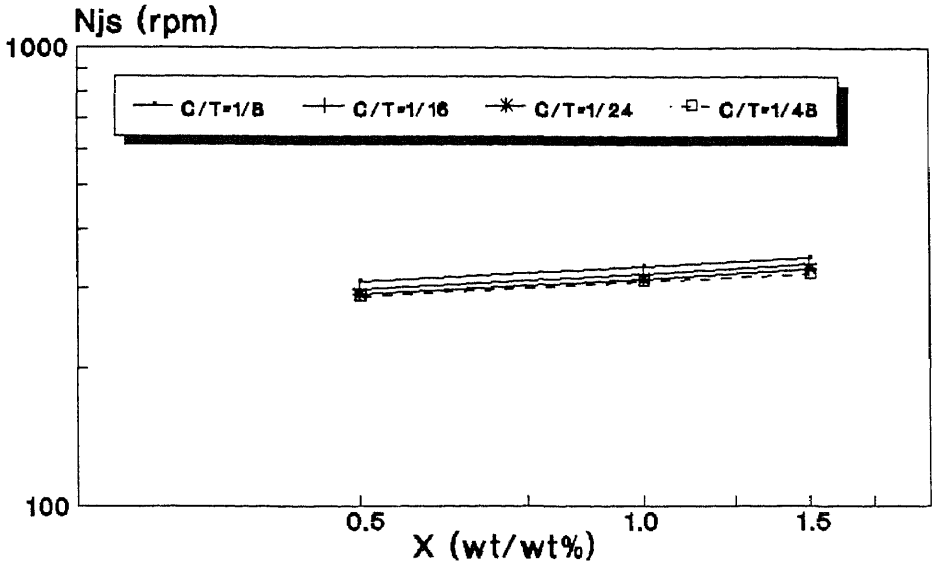

Figure 17(c) Effect of X on Njs (C/T) (6FPT)

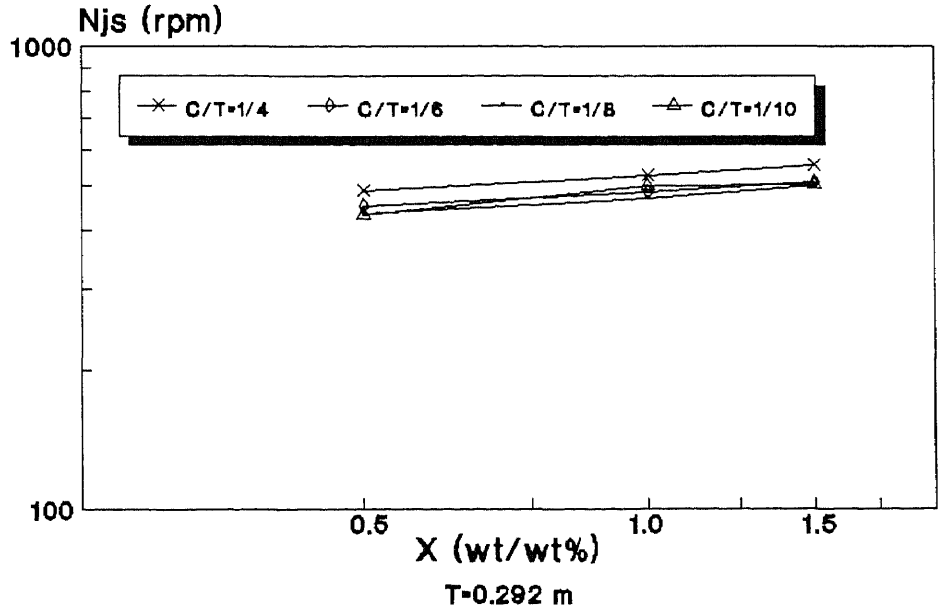

Figure 17(d) Effect of X on Njs (C/T) (CHEM)

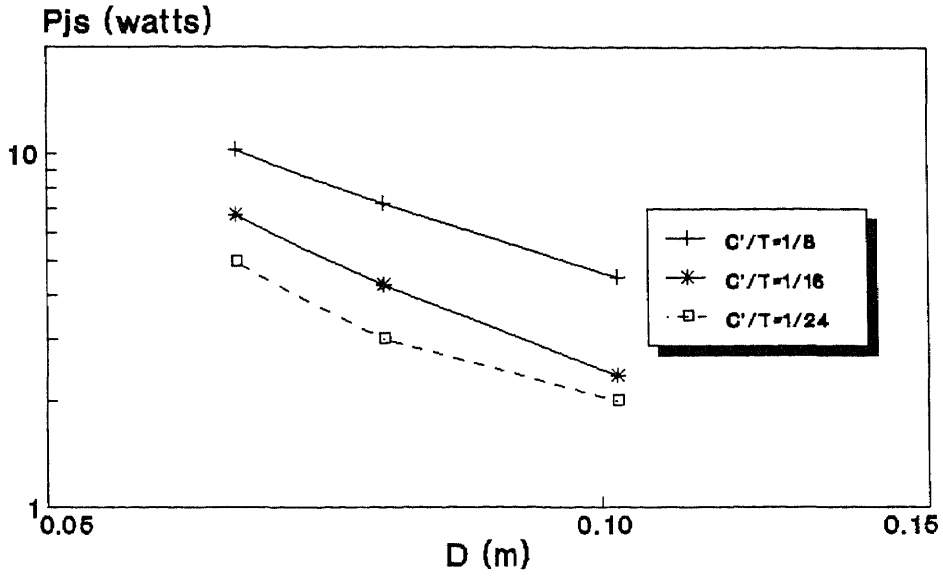

T=0.292 m, X=0.5 wt/wt%

Figure 18(a) Effect of D on Pjs (C'/T) (6FDT)

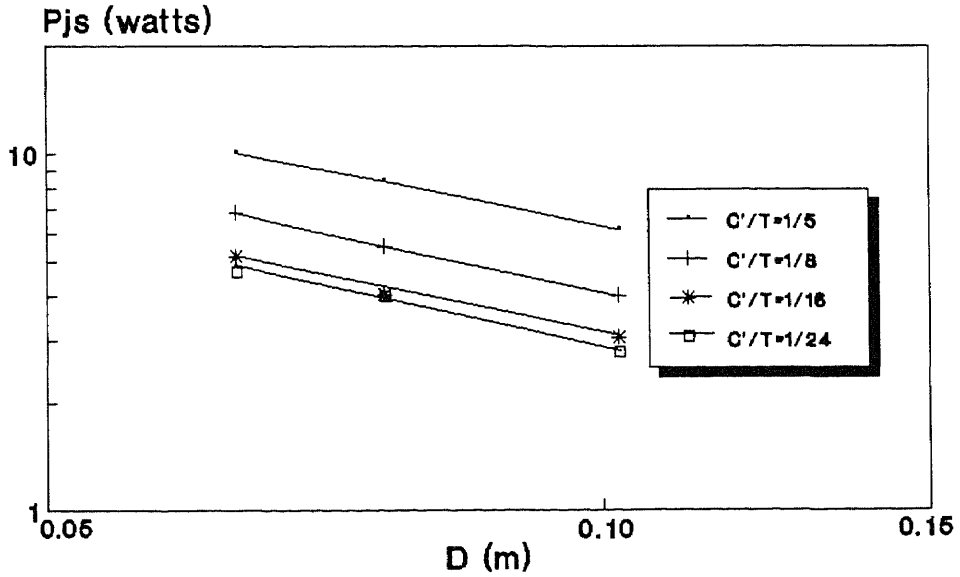

T=0.292 m, X=0.5 wt/wt%

Figure 18(b) Effect of D on Pjs (C'/T) (6FBT)

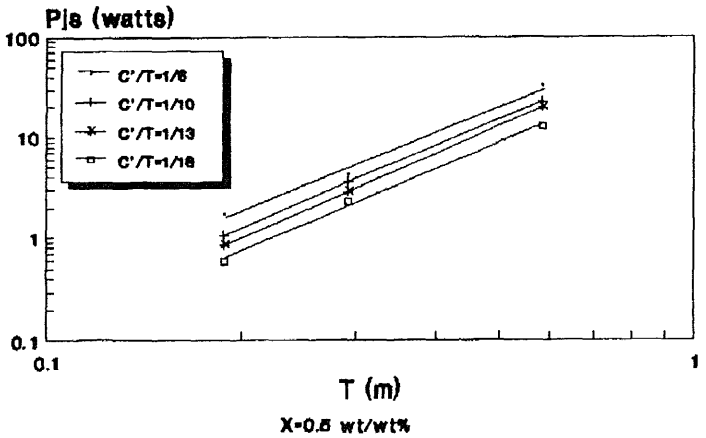

Figure 19(a) Effect of T on Pjs (D/T) (6FDT)

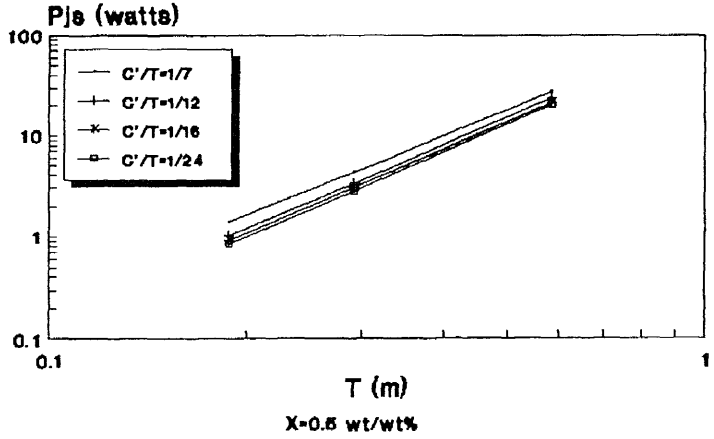

Figure 19(b) Effect of T on Pjs (D/T) (6FBT)

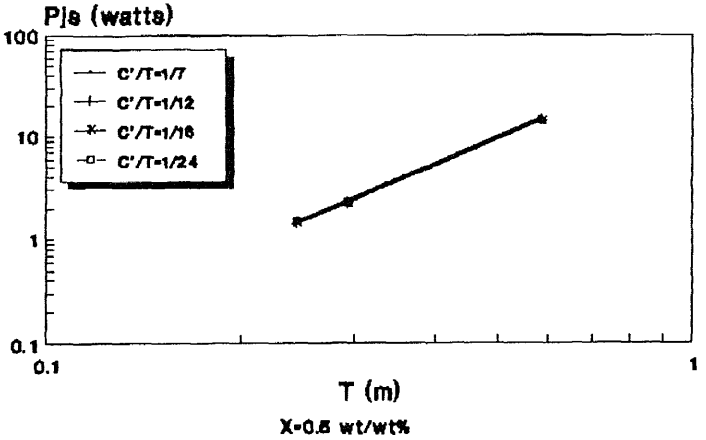

Figure 19(c) Effect of T on Pjs (D/T) (6FPT)

Effect of Tank Diameter (T) on Power Dissipation (Pjs) at Constant D/T (=0.348)

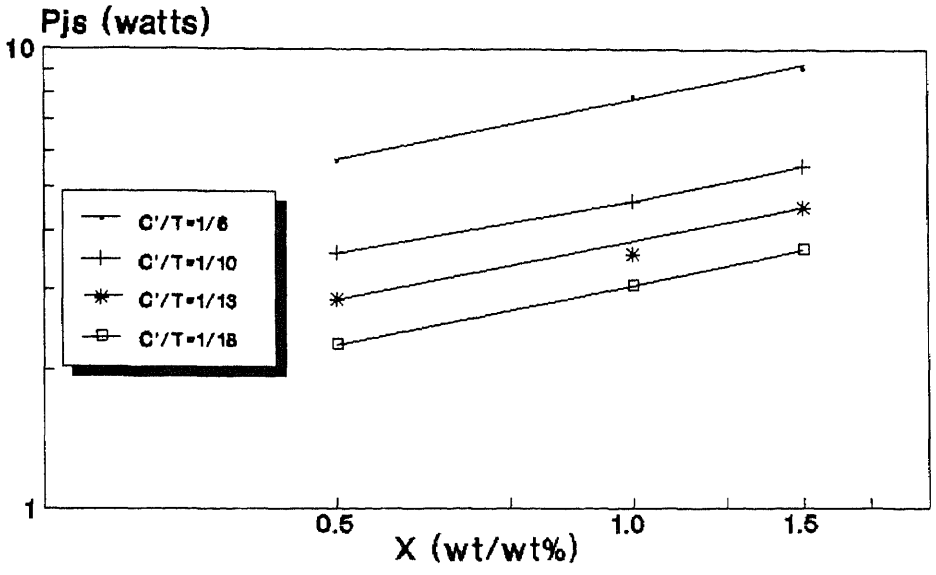

Figure 20(a) Effect of X on Pjs (C'/T) (6FDT)

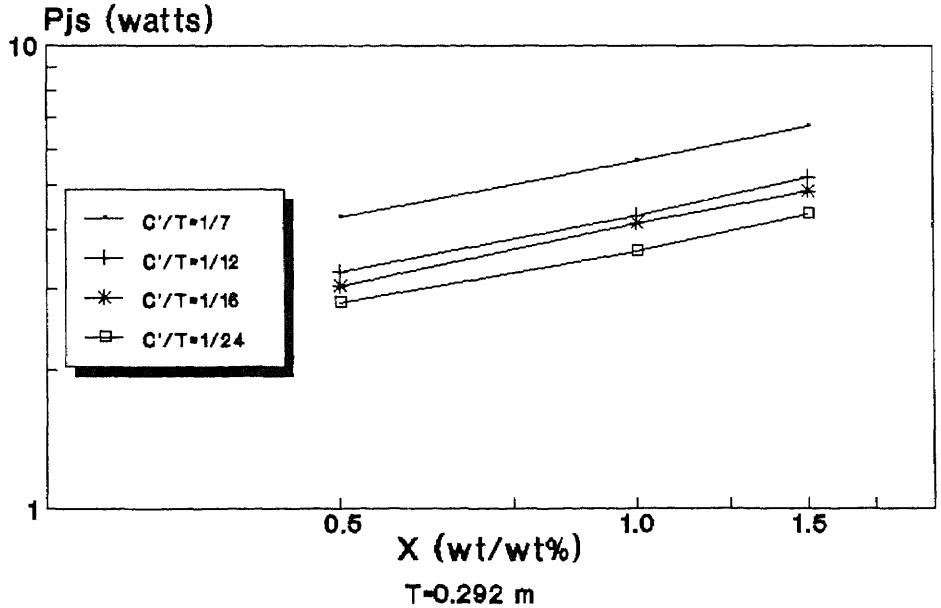

Figure 20(b) Effect of X on Pjs (C'/T) (6FBT)

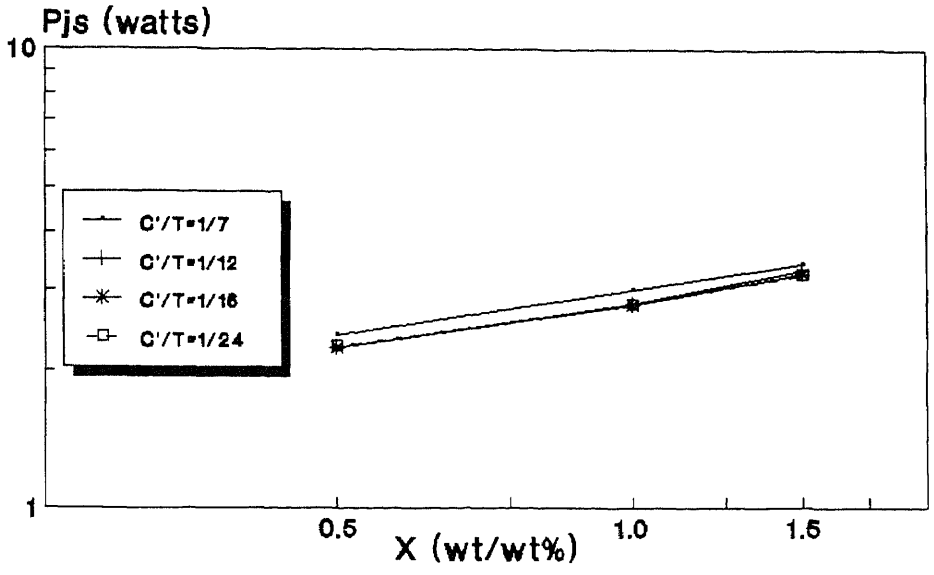

Figure 20(c) Effect of X on Pjs (C'/T) (6FPT)

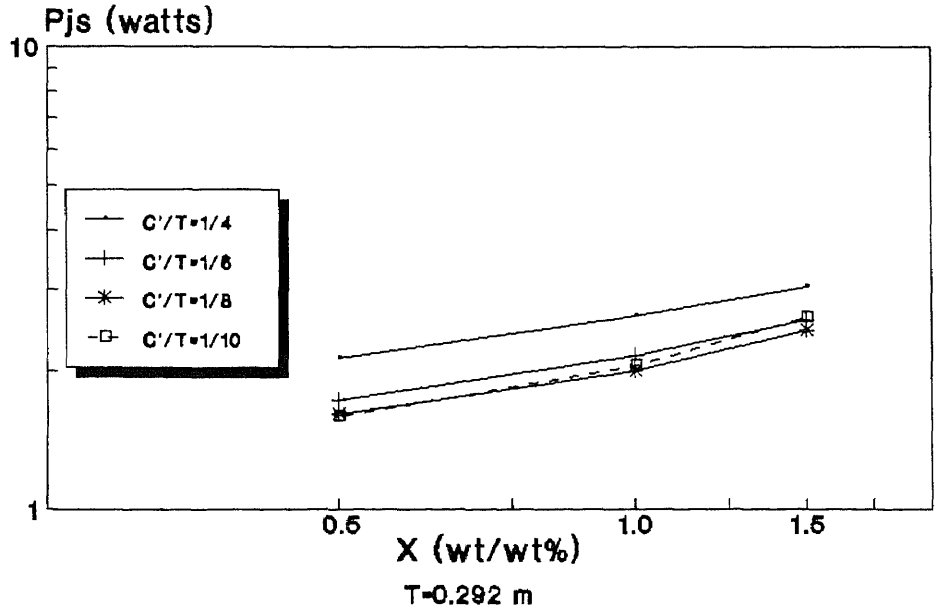

Figure 20(d) Effect of X on Pjs (C'/T) (CHEM)

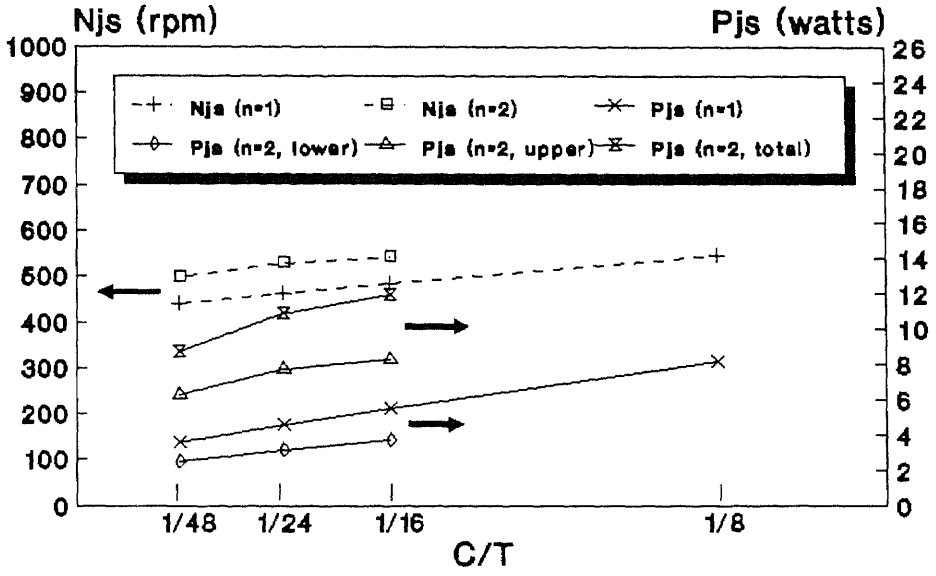

T=0.292m,D/T=0.261,S/D=1,X=0.5wt/wt%

Figure 21(a) Dual-6FDT System
(Effect of C/T on Njs and Pjs)

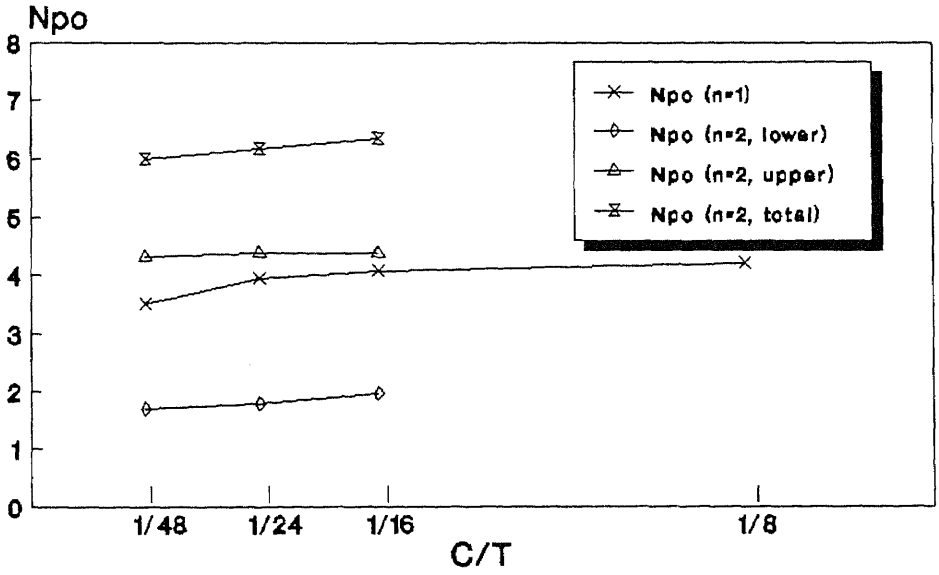

T=0.292m,D/T=0.261,S/D=1,X=0.5wt/wt%

Figure 21(b) Dual-6FDT System
(Effect of C/T on Npo)

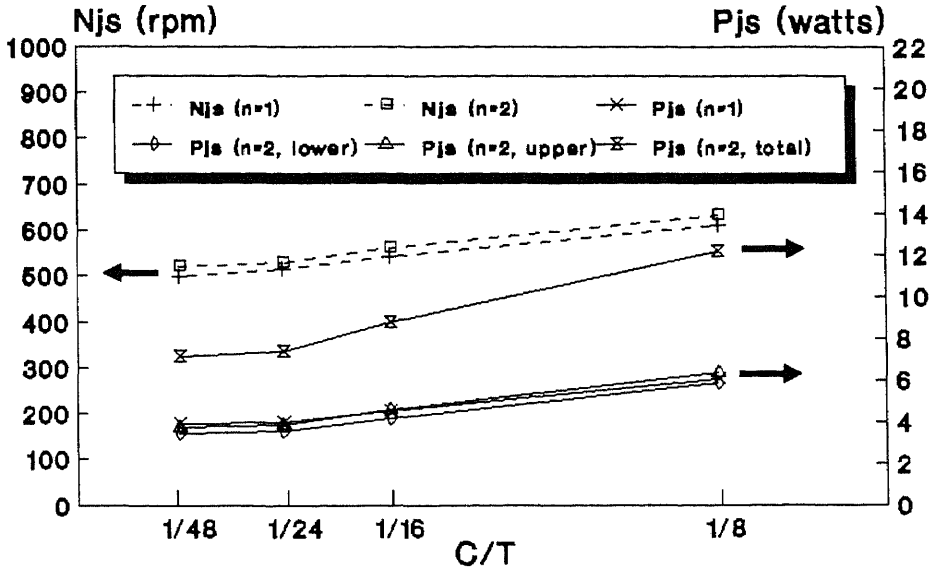

T=0.292m,D/T=0.261,S/D=1,X=0.5wt/wt%

Figure 22(a) Dual-6FBT System
(Effect of C/T on Njs and Pjs)

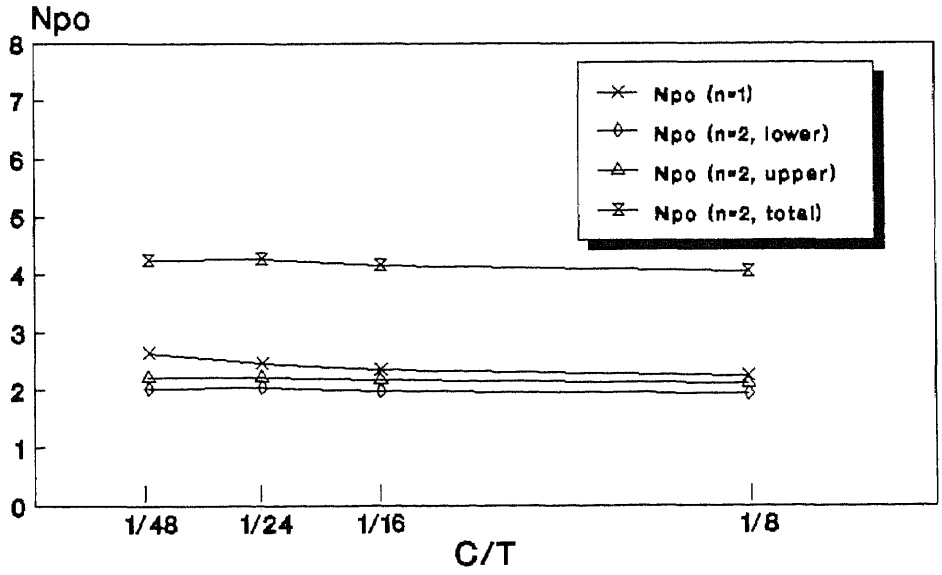

T=0.292m,D/T=0.261,S/D=1,X=0.5wt/wt%

Figure 22(b) Dual-6FBT System
(Effect of C/T on Npo)

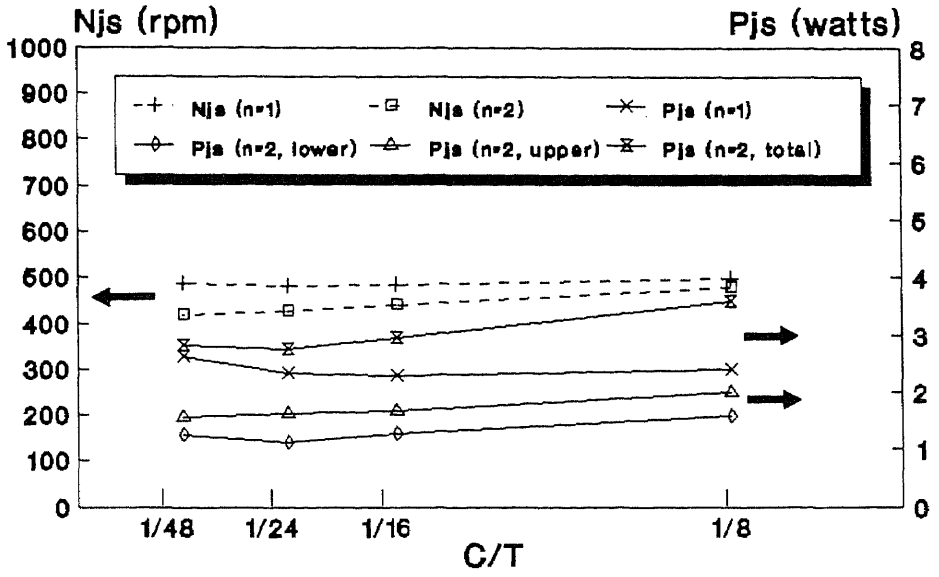

T=0.292m,D/T=0.261,S/D=1,X=0.5wt/wt%

Figure 23(a) Dual-6FPT System
(Effect of C/T on Njs and Pjs)

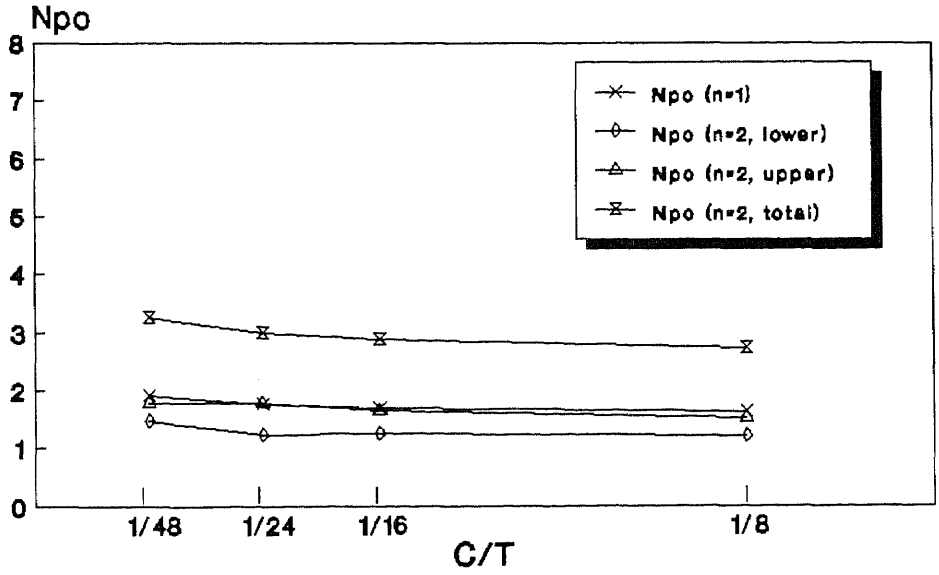

T=0.292m,D/T=0.261,S/D=1,X=0.5wt/wt%

Figure 23(b) Dual-6FPT System
(Effect of C/T on Npo)

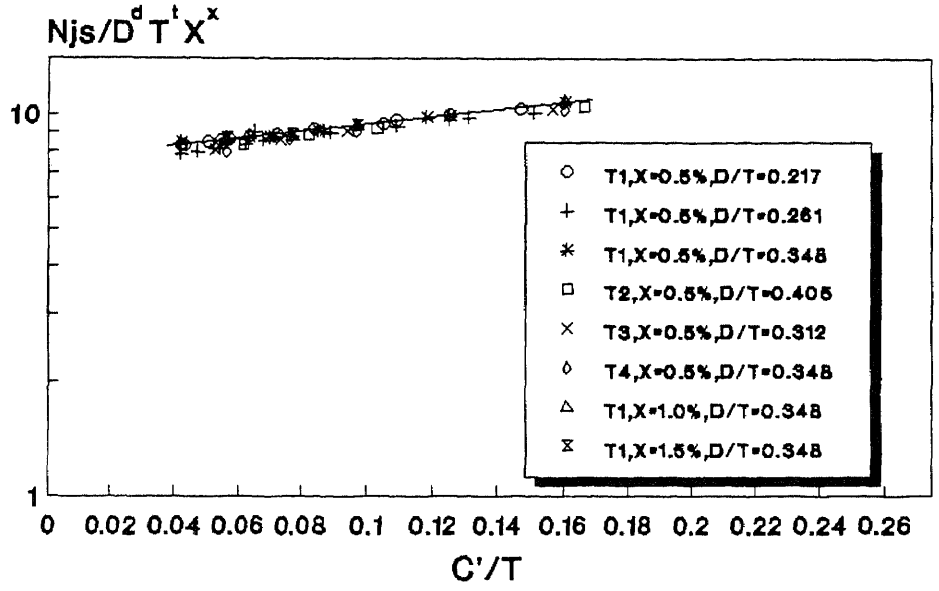

T1=0.292m,T2=0.188m,T3=0.244m,T4=0.584m

Figure 24(a) Extension of Zwietering Correlation (6FDT)

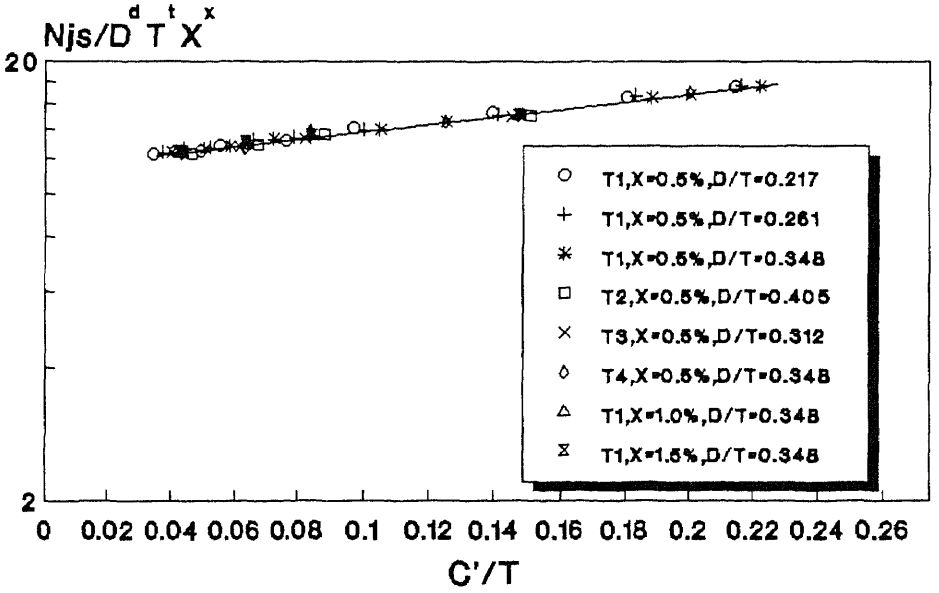

T1=0.292m,T2=0.188m,T3=0.244m,T4=0.584m

Figure 24(b) Extension of Zwietering Correlation (6FBT)

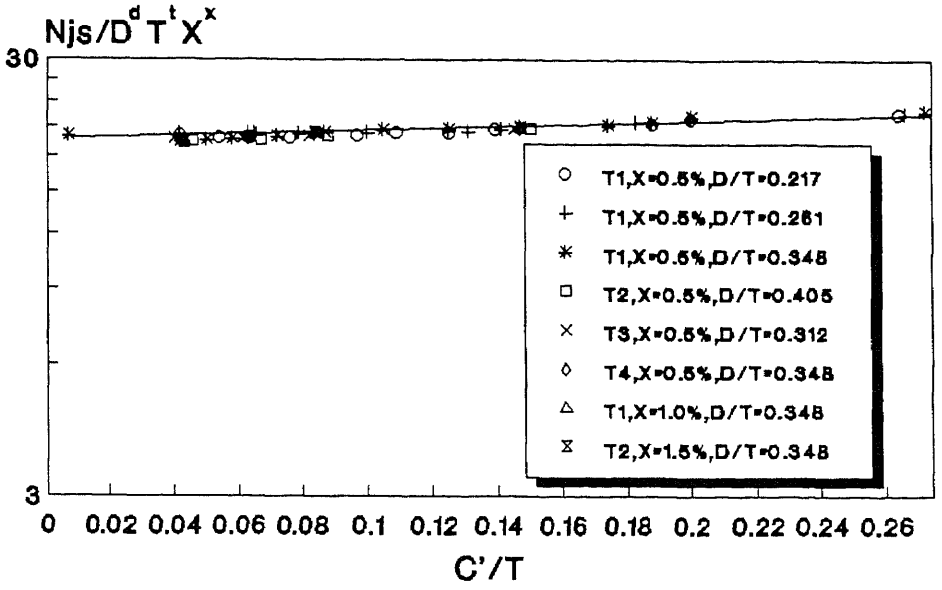

T1=0.292m,T2=0.188m,T3=0.244m,T4=0.584m

Figure 24(c) Extension of Zwietering Correlation (6FPT)

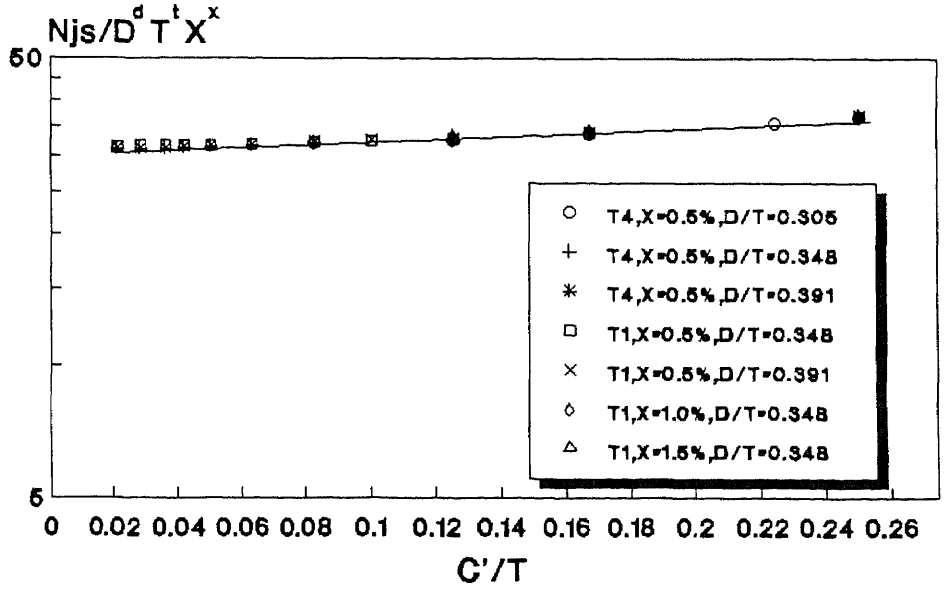

T1=0.292m,T4=0.584m

Figure 24(d) Extension of Zwietering Correlation (CHEM)

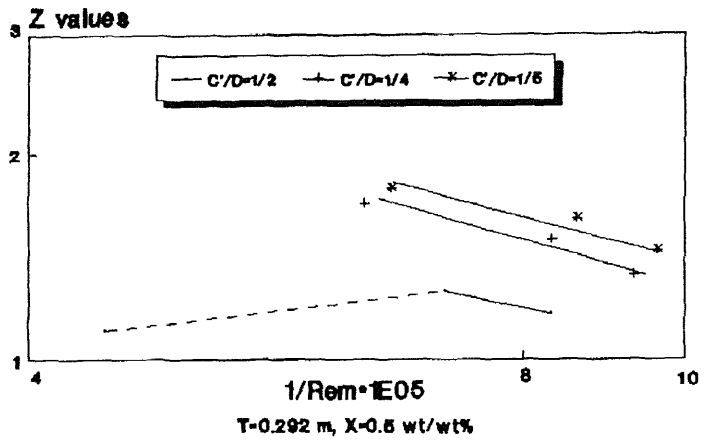

Figure 25(a) Effect of Rem on Z Values for Various C'/D Ratios (6FDT)

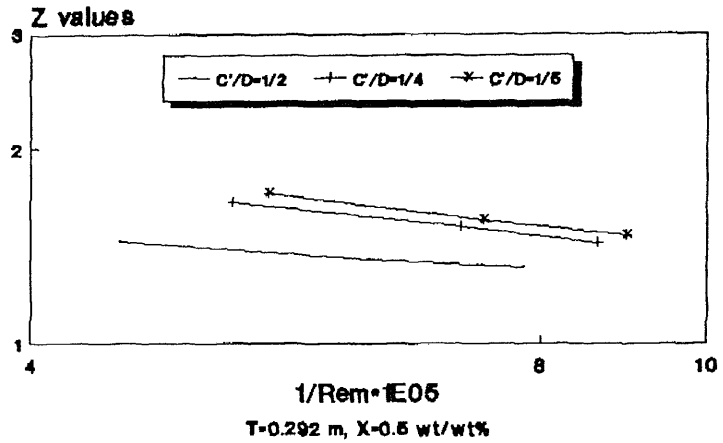

Figure 25(b) Effect of Rem on Z Values for Various C'/D Ratios (6FBT)

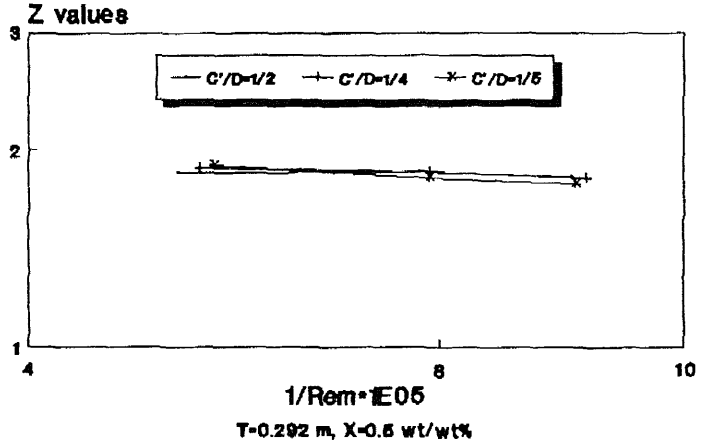

Figure 25(c) Effect of Rem on Z Values for Various C'/D Ratios (6FPT)

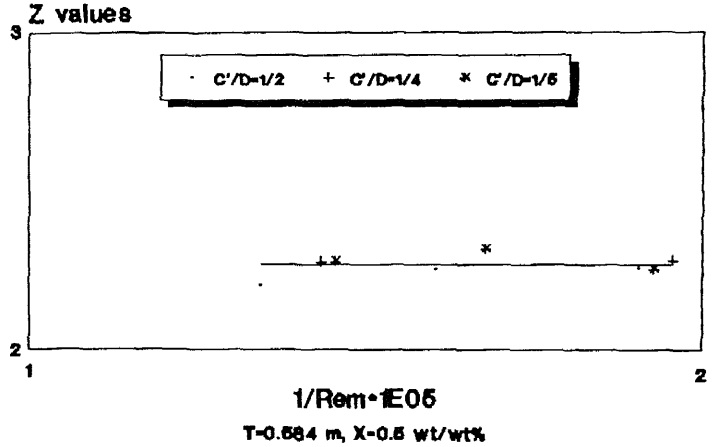

Figure 25(d) Effect of Rem on Z Values for Various C'/D Ratios (CHEM)

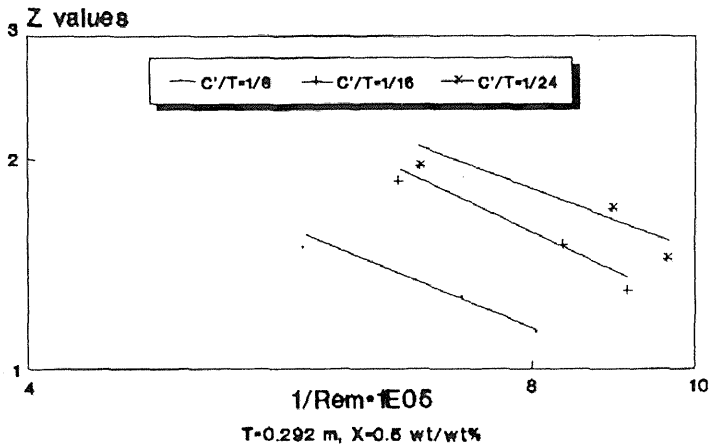

Figure 26(a) Effect of Rem on Z Values for Various C'/T Ratios (6FDT)

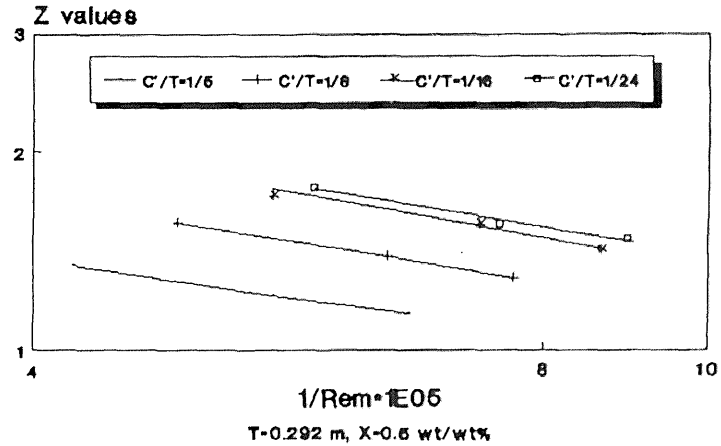

Figure 26(b) Effect of Rem on Z Values for Various C'/T Ratios (6FBT)

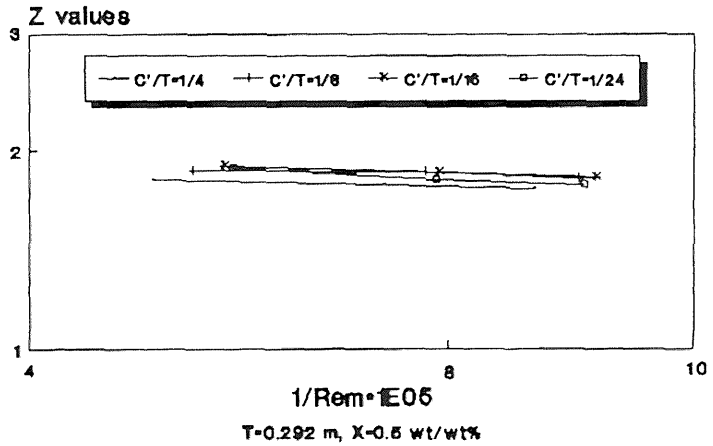

Figure 26(c) Effect of Rem on Z Values for Various C'/T Ratios (6FPT)

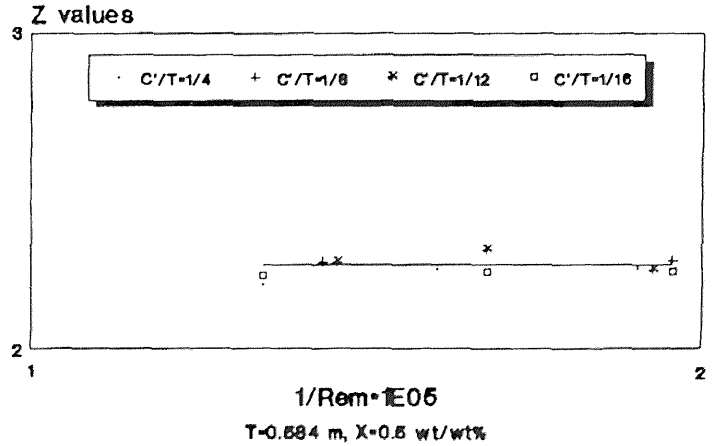

Figure 26(d) Effect of Rem on Z Values for Various C'/T Ratios (CHEM)

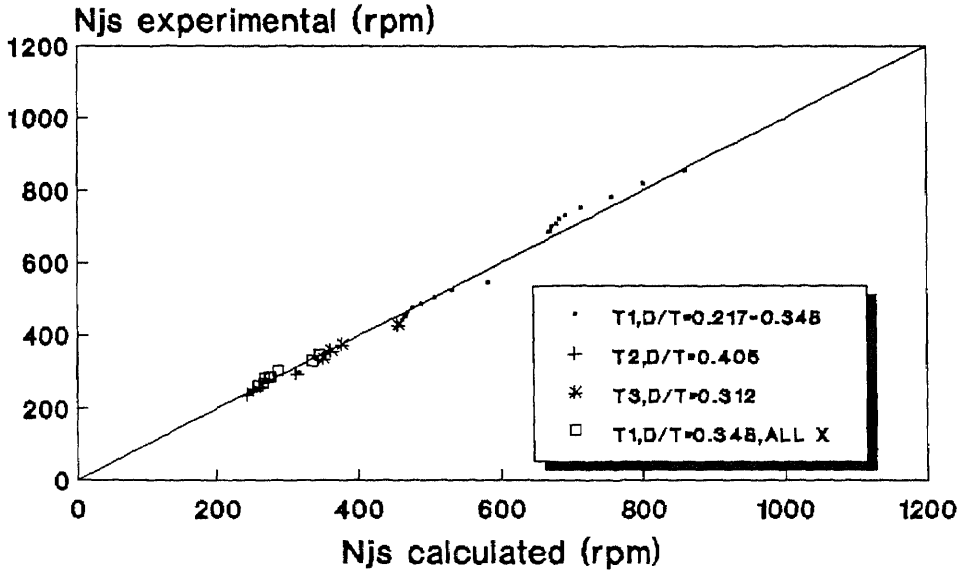

T1=0.292 m, T2=0.188 m, T3=0.244 m

Figure 27(a) Extension of Baldi et al. Model (6FDT)

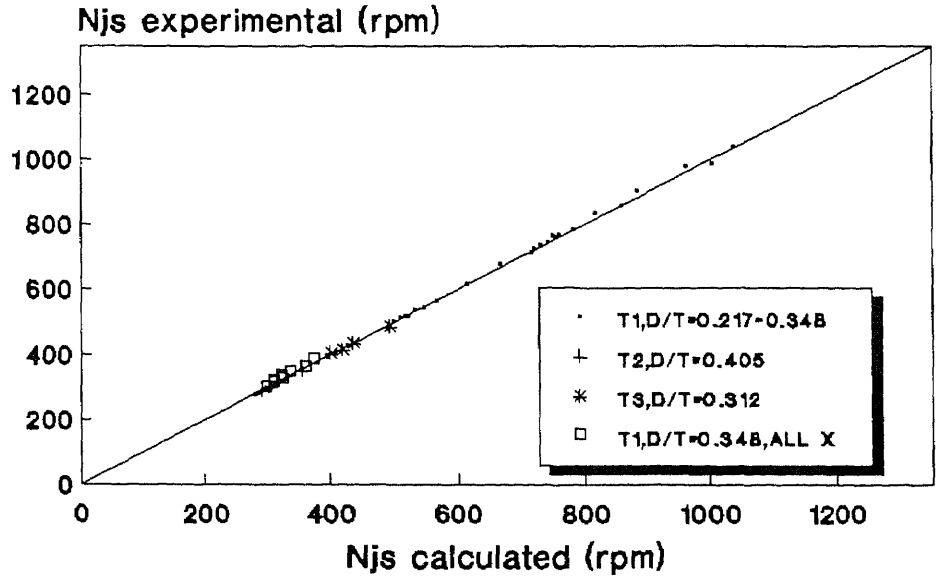

T1=0.292 m, T2=0.188 m, T3=0.244 m

Figure 27(b) Extension of Baldi et al. Model (6FBT)

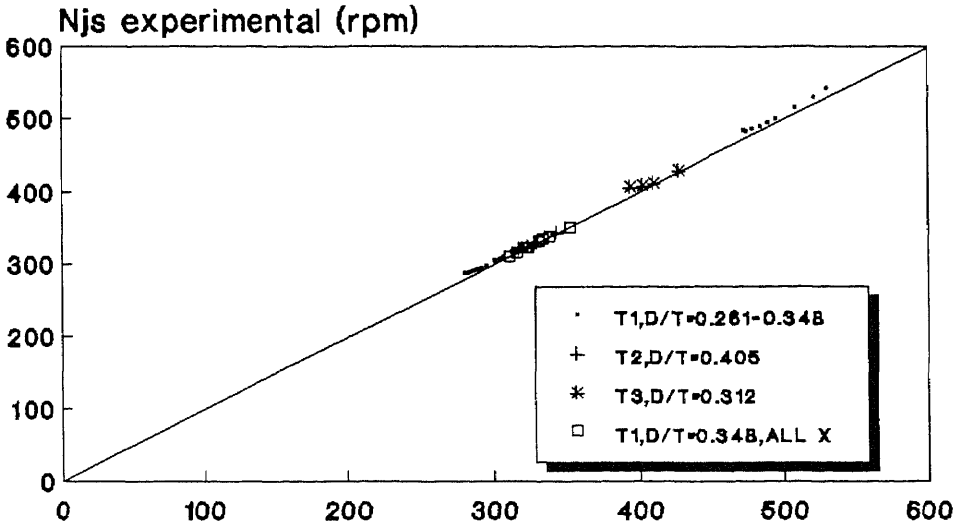

T1=0.292 m, T2=0.188 m,T3=0.244 m

Figure 27(c) Extension of Baldi et al. Model (6FPT)

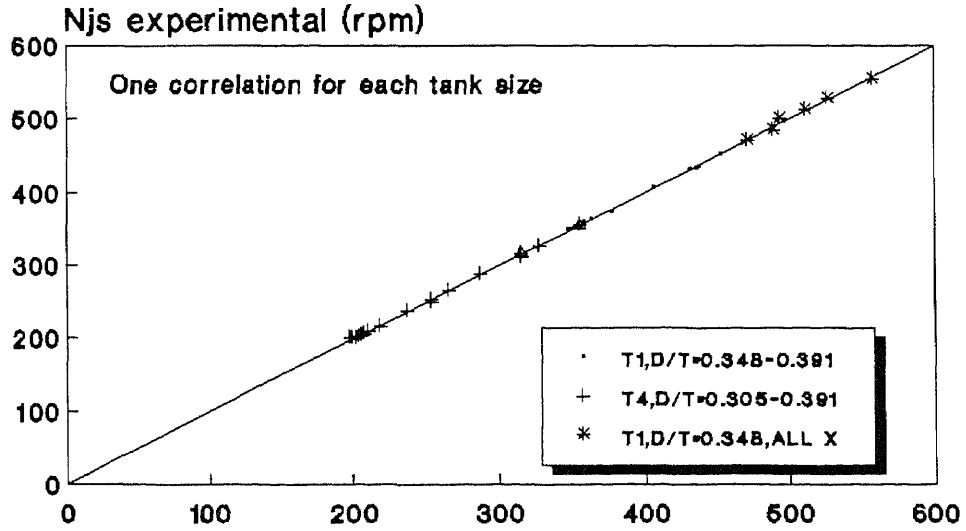

T1=0.292 m, T4=0.584 m

Figure 27(d) Extension of Baldi et al. Model (CHEM)

APPENDIX B

EXPERIMENTAL DATA

This appendix tabulates the experimental data obtained in this work. The experimental data for the effects of the impeller clearance on Njs, Pjs, and Npo include:

6FDT (Table 24-Table 26)

6FBT (Table 27-Table 29)

6FPT (Table 30-Table 31)

CHEM (Table 32-Table 34)

The experimental data for the effects of T and X include:

Effect of T (Table 35-Table 42)

Effect of X (Table 43-Table 46)

The experimental data for the dual-impeller systems include:

Dual-6FDT System (Table 47)

Dual-6FBT System (Table 47)

Dual-6FPT System (Table 47)

Table 24 Effect of C/T on Njs, Pjs, and Npo. 6FDT. T = 0.292 m

Glass Beads
dp = 110 μm
X = 0.5 wt/wt%
Tap water at 22°C

		D = 0.0635 m D/T = 0.217			D = 0.0762 m D/T = 0.261			D = 0.102 m D/T = 0.348		
C/T	C (cm)	Njs (rpm)	Pjs (watts)	Npo	Njs (rpm)	Pjs (watts)	Npo	Njs (rpm)	Pjs (watts)	Npo
1/4	7.3	1217	40.63	4.72	716	26.78	5.12	403	17.90	5.36
				4.57*			5.10+			5.25×
1/6	4.9	916	14.62	3.98	700	19.60	4.81	374	13.64	5.11
				4.00			4.77			4.98
1/8	3.7	850	11.61	3.96	546	8.16	4.21	298	5.70	4.21
				3.99			4.23			4.19
1/12	2.4	777	8.78	3.92	504	6.34	4.16	271	4.21	4.15
				3.95			4.20			4.20
1/16	1.8	749	7.73	3.85	485	5.52	4.07	259	3.59	4.02
				3.91			4.01			4.11
1/20	1.5	729	6.99	3.78	476	5.09	3.93	250	3.15	3.96
				3.88			3.96			4.06
1/24	1.2	719	6.70	3.78	462	4.59	3.93	245	2.85	3.78
				3.82			3.92			3.86
1/28	1	705	6.32	3.77	451	4.18	3.83	242	2.68	3.69
				3.58			3.89			3.75
1/36	0.8	696	5.58	3.46	441	3.56	3.49	241	2.35	3.30
				3.42			3.47			3.48
1/48	0.6	682	4.95	3.27	430	3.12	3.29	240	2.27	3.21
				3.31			3.35			3.36

* Using water only: 500-600 rpm
+ Using water only: 400-500 rpm
× Using water only: 300-400 rpm

Table 25 Effect of C'/D and C'/T on Njs, Pjs, and Npo. 6FDT. T = 0.292 m

Glass Beads
dp = 110 μm
X = 0.5 wt/wt%
Tap water at 22°C

C'/D (C/D)

		D = 0.0635 m D/T = 0.217			D = 0.0762 m D/T = 0.261			D = 0.102 m D/T = 0.348		
C/D	**C'/D**	**Njs (rpm)**	**Pjs (watts)**	**Npo**	**Njs (rpm)**	**Pjs (watts)**	**Npo**	**Njs (rpm)**	**Pjs (watts)**	**Npo**
2/5	**1/2**	791	9.36	3.96	530	7.44	4.20	360	11.40	4.78
3/20	**1/4**	705	6.21	3.81	457	4.41	4.16	247	3.23	4.17
1/10	**1/5**	682	4.95	3.26	441	3.56	3.59	241	2.35	3.28

C'/T

		D = 0.0635 m D/T = 0.217			D = 0.0762 m D/T = 0.261			D = 0.102 m D/T = 0.348		
C'/T	**C' (cm)**	**Njs (rpm)**	**Pjs (watts)**	**Npo**	**Njs (rpm)**	**Pjs (watts)**	**Npo**	**Njs (rpm)**	**Pjs (watts)**	**Npo**
1/8	**3.7**	815	10.27	3.97	524	7.22	4.22	275	4.50	4.23
1/16	**1.8**	719	6.70	3.77	455	4.28	3.82	241	2.35	3.28
1/24	**1.2**	682	4.95	3.26	426	3.00	3.26	234	2.00	3.05

Table 26 Effect of C/T on Njs, Pjs, and Npo. 6FDT. T = 0.292 m
Transition Region

Glass Beads
dp = 110 μm
X = 0.5 wt/wt%
Tap water at 22°C

		D = 0.0635 m D/T = 0.217			**D = 0.0762 m D/T = 0.261**			**D = 0.102 m D/T = 0.348**		
C/T	**C (cm)**	**Njs (rpm)**	**Pjs (watts)**	**Npo**	**Njs (rpm)**	**Pjs (watts)**	**Npo**	**Njs (rpm)**	**Pjs (watts)**	**Npo**
-	**6**	1100	29.09	4.52	-	-	-	-	-	-
-	**5.5**	1054	25.33	4.57	-	-	-	-	-	-
-	**5**	-	-	-	-	-	-	-	-	-
-	**4.5**	-	-	-	652	14.58	4.42	371	12.62	4.96
-	**4**	-	-	-	600	11.06	4.30	362	10.38	4.27

Table 27 Effect of C/T on Njs, Pjs, and Npo. 6FBT. T = 0.292 m

Glass Beads
dp = 110 μm
X = 0.5 wt/wt%
Tap water at 22°C

		D = 0.063 m D/T = 0.217			D = 0.0762 m D/T = 0.261			D = 0.102 m D/T = 0.348		
C/T	C (cm)	Njs (rpm)	Pjs (watts)	Npo	Njs (rpm)	Pjs (watts)	Npo	Njs (rpm)	Pjs (watts)	Npo
1/4	7.3	1359	27.83	2.32	872	18.23	2.31	495	14.25	2.30
				2.37*			2.39+			2.39×
1/5	5.8	1035	11.37	2.18	710	9.21	2.19	387	6.49	2.18
				2.20			2.18			2.16
1/6	4.9	978	9.89	2.22	675	8.11	2.22	365	5.55	2.24
				2.25			2.26			2.25
1/8	3.7	903	7.94	2.26	611	6.07	2.24	332	4.28	2.28
				2.31			2.29			2.30
1/12	2.4	830	6.27	2.30	562	4.97	2.35	309	3.53	2.33
				2.35			2.30			2.34
1/16	1.8	779	5.34	2.36	542	4.50	2.36	299	3.26	2.39
				2.37			2.33			2.37
1/20	1.5	766	5.19	2.42	534	4.31	2.42	293	3.14	2.44
				2.41			2.35			2.43
1/24	1.2	760	5.10	2.43	515	3.99	2.46	289	3.04	2.45
				2.42			2.40			2.48
1/28	1	740	4.75	2.44	513	4.00	2.50	283	2.92	2.52
				2.43			2.44			2.51
1/36	0.8	734	4.69	2.48	510	4.00	2.53	278	2.83	2.57
				2.48			2.49			2.55
1/48	0.6	724	4.55	2.50	499	3.90	2.64	275	2.80	2.63
				2.49			2.54			2.57

* Using water only: 500-600 rpm
+ Using water only: 400-500 rpm
× Using water only: 300-400 rpm

Table 28 Effect of C'/D and C'/T on Njs, Pjs, and Npo. 6FBT. T = 0.292 m

Glass Beads
dp = 110 μm
X = 0.5 wt/wt%
Tap water at 22°C

C'/D (C/D)

		D = 0.0635 m D/T = 0.217			D = 0.0762 m D/T = 0.261			D = 0.102 m D/T = 0.348		
C/D	**C'/D**	**Njs (rpm)**	**Pjs (watts)**	**Npo**	**Njs (rpm)**	**Pjs (watts)**	**Npo**	**Njs (rpm)**	**Pjs (watts)**	**Npo**
7/16	**1/2**	840	6.65	2.35	600	5.95	2.32	355	4.75	2.08
3/16	**1/4**	760	5.10	2.43	529	4.25	2.41	304	3.36	2.34
1/8	**1/5**	732	4.65	2.48	513	4.00	2.49	290	3.07	2.46

C'/T

		D = 0.0635 m D/T = 0.217			D = 0.0762 m D/T = 0.261			D = 0.102 m D/T = 0.348		
C'/T	**C' (cm)**	**Njs (rpm)**	**Pjs (watts)**	**Npo**	**Njs (rpm)**	**Pjs (watts)**	**Npo**	**Njs (rpm)**	**Pjs (watts)**	**Npo**
1/5	**5.8**	985	10.05	2.20	685	8.41	2.20	380	6.15	2.19
1/8	**3.7**	855	6.85	2.29	587	5.51	2.29	329	4.00	2.20
1/16	**1.8**	758	5.15	2.47	518	4.01	2.43	289	3.04	2.46
1/24	**1.2**	732	4.65	2.48	505	3.95	2.58	274	2.76	2.62

Table 29 Effect of C/T on Njs, Pjs, and Npo. 6FBT. T = 0.292 m
Transition Region

Glass Beads
dp = 110 μm
X = 0.5 wt/wt%
Tap water at 22°C

		D = 0.0635 m D/T = 0.217			**D = 0.0762 m D/T = 0.261**			**D = 0.102 m D/T = 0.348**		
C/T	**C (cm)**	**Njs (rpm)**	**Pjs (watts)**	**Npo**	**Njs (rpm)**	**Pjs (watts)**	**Npo**	**Njs (rpm)**	**Pjs (watts)**	**Npo**
-	7	1284	22.30	2.21	869	17.27	2.21	488	13.37	2.25
-	**6.5**	1089	13.19	2.14	860	16.52	2.19	472	11.67	2.17
-	**6**	1059	12.22	2.15	849	15.73	2.16	458	10.59	2.15

Table 30 Effect of C/T on Njs, Pjs, and Npo. 6FPT. T = 0.292 m

Glass Beads
dp = 110 μm
X = 0.5 wt/wt%
Tap water at 22°C

		D = 0.0635 m D/T = 0.217			**D = 0.0762 m D/T = 0.261**			**D = 0.102 m D/T = 0.348**		
C/T	**C (cm)**	**Njs (rpm)**	**Pjs (watts)**	**Npo**	**Njs (rpm)**	**Pjs (watts)**	**Npo**	**Njs (rpm)**	**Pjs (watts)**	**Npo**
1/4	**7.3**	732	2.89	1.54	540	2.75	1.47	335	2.75	1.43
				1.55*			1.46+			1.41×
1/6	**4.9**	691	2.69	1.70	515	2.52	1.55	316	2.50	1.55
				1.64			1.54			1.58
1/8	**3.7**	675	2.55	1.73	499	2.39	1.62	309	2.39	1.59
				1.76			1.59			1.62
1/12	**2.4**	654	2.42	1.81	488	2.33	1.68	303	2.31	1.62
				1.80			1.69			1.66
1/16	**1.8**	643	2.39	1.88	484	2.29	1.70	297	2.24	1.68
				1.87			1.74			1.73
1/20	**1.5**	642	2.40	1.90	482	2.30	1.73	293	2.22	1.73
				1.92			1.76			1.78
1/24	**1.2**	645	2.50	1.94	482	2.34	1.76	291	2.23	1.76
				1.98			1.80			1.79
1/28	**1**	652	2.60	1.97	484	2.48	1.84	289	2.24	1.80
				1.99			1.84			1.82
1/36	**0.8**	655	2.67	1.99	485	2.54	1.87	287	2.23	1.85
				2.00			1.88			1.85
1/48	**0.6**	660	2.81	2.04	486	2.61	1.91	286	2.25	1.88
				2.06			1.91			1.90

* Using water only: 500-600 rpm
+ Using water only: 400-500 rpm
× Using water only: 300-400 rpm

Table 31 Effect of C'/D and C'/T on Njs, Pjs, and Npo. 6FPT. T = 0.292 m

Glass Beads
dp = 110 μ
X = 0.5 wt/wt%
Tap water at 22°C

C'/D (C/D)

		D = 0.0635 m D/T = 0.217			D = 0.0762 m D/T = 0.261			D = 0.102 m D/T = 0.348		
C/D	C'/D	Njs (rpm)	Pjs (watts)	Npo	Njs (rpm)	Pjs (watts)	Npo	Njs (rpm)	Pjs (watts)	Npo
7/16	1/2	660	2.47	1.80	492	2.35	1.66	311	2.41	1.57
3/16	1/4	645	2.50	1.95	483	2.33	1.74	300	2.28	1.65
1/8	1/5	654	2.67	1.98	484	2.48	1.84	293	2.23	1.73

C'/T

		D = 0.0635 m D/T = 0.217			D = 0.0762 m D/T = 0.261			D = 0.102 m D/T = 0.348		
C'/T	C' (cm)	Njs (rpm)	Pjs (watts)	Npo	Njs (rpm)	Pjs (watts)	Npo	Njs (rpm)	Pjs (watts)	Npo
1/5	5.8	712	2.76	1.60	528	2.66	1.52	327	2.59	1.45
1/8	3.7	661	2.48	1.80	493	2.35	1.65	306	2.35	1.60
1/16	1.8	644	2.45	1.92	483	2.33	1.74	291	2.23	1.77
1/24	1.2	654	2.65	1.98	485	2.54	1.87	286	2.28	1.91

Table 32 Effect of C/T on Njs, Pjs, and Npo. CHEM. T = 0.292 m

Glass Beads
dp = 110 μm
X = 0.5 wt/wt%
Tap water at 22°C

		D = 0.102 m D/T = 0.348			**D = 0.114 m D/T = 0.391**		
C/T	**C (cm)**	**Njs (rpm)**	**Pjs (watts)**	**Npo**	**Njs (rpm)**	**Pjs (watts)**	**Npo**
1/4	**7.3**	489	2.12	0.35	407	2.09	0.34
				0.35*			0.34+
1/6	**4.9**	452	1.72	0.37	373	1.67	0.36
				0.36			0.36
1/8	**3.7**	435	1.61	0.38	362	1.57	0.37
				0.38			0.36
1/10	**2.9**	432	1.59	0.39	359	1.56	0.37
				0.38			0.38
1/12	**2.4**	431	1.58	0.39	357	1.54	0.38
				0.39			0.37
1/16	**1.8**	431	1.60	0.39	353	1.54	0.39
				0.40			0.37
1/20	**1.5**	432	1.65	0.40	351	1.53	0.39
				0.40			0.38
1/24	**1.2**	436	1.72	0.41	350	1.55	0.40
				0.41			0.39
1/28	**1**	437	1.77	0.41	350	1.56	0.40
				0.41			0.39
1/36	**0.8**	438	1.83	0.43	349	1.57	0.41
				0.42			0.40
1/48	**0.6**	439	1.86	0.43	348	1.61	0.42
				0.42			0.42

* Using water only: 500-600 rpm
+ Using water only: 400-500 rpm

Table 33 Effect of C/T on Njs, Pjs, and Npo. CHEM. T = 0.584 m

Glass Beads
dp = 110 μm
X = 0.5 wt/wt%
Tap water at 22°C

		D = 0.178 m D/T = 0.304			**D = 0.203 m D/T = 0.348**			**D = 0.229 m D/T = 0.391**		
C/T	**C (cm)**	**Njs (rpm)**	**Pjs (watts)**	**Npo**	**Njs (rpm)**	**Pjs (watts)**	**Npo**	**Njs (rpm)**	**Pjs (watts)**	**Npo**
1/4	**14.6**	355	10.69	0.29	287	10.83	0.28	237	10.93	0.28
				0.29*			0.29*			0.29*
1/6	**9.7**	326	8.75	0.31	265	8.80	0.30	216	8.80	0.30
				0.30			0.30			0.30
1/8	**7.3**	315	8.37	0.32	253	8.40	0.32	210	8.38	0.31
				0.31			0.31			0.31
1/12	**4.9**	310	8.20	0.33	250	8.27	0.33	206	8.30	0.33
				0.33			0.33			0.33
1/16	**3.7**	312	8.45	0.34	248	8.36	0.34	204	8.32	0.34
				0.34			0.34			0.34
1/20	**2.9**	316	8.99	0.35	248	8.56	0.35	202	8.47	0.35
				0.34			0.35			0.35
1/24	**2.4**	320	9.59	0.36	249	8.90	0.36	201	8.52	0.36
				0.36			0.36			0.36
1/28	**2.1**	322	10.15	0.37	249	9.03	0.36	201	8.59	0.37
				0.36			0.37			0.36
1/36	**1.6**	326	10.82	0.38	250	9.31	0.37	200	8.74	0.38
				0.37			0.37			0.37
1/48	**1.2**	330	11.28	0.38	250	9.49	0.38	200	8.84	0.38
				0.38			0.38			0.38

* Using water only: 200-300 rpm

Table 34 Effect of C'/D on Njs, Pjs, and Npo. CHEM. T = 0.584 m

Glass Beads
dp = 110 μm
X = 0.5 wt/wt%
Tap water at 22°C

		D = 0.178 m D/T = 0.304			**D = 0.203 m D/T = 0.348**			**D = 0.229 m D/T = 0.391**		
C/D	**C'/D**	**Njs (rpm)**	**Pjs (watts)**	**Npo**	**Njs (rpm)**	**Pjs (watts)**	**Npo**	**Njs (rpm)**	**Pjs (watts)**	**Npo**
1/2	**1/2**	320	8.61	0.32	264	8.85	0.30	221	9.53	0.31
1/4	**1/4**	308	8.23	0.34	250	8.27	0.33	208	8.31	0.32
1/5	**1/5**	315	8.71	0.34	250	8.27	0.33	206	8.31	0.33

Table 35 Effect of T on Njs, Pjs, and Npo at Constant D/T (= 0.384). 6FDT Constant C/T (C'/T)

Glass Beads
dp = 110 μm
X = 0.5 wt/wt%
Tap water at 22°C

		T = 0.188 m* **D = 0.0636 m**			**T = 0.292 m** **D = 0.102 m**			**T = 0.584 m** **D = 0.203 m**		
C/T	**C'/T**	**Njs (rpm)**	**Pjs (watts)**	**Npo**	**Njs (rpm)**	**Pjs (watts)**	**Npo**	**Njs (rpm)**	**Pjs (watts)**	**Npo**
1/8	**1/6**	421	1.74	4.21	298	5.70	4.21	163	32.74	4.70
							4.19[+]			4.70[×]
1/16	**1/10**	361	1.05	4.05	259	3.59	4.02	143	22.62	4.78
							4.11			4.76
1/24	**1/13**	341	0.85	3.87	245	2.85	3.78	137	19.89	4.78
							3.86			4.78
1/48	**1/18**	318	0.59	3.31	240	2.27	3.21	127	12.47	3.81
							3.26			3.79

* Corrected values: Njs calculated from Njs α $D^{-2.25}$, Npo taken from average value (Npo for D = 0.0762 m and D = 0.102 m) and Pjs calculated from Rushton expression (Pjs = ρ Npo $Njs^3 D^5$)

[+] Using water only: 300-400 rpm

[×] Using water only: 100-200 rpm

Table 36 Effect of T on Njs, Pjs, and Npo at Constant D (= 0.0762 m). 6FDT Constant C/T

Glass Beads
dp = 110 μm
X = 0.5 wt/wt%
Tap water at 22°C

		T = 0.188 m D/T = 0.405			**T = 0.244 m D/T = 0.312**			**T = 0.292 m D/T = 0.261**		
C/T	**C (cm)**	**Njs (rpm)**	**Pjs (watts)**	**Npo**	**Njs (rpm)**	**Pjs (watts)**	**Npo**	**Njs (rpm)**	**Pjs (watts)**	**Npo**
1/8	-	295	1.28	4.16	426	3.88	4.23	546	8.16	4.21
				4.15*			4.23*			4.23*
1/16	-	260	0.84	4.05	374	2.59	4.16	485	5.52	4.07
				4.08			4.09			4.01
1/24	-	250	0.71	3.82	356	2.07	3.84	462	4.59	3.93
				3.91			3.98			3.92
1/48	-	234	0.49	3.23	334	1.51	3.33	430	3.12	3.29
				3.25			3.46			3.35

* Using water only: 400-500 rpm

Table 37 Effect of T on Njs, Pjs, and Npo at Constant D (= 0.0635 m). 6FDT Constant C/T

Glass Beads
dp = 110 μm
X = 0.5 wt/wt%
Tap water at 22°C

		T = 0.188 m D/T = 0.338			**T = 0.244 m D/T = 0.261**			**T = 0.292 m D/T = 0.217**		
C/T	**C (cm)**	**Njs (rpm)**	**Pjs (watts)**	**Npo**	**Njs (rpm)**	**Pjs (watts)**	**Npo**	**Njs (rpm)**	**Pjs (watts)**	**Npo**
1/8	-	450	1.75	4.00	639	5.06	4.06	850	11.61	3.96
				3.98*			3.91*			3.99*
1/16	-	385	1.06	3.89	566	3.35	3.85	749	7.73	3.85
				3.89			3.87			3.91
1/24	-	364	0.89	3.84	536	2.78	3.78	719	6.70	3.78
				3.83			3.79			3.82
1/48	-	340	0.66	3.48	502	1.97	3.25	682	4.95	3.27
				3.32			3.27			3.31

* Using water only: 500-600 rpm

Table 38 Effect of T on Njs, Pjs, and Npo at Constant D/T (= 0.348). 6FBT Constant C/T (C'/T)

Glass Beads
dp = 110 μm
X = 0.5 wt/wt%
Tap water at 22°C

		T = 0.188 m* **D = 0.0636 m**			**T = 0.292 m** **D = 0.102 m**			**T = 0.584 m** **D = 0.203 m**		
C/T	**C'/T**	**Njs (rpm)**	**Pjs (watts)**	**Npo**	**Njs (rpm)**	**Pjs (watts)**	**Npo**	**Njs (rpm)**	**Pjs (watts)**	**Npo**
1/8	**1/7**	480	1.40	2.29	332	4.28	2.28	190	27.93	2.52
							2.30[+]			2.45[×]
1/16	**1/12**	431	1.04	2.36	299	3.26	2.39	175	23.92	2.76
							2.37			2.73
1/24	**1/16**	410	0.93	2.44	284	3.04	2.45	160	21.49	2.93
							2.48			2.92
1/48	**1/24**	393	0.85	2.54	275	2.80	2.63	155	19.95	3.02
							2.57			3.07

* Corrected values: Njs calculated from Njs α $D^{-2.07}$, Npo taken from average value and Pjs calculated from Rushton expression (Pjs = Npo ρ Njs^3 D^5)

[+] Using water only: 300-400 rpm

[×] Using water only: 100-200 rpm

Table 39 Effect of T on Njs, Pjs, and Npo at Constant D (= 0.0762 m). 6FBT Constant C/T

Glass Beads
dp = 110 μm
X = 0.5 wt/wt%
Tap water at 22°C

		T = 0.188 m D/T = 0.405			**T = 0.244 m D/T = 0.312**			**T = 0.292 m D/T = 0.261**		
C/T	**C (cm)**	**Njs (rpm)**	**Pjs (watts)**	**Npo**	**Njs (rpm)**	**Pjs (watts)**	**Npo**	**Njs (rpm)**	**Pjs (watts)**	**Npo**
1/8	-	350	1.17	2.30	483	3.05	2.27	611	6.07	2.24
				2.33*			2.30*			2.29*
1/16	-	317	0.90	2.39	430	2.25	2.39	542	4.50	2.36
				2.39			2.36			2.33
1/24	-	299	0.78	2.45	411	1.99	2.41	515	3.99	2.46
				2.51			2.43			2.40
1/48	-	286	0.72	2.58	399	1.86	2.46	499	3.90	2.64
				2.57			2.58			2.54

* Using water only: 500-600 rpm

Table 40 Effect of T on Njs, Pjs, and Npo at Constant D (= 0.0635 m). 6FBT Constant C/T

Glass Beads
dp = 110 μm
X = 0.5 wt/wt%
Tap water at 22°C

		T = 0.188 m D/T = 0.338			**T = 0.244 m D/T = 0.261**			**T = 0.292 m D/T = 0.217**		
C/T	**C (cm)**	**Njs (rpm)**	**Pjs (watts)**	**Npo**	**Njs (rpm)**	**Pjs (watts)**	**Npo**	**Njs (rpm)**	**Pjs (watts)**	**Npo**
1/8	-	510	1.47	2.31	710	3.77	2.20	903	7.94	2.26
				2.32*			2.29*			2.31*
1/16	-	458	1.07	2.34	629	2.72	2.28	779	5.34	2.36
				2.37			2.32			2.37
1/24	-	436	0.97	2.45	595	2.38	2.36	760	5.10	2.43
				2.47			2.35			2.42
1/48	-	417	0.87	2.52	578	2.33	2.52	724	4.55	2.50
				2.51			2.46			2.49

* Using water only: 500-600 rpm

Table 41 Effect of T on Njs, Pjs, and Npo at Constant D/T (= 0.348). 6FPT Constant C/T (C'/T)

Glass Beads
dp = 110 μm
X = 0.5 wt/wt%
Tap water at 22°C

		T = 0.244 m* **D = 0.0762 m**			**T = 0.292 m** **D = 0.102 m**			**T = 0.584 m** **D = 0.203 m**		
C/T	**C'/T**	**Njs (rpm)**	**Pjs (watts)**	**Npo**	**Njs (rpm)**	**Pjs (watts)**	**Npo**	**Njs (rpm)**	**Pjs (watts)**	**Npo**
1/8	**1/7**	356	1.50	1.62	309	2.39	1.59	175	15.25	1.76
							1.62+			1.78×
1/16	**1/12**	342	1.42	1.73	297	2.31	1.73	170	14.37	1.82
							1.78			1.86
1/24	**1/16**	338	1.42	1.79	291	2.25	1.76	165	14.11	1.96
							1.79			1.90
1/48	**1/24**	337	1.50	1.91	286	2.25	1.88	163	13.86	2.00
							1.90			1.96

* Corrected values: Njs calculated from Njs α $D^{-1.66}$, Npo taken from average value (Npo for D = 0.0762 m and D = 0.102 m) and Pjs calculated from Rushton expression (Pjs = Npo ρ Njs^3 D^5)

+ Using water only: 300-400 rpm

× Using water only: 100-200 rpm

Table 42 Effect of T on Njs, Pjs, and Npo at Constant D (= 0.0762 m). 6FPT Constant C/T

Glass Beads
dp = 110 μm
X = 0.5 wt/wt%
Tap water at 22°C

		T = 0.188 m D/T = 0.405			**T = 0.244 m D/T = 0.312**			**T = 0.292 m D/T = 0.261**		
C/T	**C (cm)**	**Njs (rpm)**	**Pjs (watts)**	**Npo**	**Njs (rpm)**	**Pjs (watts)**	**Npo**	**Njs (rpm)**	**Pjs (watts)**	**Npo**
1/8	-	341	0.75	1.59	427	1.47	1.58	499	2.39	1.62
				1.55*			1.59*			1.59*
1/16	-	328	0.71	1.69	410	1.38	1.68	484	2.29	1.70
				1.68			1.68			1.74
1/24	-	323	0.71	1.78	406	1.39	1.74	482	2.34	1.76
				1.78			1.75			1.80
1/48	-	320	0.73	1.86	404	1.51	1.92	486	2.61	1.91
				1.90			1.81			1.91

* Using water only: 500-600 rpm

Table 43 Effect of X on Njs, Pjs, and Npo. 6FDT. D/T = 0.348
Constant C/T (C'/T)

Glass Beads
dp = 110 μm
Tap water at 22°C

		X = 0.5 wt/wt%			X = 1.0 wt/wt%			X = 1.5 wt/wt%		
C/T	**C'/T**	**Njs (rpm)**	**Pjs (watts)**	**Npo**	**Njs (rpm)**	**Pjs (watts)**	**Npo**	**Njs (rpm)**	**Pjs (watts)**	**Npo**
1/8	**1/6**	298	5.70	4.21	329	7.85	4.31	347	9.04	4.19
				4.19*			4.19*			4.19*
1/16	**1/10**	259	3.59	4.02	282	4.67	4.08	299	5.57	4.05
				4.11			4.11			4.02
1/24	**1/13**	245	2.85	3.78	266	3.58	3.70	284	4.53	3.85
				3.86			3.86			3.86
1/48	**1/18**	240	2.27	3.21	260	3.06	3.40	278	3.68	3.32
				3.26			3.26			3.26

* Using water only: 300-400 rpm

Table 44 Effect of X on Njs, Pjs, and Npo. 6FBT. D/T = 0.348
Constant C/T (C'/T)

Glass Beads
dp = 110 μm
Tap water at 22°C

		X = 0.5 wt/wt%			X = 1.0 wt/wt%			X = 1.5 wt/wt%		
C/T	**C'/T**	**Njs (rpm)**	**Pjs (watts)**	**Npo**	**Njs (rpm)**	**Pjs (watts)**	**Npo**	**Njs (rpm)**	**Pjs (watts)**	**Npo**
1/8	**1/7**	332	4.28	2.28	363	5.65	2.30	384	6.71	2.30
				2.30*			2.30*			2.30*
1/16	**1/12**	299	3.26	2.39	327	4.29	2.41	346	5.20	2.43
				2.37			2.37			2.37
1/24	**1/16**	289	3.04	2.45	316	4.14	2.56	334	4.84	2.52
				2.48			2.48			2.48
1/48	**1/24**	275	2.80	2.63	299	3.59	2.62	317	4.33	2.63
				2.57			2.57			2.57

* Using water only: 300-400 rpm

Table 45 Effect of X on Njs, Pjs, and Npo. 6FPT. D/T = 0.348
Constant C/T (C'/T)

Glass Beads
dp = 110 μm
Tap water at 22°C

		X = 0.5 wt/wt%			X = 1.0 wt/wt%			X = 1.5 wt/wt%		
C/T	**C'/T**	**Njs (rpm)**	**Pjs (watts)**	**Npo**	**Njs (rpm)**	**Pjs (watts)**	**Npo**	**Njs (rpm)**	**Pjs (watts)**	**Npo**
1/8	**1/7**	309	2.39	1.59	333	3.00	1.60	348	3.43	1.58
				1.62*			1.62*			1.62*
1/16	**1/12**	297	2.24	1.68	321	2.80	1.65	337	3.31	1.68
				1.78			1.78			1.78
1/24	**1/16**	291	2.23	1.76	314	2.78	1.75	329	3.26	1.77
				1.79			1.79			1.79
1/48	**1/24**	286	2.25	1.88	309	2.17	1.82	321	3.23	1.89
				1.90			1.90			1.90

* Using water only: 300-400 rpm

Table 46 Effect of X on Njs, Pjs, and Npo. CHEM. D/T = 0.348
Constant C/T (C'/T)

Glass Beads
dp = 110 μm
Tap water at 22°C

		X = 0.5 wt/wt%			X = 1.0 wt/wt%			X = 1.5 wt/wt%		
C/T	**C'/T**	**Njs (rpm)**	**Pjs (watts)**	**Npo**	**Njs (rpm)**	**Pjs (watts)**	**Npo**	**Njs (rpm)**	**Pjs (watts)**	**Npo**
1/4	**1/4**	489	2.12	0.35	528	2.62	0.35	555	3.03	0.34
				0.35*			0.35*			0.35*
1/6	**1/6**	452	1.72	0.37	484	2.15	0.37	512	2.57	0.37
				0.36			0.36			0.36
1/8	**1/8**	435	1.61	0.38	470	2.00	0.38	500	2.44	0.38
				0.38			0.38			0.38
1/10	**1/10**	432	1.59	0.38	472	2.05	0.38	504	2.60	0.40
				0.38			0.38			0.38
1/12	**1/12**	431	1.58	0.39	478	2.23	0.40	512	2.71	0.39
				0.39			0.39			0.39
1/16	**1/16**	431	1.6	0.39	490	2.48	0.41	528	3.02	0.40
				0.40			0.40			0.40
1/20	**1/20**	432	1.65	0.40	498	2.57	0.41	544	3.3	0.40
				0.40			0.40			0.40
1/24	**1/24**	436	1.72	0.41	506	2.75	0.41	556	3.57	0.40
				0.41			0.41			0.41
1/36	**1/36**	438	1.83	0.43	520	3.02	0.42	574	3.97	0.41
				0.42			0.42			0.42

* Using water only: 500-600 rpm

Table 47 Dual-6FDT System. Effect of C/T on Njs, Pjs, and Npo
T = 0.292 m, D/T = 0.261, S/D = 1

Glass Beads
dp = 110 μ
X = 0.5 wt/wt%
Tap water at 22°C

		n = 1			n = 2					
C/T	**C (cm)**	**Njs (rpm)**	**Pjs (watts)**	**Npo**	**Njs (rpm)**	**$\frac{Pj_{Supper}}{Pj_{Slower}}$**	**Pjs total (watts)**	**Npo lower**	**Npo upper**	**Npo total**
1/8	**3.7**	546	8.16	4.21	-	-	-	-	-	-
				4.23*				3.68*		8.23*
1/16	**1.8**	485	5.52	4.07	541	2.26	11.95	1.95	4.39	6.33
				4.01				1.9		6.21
1/24	**1.2**	462	4.59	3.93	529	2.45	10.88	1.79	4.38	6.17
				3.92				1.78		6.13
1/48	**0.6**	441	3.56	3.49	497	2.57	8.74	1.68	4.31	5.99
				3.47				1.61		6.10

* Using water only: 400-500 rpm

Table 48 Dual-6FBT System. Effect of C/T on Njs, Pjs, and Npo
T = 0.292 m, D/T = 0.261, S/D = 1

Glass Beads
dp = 110 μ
X = 0.5 wt/wt%
Tap water at 22°C

		n = 1			n = 2					
C/T	**C (cm)**	**Njs (rpm)**	**Pjs (watts)**	**Npo**	**Njs (rpm)**	**$\frac{Pj_{Supper}}{Pj_{Slower}}$**	**Pjs total (watts)**	**Npo lower**	**Npo upper**	**Npo total**
1/8	**3.7**	611	6.07	2.24	632	1.09	12.19	1.94	2.11	4.05
				2.29*				1.88*		4.05*
1/16	**1.8**	542	4.50	2.36	562	1.10	8.76	1.98	2.17	4.15
				2.33				1.92		4.14
1/24	**1.2**	515	3.99	2.46	526	1.09	7.38	2.04	2.23	4.27
				2.40				1.94		4.21
1/48	**0.6**	499	3.90	2.64	520	1.09	7.12	2.03	2.22	4.26
				2.54				1.97		3.29

* Using water only: 400-500 (rpm)

Table 49 Dual-6FPT System. Effect of C/T on Njs, Pjs, and Npo
T = 0.292 m, D/T = 0.261, S/D = 1

Glass Beads
dp = 110 μ
X = 0.5 wt/wt%
Tap water at 22°C

		n = 1			n = 2					
C/T	**C (cm)**	**Njs (rpm)**	**Pjs (watts)**	**Npo**	**Njs (rpm)**	**$\frac{Pj_{upper}}{Pj_{lower}}$**	**Pjs total (watts)**	**Npo lower**	**Npo upper**	**Npo total**
1/8	**3.7**	499	2.39	1.62	480	1.26	3.59	1.2	1.52	2.72
				1.59*				1.15*		2.70*
1/16	**1.8**	484	2.29	1.70	441	1.31	2.94	1.25	1.64	2.89
				1.74				1.21		2.84
1/24	**1.2**	482	2.34	1.76	426	1.46	2.75	1.23	1.77	3.00
				1.80				1.26		2.97
1/48	**0.6**	486	2.61	1.91	417	1.23	2.82	1.46	1.79	3.24
				1.91				1.35		3.17

* Using water only: 400-500 rpm

REFERENCES

Aravinth, S., Gangaghar Rao P., and Murugesan, T., 1996, Critical Impeller Speed for Solid Suspension in Turbine Agitated Contactors, *Bioproc. Eng.*, **14**: 97-99.

Armenante, P. M., and Li, T., 1993, Minimum Agitation Speed for Off-Bottom Suspension of Solids in Agitated Vessels Provided with Multiple Flat-Blade Impellers, *A.I.Ch.E. Symp. Ser.*, **89**: 105-111.

Armenante, P. M., Huang, Y. T., and Li, T., 1992, Determination of the Minimum Agitation Speed to Attain the Just Dispersed State in Solid-Liquid and Liquid-Liquid Reactors Provided with Multiple Impellers, *Chem. Eng. Sci.*, **47**: 2865-2870.

Baldi, G., Conti, R., and Alaria, E., 1978, Complete Suspension of Particles in Mechanically Agitated Vessels, *Chem. Eng. Sci.*, **33**: 21-25.

Bates, R. L., Fondy, P. L., and Corpstein, R. R., 1963, An Examination of Some Geometric Parameters on Impeller Power, *Ind. Eng. Chem. Process Des. Dev.*, **2**:310-314.

Chang, G-M, 1993, Power Consumption in Single-Phase Agitated Vessels Provided with Multiple Impellers, M. S. Thesis, New Jersey Institute of Technology, Newark, NJ.

Chapman, C. M., Nienow, A. W., Cooke, M., and Middleton, J. C., 1983, Particle-Gas-Liquid Mixing in Stirred Vessels. Part I: Particle-Liquid Mixing, *Trans. Inst. Chem. Eng.*, **61**: 71-81.

Chudacek, M. W., 1985, Solids Suspension Behavior in Profiled Bottom and Flat Bottom Mixing Tanks, *Chem. Eng. Sci.*, **40**: 385-392.

Chudacek, M. W., 1986, Relationships between Solids Suspension Criteria, Mechanism of Suspension, Tank Geometry, and Scale-Up Parameters in Stirred Tanks, *Ind. Eng. Chem. Fundam.*, **25**: 391-401.

Conti, R., Sicardi, S., and Specchia, V., 1981, Effect of the Stirrer Clearance on Suspension in Agitated Vessels, *Chem. Eng. J.*, **22**: 247-249.

Einenkel, W-D, 1980, Influence of Physical Properties and Equipment Design on the Homogeneity of Suspensions in Agitated Vessels, *Ger. Chem. Eng.*, **3**: 118-124.

Gray, D. J., 1987, Impeller Clearance Effect on Off-Bottom Particle Suspension in Agitated Vessels, *Chem. Eng. Commun.*, **61**: 151-158.

Gray, D. J., Treybal, R. E., and Barnett, S. M., 1982, Mixing of Single and Two Phase Systems: Power Consumption of Impellers, *A.I.Ch.E. J.*, **28**: 195-199.

Janzon, J., and Theliander, H., 1994, On the Suspension of Particles in an Agitated Vessel, *Chem. Eng. Sci.*, **49**: 3522-3526.

Kolar, V., 1961, Studies on Mixing. X: Suspending Solid Particles in Liquids by means of Mechanical Agitation, *Collec. Czech. Chem. Commun.*, **26**: 613-627.

Molerus, M., and Latzel, W., 1987a, Suspension of Solid Particles in Agitated Vessels-I. Archimedes Number < 40, *Chem. Eng. Sci.*, **42**: 1423-1430.

Molerus, M., and Latzel, W., 1987b, Suspension of Solid Particles in Agitated Vessels-II. Archimedes Number > 40, Reliable Prediction of Minimum Stirrer Angular Velocities, *Chem. Eng. Sci.*, **42**: 1431-1437.

Musil, L., and Vlk, J., 1978, Suspending Solid Particles in an Agitated Conical-Bottom Tank, *Chem. Eng. Sci.*, **33**: 1123-1131.

Musil, L., Vlk, J., and Jiroudkova, H., 1984, Suspending Solid Particles in an Agitated Tank with Axial-Type Impellers, *Chem. Eng. Sci.*, **39**: 621-627.

Myers, K. J., and Fasano, J. B., 1992, The Influence of Baffle Off-Bottom Clearance on the Solids Suspension Performance of Pitched-Blade and High-Efficiency Impellers, *Can. J. Chem. Eng.*, **70**: 596-599.

Myers, K. J., Corpstein, R. R., Bakker, A., and Fasano, J., 1994a, Solids Suspension Agitator Design with Pitched-Blade and High-Efficiency Impellers, *A.I.Ch.E. Symp. Ser.*, **90**: 186-190.

Myers, K. J., Fasano, J. B., and Corpstein, R. R., 1994b, The Influence of Solid Properties on the Just-Suspended Agitation Requirements of Pitched-Blade and High-Efficiency Impellers, *Can. J. Chem. Eng.*, **72**: 745-748.

Narayanan, S., Bhathia, V. K., Guha, D. K., and Rao, M. N., 1969, Suspension of Solids by Mechanical Agitation, *Chem. Eng. Sci.*, **24**: 223-230.

Nienow, A. W., 1968, Suspension of Solid Particles in Turbine-agitated, Baffled Vessels, *Chem. Eng. Sci.*, **23**: 1453-1459.

Nienow, A. W., and Miles, D., 1971, Impeller Power Numbers in Closed Vessels, *Ind. Eng. Chem. Process Des. Dev.*, **10**: 41-43.

Nienow, A. W., and Miles, D., 1978, The Effect of Impeller/Tank Configurations on Fluid-Particle Mass Transfer, *Chem. Eng. J.*, **15**: 13-24.

Niewow, A. W., 1985, The Dispersion of Solids in Liquids, in *Mixing of Liquids by Mechanical Agitation*, by J. J. Ulbrecht and G. K. Patterson (editors), pp. 273-307, Gordon and Breach Science Publishers, London.

Oldshue, J. Y., 1983, Solids Suspensions, in *Fluid Mixing Technology*, pp. 94-124, McGraw-Hill, New York, NY.

Oldshue, J. Y., and Sharma, R. N., 1992, The Effect of Off-Bottom Distance of an Impeller for the "Just Suspended Speed", Njs, *A.I.Ch.E. Symp. Ser.*, **88**: 72-76.

O'Okane, K., 1974, The Effect of Geometric Parameters on the Power Consumption of Turbine Impellers Operating in Non-viscous Fluids , *Proc. 1st Europ. Conf. on Mixing, Cambridge, England, Sept. 9-11*, paper A3: 23-31.

Raghava Rao, K. S. M. S., and Joshi, J. B., 1988a, Liquid Phase Mixing in Mechanically Agitated Vessels, *Chem. Eng. Commun.*, **74**: 1-25.

Raghava Rao, K. S. M. S., Rewatkar, V. B., and Joshi, J. B., 1988b, Critical Impeller Speed for Solid Suspension in Mechanically Agitated Contactors, *A.I.Ch.E. J.*, **34**: 1332-1340.

Rewatkar, V. B., Raghava Rao, K. S. M. S., and Joshi, J. B., 1990, Power Consumption in Mechanically Agitated Contactors Using Pitched Bladed Turbine Impeller, *Chem. Eng. Commun.*, **88**: 69-90.

Rieger, F., and Ditl, P., 1994, Suspension of Solid Particles, *Chem. Eng. Sci.*, **49**: 2219-2227.

Rushton, J. H., Costich, E. W., and Everett, H. J., 1950, Power Characteristics of Mixing Impellers — Part I, *Chem. Eng. Prog.*, **46**: 395-404.

Weisman, J., and Efferding, L. E., 1960, Suspension of Slurries by Mechanical Mixers, *A.I.Ch.E. J.*, **6**: 419-426.

Wichterle, K., 1988, Conditions for Suspension of Solids in Agitated Vessels, *Chem. Eng. Sci.*, **43**: 467-471.

Zwietering, T. N., 1958, Suspending Solid Particles in Liquids by Agitators, *Chem. Eng. Sci.*, **8**: 244-253.